UNIVERSITY OF OXFORD

Identification of methylation sites in *Rhodobacter* chemoreceptors

Thesis for Master of Science by Research

Ayse Ozhan

Lady Margaret Hall

Trinity 2010

Abstract

Chemotaxis in *Rhodobacter sphaeroides* occurs through the alteration of the level of rotational switching of its flagellum. The presence of attractants and repellents are sensed by methyl-accepting chemotaxis proteins (MCPs). The reversible methylation of certain glutamate residues in the methylation helices of MCPs is important in the adaptation aspect of chemotaxis. Previously established consensus methylation sites in other organisms were used for searches in the sequences of *R. sphaeroides* chemoreceptors for putative methylation sites. Site-directed mutagenesis was used to convert glutamine/glutamate residues to alanine in these putative sites on the cytoplasmic receptor TlpT and the transmembrane receptor McpH. Motility analyses of mutants showed that $TlpT_{(Q475A)}$ and $TlpT_{(Q528A)}$ cells have reduced motility. This indicates that these sites in TlpT could be important for methylation by $CheR_3$ and demethylation by the CheBs.

Acknowledgments

I would like to express my gratitude to Prof Judy Armitage for allowing me to work in her laboratory, and also to Dr Mark Roberts for his continuous support throughout the completion process of the project. I should also like to thank the other members of the Armitage Lab for creating a friendly and supportive working environment.

Abbreviation	Meaning
Amp	Ampicillin
ATP	Adenosine triphosphate
bp	Base pair
BSA	Bovine serum albumin
CI	*R. sphaeroides* chromosome one
CII	*R. sphaeroides* chromosome two
CA	Catalytic and ATP binding domain
Cm	Chloramphenicol
Che	Chemotaxis
DHp	Dimerization and histidine phosphotransfer domain
DIG	Digoxigenin
DMSO	Dimethyl sulphoxide
DNA	Deoxyribosenucleic acid
dNTP	Deoxynucleoside 5'-triphosphate
HAP	Histidine-aspartate-phosphorelay
HEPES	Sodium N-2-hydroxyethylpiperazine-N'-2-ethanesulphonic acid
HCD	Highly conserved domain
HK	Histidine kinase
Kan	Kanamycin
kDa	Kilodalton
LB	Luria-Bertani
Nal	Nalidixic acid
PBP	Periplasmic binding protein
PCR	Polymerase chain reaction
RR	Response regulator
SSC	Saline-sodium citrate
Sm	Streptomycin
Tet	Tetracyclin
UV	Ultraviolet

Table 1: Abbreviations used in the study are listed above.

Contents

1 Introduction 6
1.1 Bacterial motility 6
1.1.1 The flagellum 8
1.2 Two-component regulatory systems 9
1.3 Bacterial chemotaxis 11
1.3.1 The *Escherichia coli* chemotaxis model 12
1.3.2 *Rhodobacter sphaeroides* 25
1.4 Aims of the study 34
2 Materials and Methods 34
2.1 Plasmids 34
2.2 Strains 37
2.3 Growth conditions 38
2.3.6 Storage of bacterial cells 39
2.4 Genetic techniques 39
2.4.1 Extraction of *R. sphaeroides* genomic DNA 39
2.4.2 Agarose gel electrophoresis 40
2.4.3 Extraction of DNA from TBE agarose gels 40
2.4.4 Polymerase Chain Reactions (PCRs) 40
2.4.5 Restriction enzyme digests 45
2.4.6 Dephosphorylation of plasmid DNA 46
2.4.7 DNA ligations 46
2.4.8 Competent cells 48
2.4.9 Transformation of plasmid DNA into *E. coli* 48
2.4.10 Plasmid preparations 48
2.5 Gene insertion strategy 48
2.5.1 Insertion constructs 48
2.5.2 Conjugations 49
2.5.3 Selection for 2nd round recombination 49
2.5.4 DNA sequencing 51
2.5.5 Preparation of labelled DNA probes 51
2.5.6 Southern blots 51

2.6 Phenotypic techniques 52
2.6.1 Swarm plates 52
2.6.2 Tethered cell analysis 52
2.7 Bioinformatics techniques 53
3 Results 54
4 Discussion 71
5 References 80
A1 Appendix 1 – Primers 87
A2 Appendix 2 – Reagent recipes 91
A2.1 Succinate medium 91
A2.2 Concentrated Base 91
A2.3 Metals 44 Solution 92
A2.4 Growth Factors 92
A2.5 M22 medium 93
A2.6 DNA loading dye (5x) 93
A2.7 TBE (10x) 94
A2.8 L-broth 94
A2.9 Chromosomal DNA preparation lysis buffer 94

1 Introduction

Chemotaxis is the ability of a bacterial cell to respond to chemical gradients by moving towards higher concentrations of attractants and lower concentrations of repellents (Falke and Hazelbauer 2001). It is an important survival strategy for many bacterial species and is frequently used in pathogenesis (Mowbray and Sandgren 1998). In the chemotaxis process, chemical signals received from the environment are transmitted inside the cell by the cooperative function of proteins to affect swimming behaviour.

1.1 Bacterial motility

Bacteria such as *Escherichia coli* and *Salmonella typhimurium* swim smoothly about their environment in one direction for a while, and then tumble and choose an arbitrary new direction. This is the case in the absence of a chemoeffector or in the presence of increasing concentrations of repellent (Figure 1A). They swim fairly smoothly in the presence of increasing concentrations of attractant or decreasing concentrations of repellent (Figure 1B). Attractants suppress tumbling and prolong smooth swimming to carry the cell up the gradient, whereas repellents increase the frequency of tumbles and shorten smooth swimming in an unfavourable direction (Blair 1995).

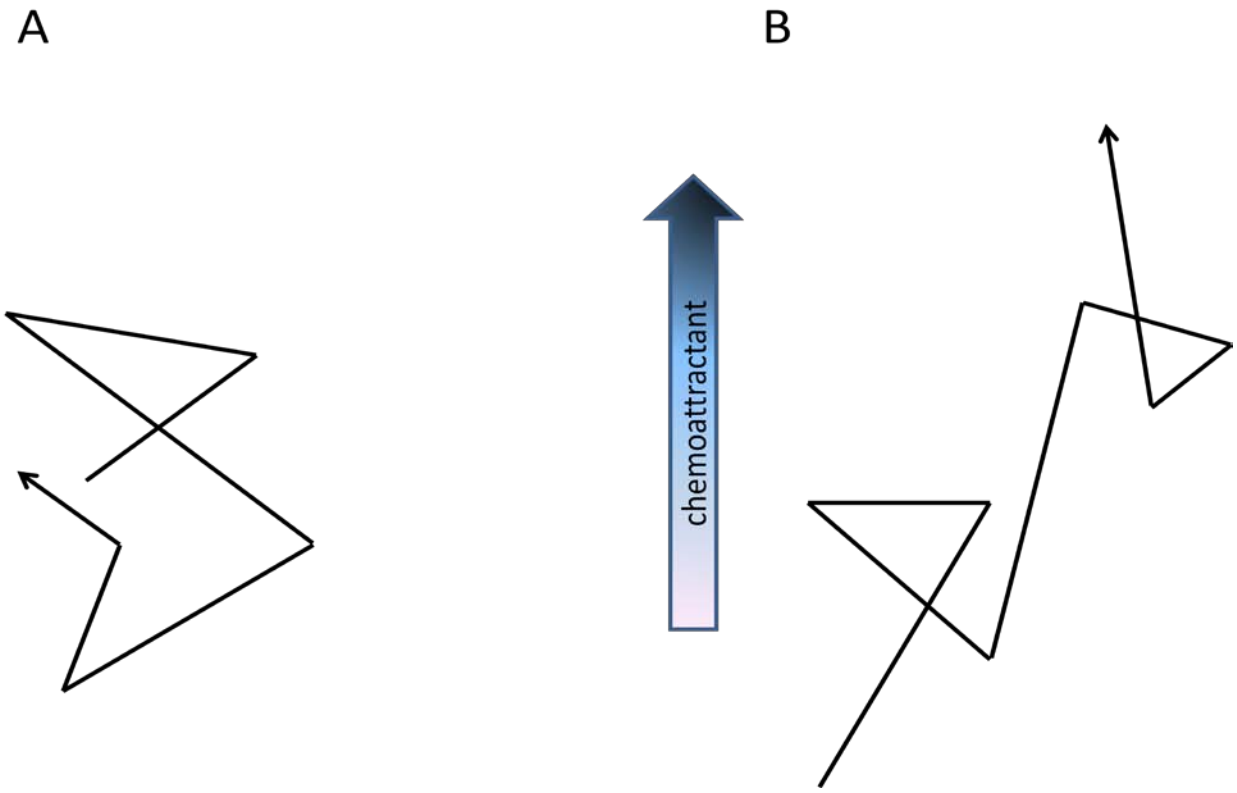


Figure 1: Swimming behaviour in the absence and presence of a chemoattractant. **(A)** In the absence of a chemoeffector, the swimming pattern is smooth swimming for a few seconds and then tumbling. After tumbling, the bacterium swims in a randomly different direction. **(B)** In the presence of a chemoattractant, tumbling frequency is decreased and smooth swimming periods are prolonged. This results in the bacterium swimming towards higher concentrations of attractant. Repellents have the opposite effect.

1.1.1 The flagellum

Many motile bacteria use flagella which, by rotating, enable them to swim towards favourable environments. Monomers of the flagellin protein polymerize to form the semi-rigid helix of the flagellar filament (Armitage 1992). The hook connects the filament to the basal body. The hook is made up of the FlgE protein.

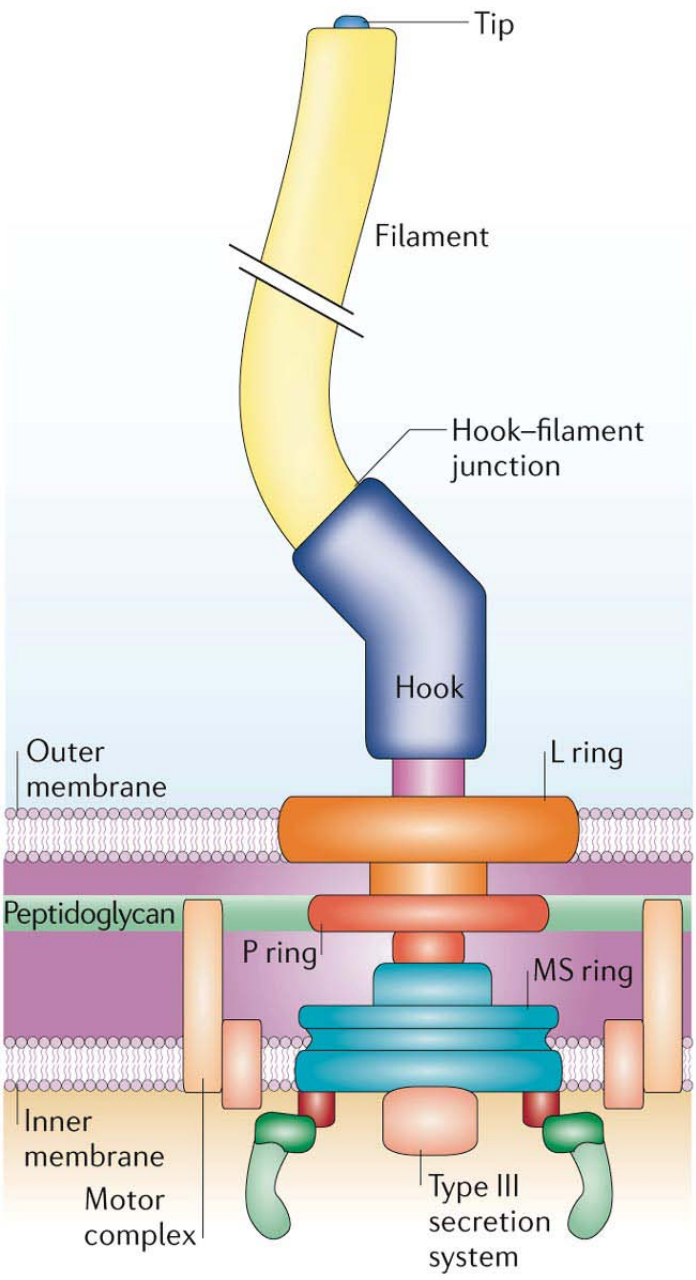


Figure 2: Structure of the bacterial flagellum from the gram-negative *S. typhimurium*. Figure taken from Pallen and Matzke 2006.

The basal body of the flagellum in gram-negative bacteria is composed of the C, MS, P, and L rings (Figure 2). The L ring is anchored to the lipopolisaccharide layer, the P ring is anchored to the peptidoglycan layer, the MS ring is anchored to the inner membrane, and the C ring is in the cytoplasm. The MOT proteins (formed from MotA and MotB complexes) span the cell membrane, surrounding the MS ring (Figure 2) (White 2007). The switch complex consists of three proteins: FliG, FliM, and FliN (the latter two form the C ring).

The energy required for flagellar rotation comes from the proton-motive force that is generated when protons influx through the MOT proteins. FliG interacts with the MOT proteins and transmits the torque to the basal body (Pallen and Matzke 2006).

1.2 Two-component regulatory systems

The two-component system is a commonly used sensory pathway in nature. Bacterial two-component systems control a large variety of functions including cell division, virulence, antibiotic resistance, metabolite fixation and utilization, response to environmental stress, sporulation, and taxis (Falke, Bass, et al. 1997). Eukaryotic homologues of two-component pathways have been discovered in *Saccharomyces cerevisiae*, *Arabidopsis thaliana*, *Neurospora crassa*, and *Dictyostelium discoideum* (Appleby, Parkinson and Bourret 1996).

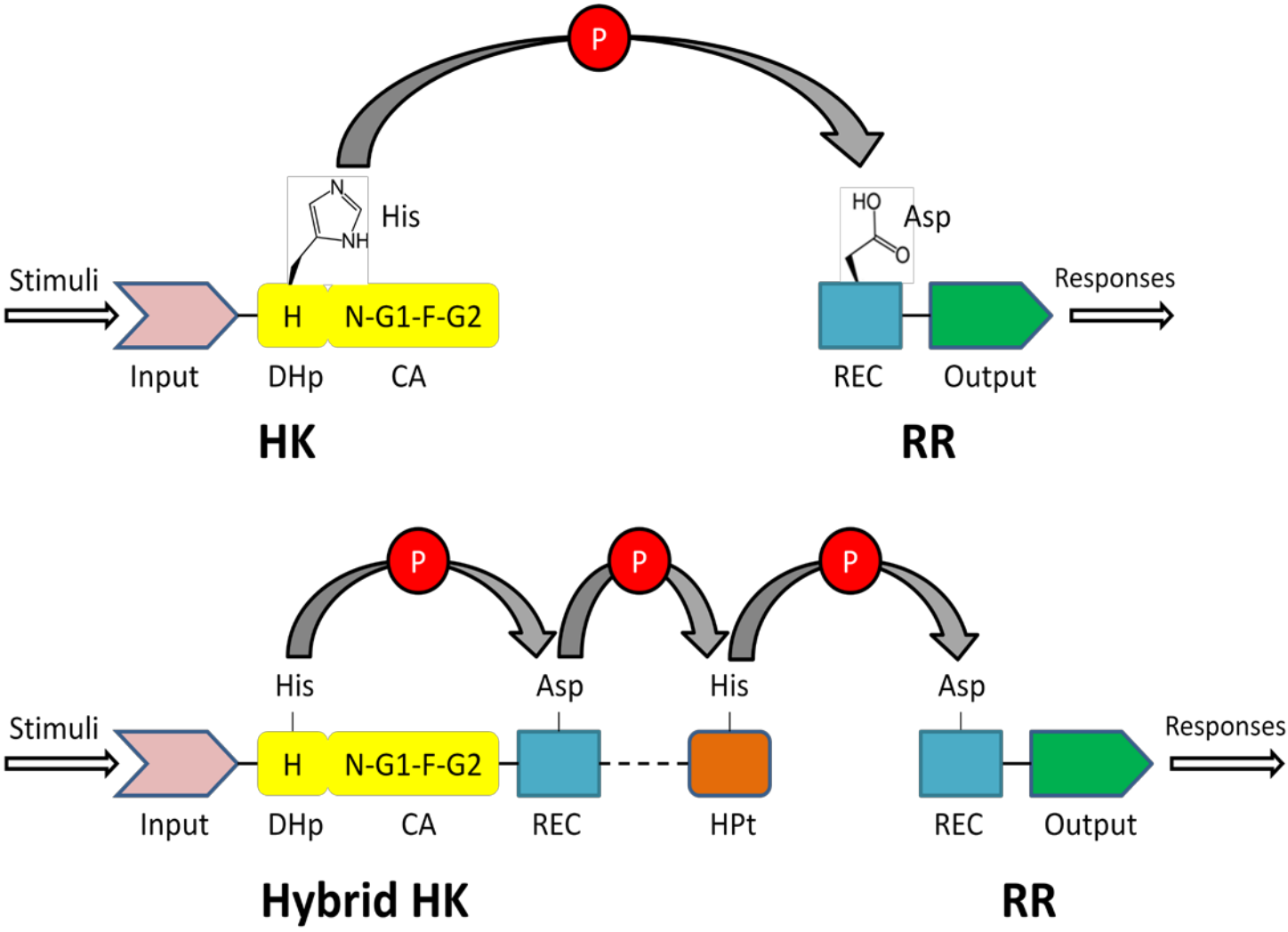


Figure 3: Diagram showing two-component systems. **(A)** The basic two-component system is composed of an HK and an RR. The HK *auto*-phosphorylates at a His residue in its DHp domain, which is transferred to an Asp residue in the REC domain of the RR. **(B)** Histidine-aspartate phosphorelay systems involve two or more phosphotransfers between multiple His- and Asp- containing proteins. Figure adapted from Gao and Stock 2009.

The basic system includes two proteins: a histidine kinase (HK) and a cytoplasmic response regulator (RR). The HK protein typically consists of a diverse N-terminal sensory domain, a well-conserved C-terminal catalytic and ATP binding (CA) domain, and a less-conserved dimerization and histidine phosphotransfer (DHp) domain. HKs function as dimers and *trans*-autophosphorylates a specific histidine residue in the DHp domain in one of its monomers by the γ-phosphoryl group of an ATP molecule that is bound to the CA domain of the other monomer (Figure 3a).

The HK then transfers the phosphoryl group to an aspartate residue in the conserved receiver (REC) domain in the response regulator protein (RR). A phosphatase, which could be the HK, the RR, or a separate protein, dephosphorylates the RR and returns it to the nonstimulated state. An example to the prototypical system is the EnvZ/OmpR system in *E. coli* and *S. typhimurium*, which regulates porin synthesis in response to changes in osmolarity. Other examples are the FixJ/FixL system in *Rhizobium melliloti*, which responds to oxygen (Swanson and Simon 1994), and *E. coli* chemosensory system (Wadhams and Armitage 2004).

Histidine-aspartate-phosphorelay (HAP) systems are formed when hybrid HKs involve additional REC and histidine phosphotransfer (HPt) domains for multiple phosphotransfer events (Figure 3b). The intermediate HPt domain can either be an independent protein or linked to the HK (Gao and Stock 2009). An example to the HAP system is the Arc system in *E. coli*, which under anaerobic conditions represses transcription of genes that are expressed only under aerobic conditions (Stock, Robinson and Goudreau 2000). Another example is the Spo phosphorelay system of *Bacillus subtilis* for the regulation of sporulation (Wadhams and Armitage 2004).

The kinase core domains of HKs (Figure 3, yellow) are divided into blocks of common sequence (Stock, Ninfa and Stock 1989), and the blocks are referred to by their

characteristic residues ('H', 'N', 'G1', 'G2', and 'F'). Block H in the DHp domain contains the histidine residue required for *auto*-phosphorylation. This block is also implicated in phosphatase activity (Parkinson and Kofoid 1992). The N, G1, F, and G2 boxes make up the ATP binding cavity (Bilwes, et al. 1999), and between the F and G2 boxes there is a flexible ATP lid region (Gao and Stock 2009). HKs have been divided into two classes based on the position of the H box: in class I HKs the H box is directly adjacent to the ATP-binding domain, whereas in class II HKs the H box is located on a distant HPt domain at the N terminus of the protein (Gao and Stock 2009).

Two-component systems are used for more specific applications in eukaryotes such as regulating development, responding to osmotic and oxidative stress, and detecting hormones (Falke, Bass, et al. 1997). Homologues of HKs have been found in the AHK family of proteins *Arabidopsis thaliana*, which have implicated functions in osmosensing and cytokinin signalling (Hwang, Chen and Sheen 2002). The osmosensing pathway in *Saccharomyces cerevisiae* involves the SLN1/YDP1/SSK1 phosphorelay system that regulates the HOG1 MAP kinase cascade (Posas, et al. 1996).

1.3 Bacterial chemotaxis

A bacterium cannot measure changes in chemoeffector concentration spatially due to its small size. Therefore it measures changes in concentration over time by measuring the absolute concentration of a chemoeffector, and then comparing it with the previously measured concentration. (White 2007).

The chemosensory systems of enteric bacteria *E. coli* and *S. typhimurium* are the best characterized two-component systems. The HKs in chemosensory systems belong to class II HKs. They are soluble and they sense stimuli indirectly through interaction with

transmembrane chemoreceptors called methyl-accepting chemotaxis proteins (MCPs) (Kirby 2009). MCPs are so called because they contain methylation regions on their cytoplasmic surfaces, which are covalently modified for chemotactic regulation.

Increasing concentrations of attractants and decreasing concentrations of repellents promote (CCW) rotation of the flagellar motor and smooth swimming. On the other hand, increasing concentrations of repellents, decreasing concentrations of attractants, or the absence of any chemoeffector promote clockwise (CW) rotation and tumbling.

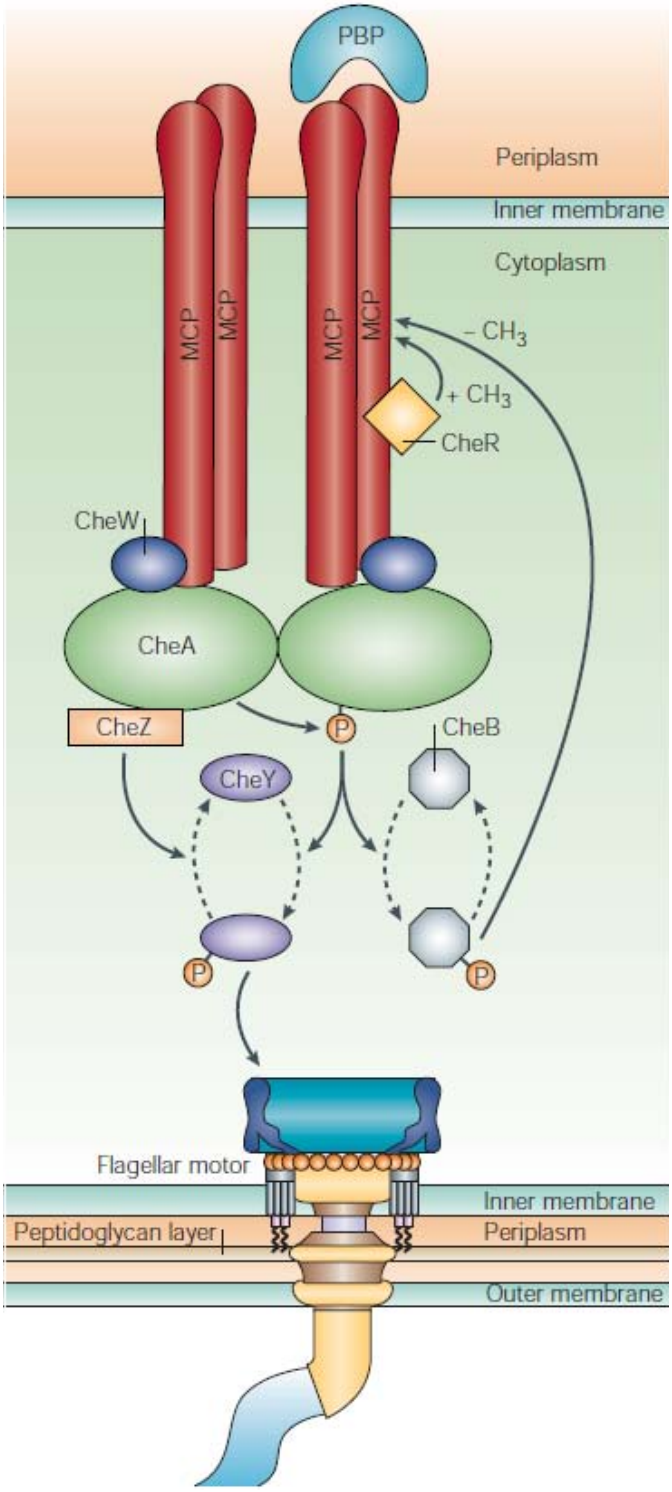


Figure 4: The chemosensory system of *E. coli*. The figure is taken from Wadhams and Armitage 2004.

1.3.1 The *Escherichia coli* chemotaxis model

Chemotaxis in *E. coli* is carried out by the cytoplasmic Che proteins. CheA is the HK in the chemotaxis system. It is coupled to the transmembrane MCPs by a scaffolding protein called CheW.

Attractant binding to an MCP decreases the rate of autophosphorylation of CheA, whereas the dissociation of the attractant increases it (Stock and Mowbray 1995). Active CheA-P transfers the phosphate

group to an aspartyl residue on CheY, one of the RRs in the system. CheY-P binds to the flagellar motor switch, promoting CW rotation and tumbling. The phosphatase CheZ terminates the CheY-P signal (Wadhams and Armitage 2004).

Efficient chemotaxis requires the bacterium to memorize the past attractant concentration and compare it to the present concentration. Adaptation to chemotactic signalling involves the transfer of methyl groups to the MCPs by the constitutively active methyltransferase CheR, and their removal by the other RR in the system, the methylesterase CheB. Because increased attractant binding reduces the rate of CheA-P formation, phosphorylation of its substrate CheB is also reduced, allowing the receptors to become more heavily methylated by CheR (Figure 4). The highly methylated MCP stimulates CheA-P activity, which in turn promotes CW rotation and tumbling, hence adaptation to that concentration of attractant (Blair 1995).

A decreased concentration of attractant or increased concentration of repellent increases the rate of CheB-P formation, which results in the receptors becoming less methylated. Demethylated MCPs have a reduced ability to stimulate CheA-P formation, so the CheA-P and CheY-P levels return to the pre-stimulus level (Wadhams and Armitage 2004).

1.3.1.1 Methyl-accepting chemotaxis proteins (MCPs)

E. coli has four MCPs used in chemotaxis: Tar (aspartate receptor), Tsr (serine receptor), Trg (ribose and galactose receptor), and Tap (receptor for dipeptides). MCPs are divided into the following domains: the N-terminal periplasmic (sensing) domain, the transmembrane domain, the HAMP domain, the methylation helices joined by the signalling domain, and a C-terminal tail (Mowbray and Sandgren 1998). MCPs are found in homodimers both in the absence and presence of ligands. Their periplasmic domains contain eight α-helices arranged in two symmetric four-helix bundles, one from each monomer, designated α1-α4 and α1'- α4' (Figure 5) (Falke and Hazelbauer 2001). Two helices from each monomer span the bilayer to form a transmembrane four-helix bundle (helices TM1, TM2, TM', TM2'). The two cytoplasmic helical hairpins, one from each subunit, form the cytoplasmic four-helix bundle (helices CD1, CD2 and CD1', CD2').

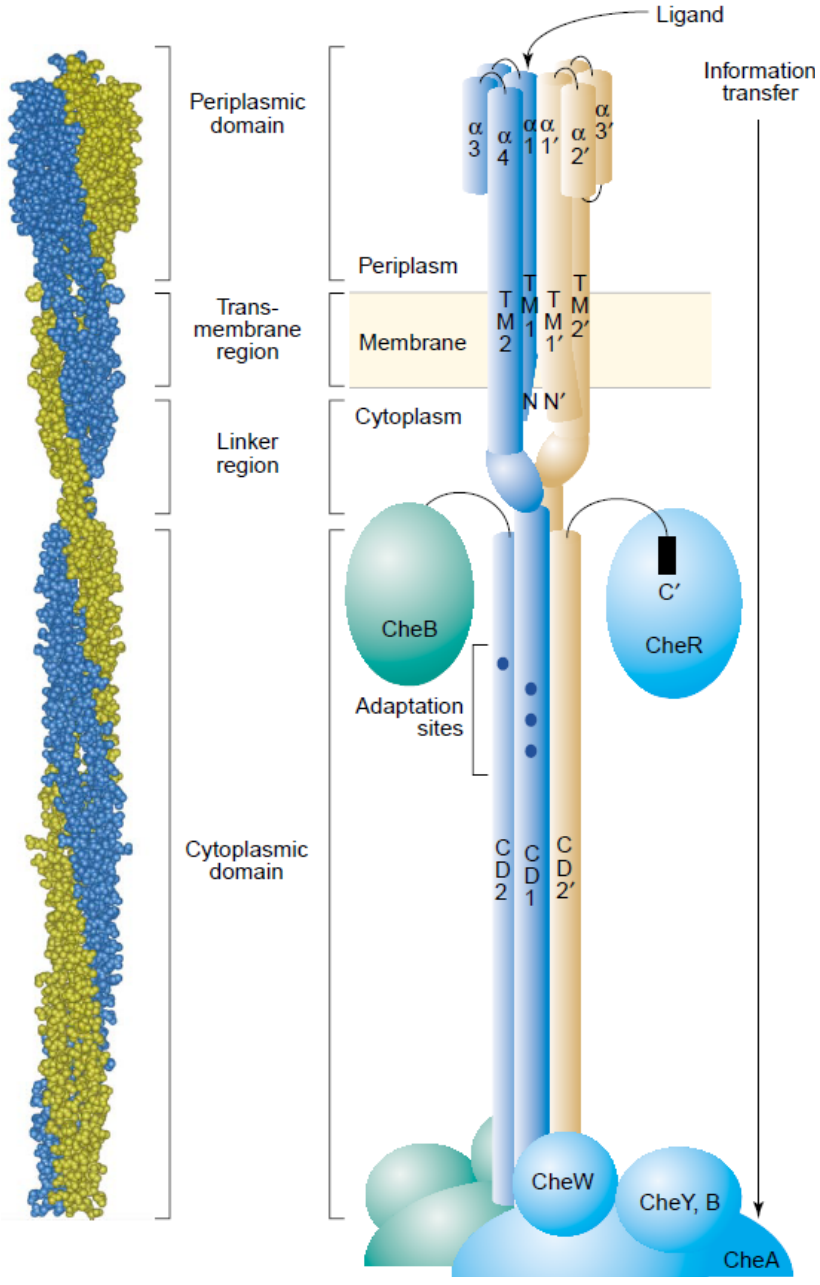


Figure 5: Structure of the dimeric MCP. The model on the left was created by combining the crystal structures of the periplasmic domain of Tar and the cytoplasmic domain of Tsr. The diagram on the right shows the functional domains and the docking sites for the chemosensory proteins. The figure was taken from Falke and Hazelbauer 2001.

Disulfide studies with the Tar receptor have revealed that cysteines and disulfides involving helix α4/TM2 significantly affect aspartate binding affinity and CheA regulation (Chervitz and Falke 1995). This assigned the α4/TM2 helix as the signalling helix, and the α1/TM1 helix as the structural helix. The aspartate-bound and unbound crystal structures of Tar were superimposed and a swinging-piston model was proposed as the transmembrane signalling mechanism. Upon ligand binding, the α4/TM2 helix is displaced downwards towards the cytoplasm by ~1.6 Å and tilted by 5° (Chervitz and Falke 1996). Structural evidence from the NarX and TorS receptors indicate that the swinging-piston model is widely conserved in bacterial receptors (Falke and Erbse 2009).

1.3.1.1.1 The N-terminal periplasmic domain

MCPs of *E. coli* interact with some ligands directly, and with other ligands indirectly through a periplasmic binding protein (PBP). Examples are MBP (maltose-binding protein) and NiBP (nickel-binding protein) for Tar, GBP (glucose/galactose-binding protein) and RBP (ribose-binding protein) for Trg and DBP (dipeptide-binding protein) for Tap (Mowbray and Sandgren 1998).

Sequence analysis of *E. coli* Tar, Tap and Tsr showed that the periplasmic domains of these receptors are 40 to 90% diverse, allowing their different ligand specificity (Krikos, et al. 1983). Structural studies with *S. typhimurium* Tar have indicated that one receptor dimer binds one aspartate molecule under physiological aspartate concentrations, although there are two ligand binding sites. Each binding pocket is formed by Arg64 and residues Tyr149 to Thr154 from one subunit, and Arg69 and Arg73 from the other. These positively charged regions in Tar form polar interactions with oppositely charged residues on aspartate (Yeh, et al. 1996).

1.3.1.1.2 The transmembrane region

In the *E. coli* Tar receptor, residues 7-30 make up TM1, and residues 189-212 make up TM2 (Mowbray and Sandgren 1998).

1.3.1.1.3 The HAMP domains

The HAMP domain connects helix TM2 to the cytoplasmic domain in MCPs. The name for HAMP domains is an abbreviation of the type of proteins in which they occur: *h*istidine kinases, *a*denylyl cyclases, *m*ethyl-accepting chemotaxis proteins and *p*hosphatases (Aravind and Ponting 1999). Receptors may have single HAMP domains or poly-HAMP chains.

Crystal structure of the putative transmembrane receptor Af1503 from *Archaeglobus fulgidus* has shown that the HAMP domain consists of two α-helices (AS1 and AS2) connected by a 13-residue loop (Hulko, et al. 2006). The HAMP dimer of one receptor monomer forms a parallel four-helix bundle with that of the other receptor monomer. The loop region contains a conserved Gly-x-HR1-x-x-x-HR2 motif (HR1 and HR2 being two hydrophobic residues) that begins immediately after AS1, which has a stabilizing function (Airola, et al. 2010).

Structural studies have been made with the *Pseudomonas aeruginosa* aerotaxis receptor Aer2, which has five HAMP units arranged in three domains. A mechanism of two-state switching (A/B) within individual HAMP domains, and alternating conformations between consecutive HAMP units (A-B-A-...) that interconvert in a binary fashion (B-A-B-...), has been proposed as to how signals are propagated through poly-HAMP chains. The two-state switching mechanism is also thought to be involved in single canonical HAMP domain signalling (Airola, et al. 2010).

1.3.1.1.4 The methylation helices

Each MCP monomer has two juxtaposed methylation (or adaptation) helices divided by the signalling domain. These helices contain multiple Glu/Gln residues which undergo reversible methylation. These sites have been determined as Gln297, Glu304, Gln311, and Glu493 in *E. coli* Tsr (Kehry, et al. 1983 and Boyd, Kendall and Simon 1983); Glu294, Glu302, Glu309, and Glu491 in *S. typhimurium* Tar (Terwilliger and Koshland 1984); and as Glu304, Glu310, Gln311, Gln318, and Glu500 in *E. coli* Trg. The *Bacillus subtilis* McpB was found to contain three methylation sites: Gln371, Glu630, and Glu637. The consensus sequence around these methylation sites is E/Q-E/Q-X-X-A-S/T (methylatable glutamate/glutamine residues are in red).

Fifteen methylation sites were identified in total on the TM0429, TM1143, TM1146, and TM1428 receptors of the hyperthermophilic *Thermotoga maritima* (Perez, Zheng and Stock 2006). The consensus methylation sequence for the longer *T. maritima* receptors is longer and symmetric: A/S-A/G/S/T-X-E/Q-E-X-A/G/S/T-A/S (methylatable glutamate/glutamine residues are in red).

1.3.1.1.5 The signalling domain

Also called the highly conserved domain (HCD), the 50-residue signalling helix contains the binding sites for CheW and CheA; and the structural features required for CheA stimulation (Ames, Yu and Parkinson 1996).

1.3.1.1.6 The C-terminal pentapeptide motif

The last five amino acids (NWETF) of the Tar and Tsr receptors from *E. coli* were found to be the binding site for CheR. Receptors which do not contain this C-terminal motif are thought to be methylated through CheR molecules bound to adjacent receptors containing the motif (Wu, et al. 1996).

1.3.1.1.7 MCP classes

MCPs have been grouped into three classes based on the presence of 14-residue insertion/deletion (indel) regions in their cytoplasmic domains (Le Moual and Koshland 1996). Class I MCPs do not contain any 14-residue insertion, class II MCPs contain two 14-residue insertions before and after the HCD. Class III MCPs contain four 14-residue insertions; two of them in the same positions as class II receptors and two additional ones at the beginning and end of the methylation regions (Le Moual and Koshland 1996).

1.3.1.2 CheA

The 71-kDa CheA kinase has five domains per monomer, designated P1-P5 from the N-terminus to the C-terminus (Wadhams and Armitage 2004). The His48 residue in the P1 domain is the site of *trans*-autophosphorylation, and it also acts as a phosphodonor for the RRs in the system (Figure 6). The crystal structure of the P1 domain revealed that this

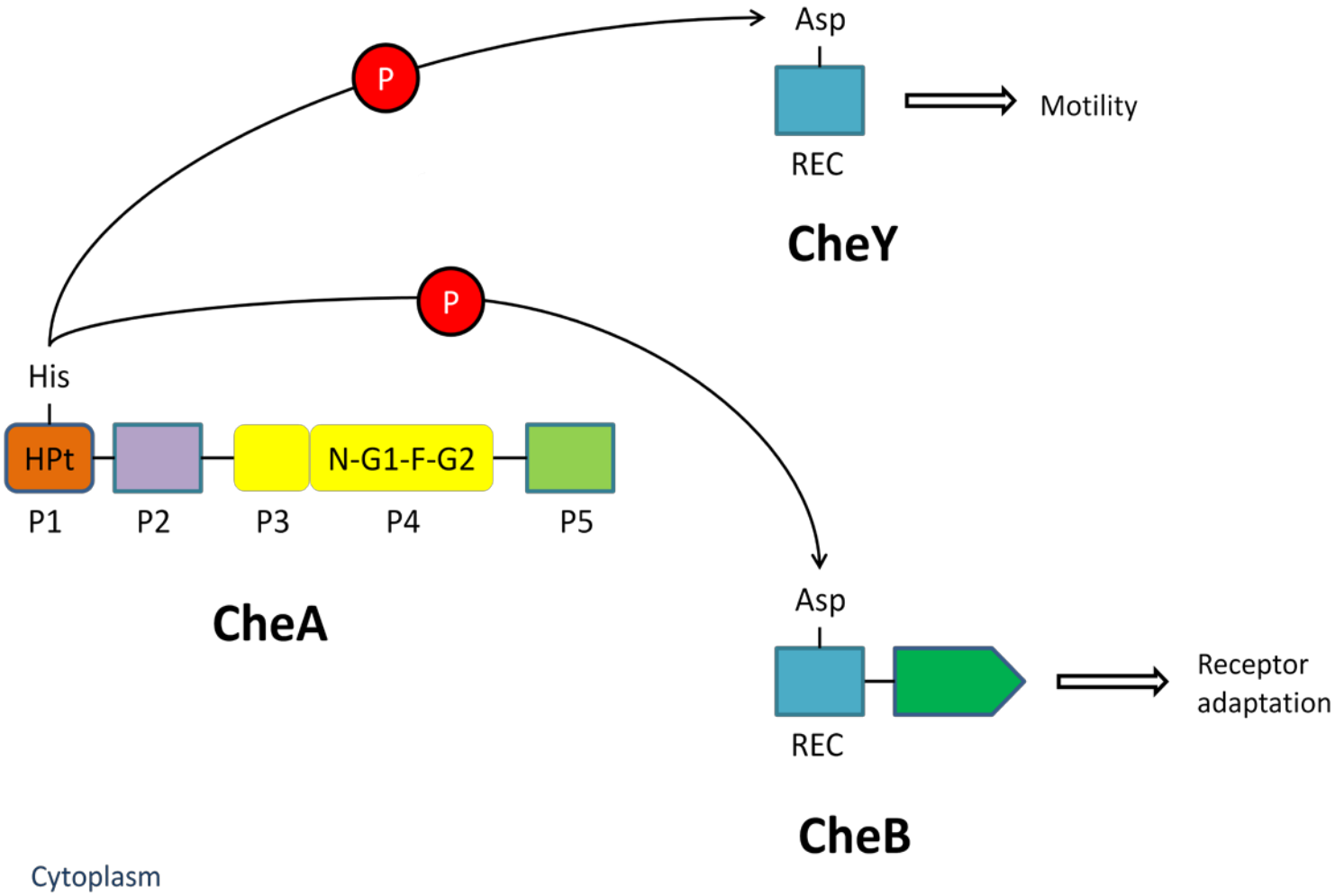


Figure 6: Domain organisation of the chemosensory two-component system. CheA, the soluble HK in the system, contains five domains (P1-P5). Figure adapted from Wadhams and Armitage 2004.

domain is composed of 5 α-helices and His48 is positioned near the middle of the B helix, with its side chain solvent exposed (Mourey, et al. 2001).

The P2 domain (residues 159-227) is the docking site for the response regulator CheY. The NMR structure of the P2 domain revealed that P2 consists of four antiparallel β-strands forming one face of the domain, and two oppositely oriented α-helices forming the other. Both helices are involved in binding and the residues involved in binding are partially or mostly exposed to the solvent (McEvoy, Muhandiram, et al. 1996). Both the P1 and P2 domains (residues 1-233) are required for binding CheB (McEvoy, Hausrath, et al. 1998).

The crystal structure of the last three domains of CheA from *T. maritima* has been solved. The dimerization domain, P3 (residues 290-354), consists of two antiparallel α-helices which form a four-helix bundle with the analogous two helices of the second subunit. The P4 domain is the CA domain, a two layered α-β sandwich made a five-stranded β sheet and six α helices. The P5 domain (residues 541-671) is the CheW interaction domain composed of two five-stranded β-barrels (Bilwes, et al. 1999).

1.3.1.3 CheW

CheW is an 18-kDa scaffolding protein with no enzymatic function. It couples CheA with the cytoplasmic tails of the MCPs (Gegner, et al. 1992). The NMR structure of CheW from *T. maritima* has shown that this protein is made up of two five-stranded β-barrels around an internal hydrophobic core. CheW is structurally similar to CheA (Griswold, et al. 2002). In *E. coli* cells, deletion of *cheW* resulted in the absence of CheB (methylesterase) activation in response to removal of attractant or addition of repellent. It was also found to be required for CheB inhibition in response to attractant addition (Stewart, Roth and Dahlquist 1990).

1.3.1.4 CheY

The levels of phosphorylated CheY in the cytoplasm determine the direction of flagellar rotation. High levels of phosphorylated CheY promote clockwise rotation, whereas low levels of phosphorylated CheY promote counterclockwise rotation. CheY achieves this by binding to FliM of the flagellar motor switch complex; phosphorylation of CheY increases its affinity to FliM (Welch, et al. 1993).

The CheY protein itself is an autocatalytic aspartate domain without an output domain. The CheY structure is a central five-stranded β-barrel flanked on both sides by five α-helices (Stock, Mottonen, et al. 1989). Mass spectrometry analysis lead to the identification of the phosphorylated residue in CheY as D57. This asparagine residue forms an acidic pocket together with D12 and D13, and these two residues are thought to coordinate the catalytic Mg^{+2} (Sanders, et al. 1989). The K109 residue is thought to be important for active phospho-CheY function (Lukat, et al. 1991). Mutagenesis and phenotypic analyses confirmed the importance of all four of these sites on chemotaxis.

1.3.1.5 CheB, CheR, and adaptation

CheB is a serine hydrolase which hydrolyzes the carboxyl-methylglutamate residues on MCPs, while releasing methanol. CheB also functions as an amidase which converts specific glutamines to glutamates on these receptors. The CheB protein has a receiver domain homologous to CheY with larger loops connecting β4 to α4 and β5 to α5 (Djordjevic, Goudreau, et al. 1998).

Sequence alignment and analysis of mutants in terms of their methylation, phosphorylation, and swarming activities lead to the corresponding functional residues in

CheB to be determined as: D10, D11, D56 (putative phosphorylation site), and K107 (Stewart, Roth and Dahlquist 1990 and Stewart 1993). The N-terminal regulatory and the C-terminal catalytic domains of CheB are connected by an 18-residue linker.

The output (catalytic) domain of CheB is a doubly wound α/β fold composed of six α-helices and nine β-strands. The crystal structure of the *S. typhimurium* CheB catalytic domain revealed that there is an antiparallel β-hairpin between strand β4 and helix αC (West, Martinez-Hackert and Stock 1995). The catalytic triad performing methylester hydrolysis involves the residues Ser164 (nucleophile), His190 (proton donor to methanol), and Asp286 (stabiliser) (West, Martinez-Hackert and Stock 1995).

The crystal structure of the full-length protein revealed that the N-terminal domain blocks access of the receptor substrate to the C-terminal domain. According to a model, phosphorylation of the N-terminal domain at D56 leads to minor reorientation of helices α4 and α5, which results in the disruption of the interdomain interface, widening the catalytic cleft (Djordjevic, Goudreau, et al. 1998).

The CheR (methyltransferase) protein catalyzes the esterification of the γ-carboxylates of the specific glutamates on MCPs using S-adenosylmethionine (SAM) as the methyl group donor, producing S-adenosylhomocysteine (AdoHcy) (Stewart 1993). The N-terminal domain of CheR consists of four α-helices, while the C-terminal domain contains a seven-stranded β-sheet with a subdomain (a three-stranded β-sheet and an α-helix) insertion (Djordjevic and Stock 1998). The β-subdomain is involved in binding the C-terminal region of the MCPs. The active site cleft lies between the two domains (Falke, Bass, et al. 1997).

The rate of demethylation of receptors by CheB is slower than the phosphorylation rate of CheY. Upon attractant binding to a receptor, CheY-P and CheB-P levels drop initially. Constitutively active CheR increases the methylation state of the receptors, causing CheY-P 1and CheB-P levels to start rising. CheY-P acts immediately on the flagella, while CheB-P

slowly returns the receptors to their non-stimulated methylation state. The result of this is that the response to change of chemoeffector concentration is transient, and cells eventually turn to their original CheY-P levels and thus tumbling rates (Meir, et al. 2010). The methylation (adaptation) system serves to keep receptor methylation levels and CheA kinase activity at an intermediate level throughout a wide range (over more than four orders of magnitude) of stimulus concentrations (Lupas and Stock 1989).

1.3.1.6 Signal termination

The CheZ protein stimulates the dephosphorylation of CheY-P, and is therefore critical in determining intracellular CheY-P concentration (Boesch, Silversmith and Bourret 2000). Each monomer of the CheZ dimer forms two amphipathic helices with a single hairpin turn, arranged 'head-to-head' to form the $CheZ_{core}$ four-helix bundle (Zhao, et al. 2002). CheZ contains an additional helix (residues 5-34) at a 100°C angle to the core bundle, and a 13-residue helix ($CheZ_c$) at its C-terminal end. The conserved Q147 from CheZ is positioned in the CheY active site, rendering CheY autodephosphorylation more efficient (Zhao, et al. 2002).

1.3.1.7 Chemotaxis in other species

In some types of bacteria such as *Rhodobacter sphaeroides*, *Rhizobium meliloti*, *Myxococcus xanthus*, and *Bacillus subtilis*, the chemotaxis system works in a different way than that of the enteric bacteria *E. coli* and *S. typhimurium*. *R. meliloti* forms nodules in the rootlets of certain legumes for nitrogen fixation. It has two cytoplasmic receptors, IcpA and McpY, in addition to six transmembrane receptors. It lacks a CheZ phosphatase, but has a CheY1 protein that shuttles phosphoryl groups back to CheA from the main flagellar regulator CheY2, and thus

works as a phosphate sink. The *R. meliloti* flagella are unidirectional (CW) and the slowing-down of flagellar rotation results in turns (Scharf and Schmitt 2002).

The soil bacterium *M. xanthus* lacks flagella and instead uses two types of gliding motility for movement: social (S-) motility, powered by the extension and retraction of type IV pili, and adventurous (A-) motility, in which protein motors attach to transient focal adhesion complexes and are thought to move on helical cytoskeletal filaments (Zusman, et al. 2007). In S-motility, the cells move in groups, and in A-motility the cells move individually. *M. xanthus* cells form biofilms and can grow by predating other microorganisms by producing antibiotics and digestive enzymes.

M. xanthus contains eight chemosensory pathways, each containing homologues of the *E. coli* chemosensory proteins. These pathways are involved in various processes in the growth and development of *M. xanthus* such as chemotaxis, motility, and fruiting-body formation (Zusman, et al. 2007). The Frz pathway, which involves the cytoplasmic chemoreceptor FrzCD, controls cellular reversal frequency. The Dif pathway controls lipid chemotaxis, the Che3 pathway controls development, the Che4 pathway regulates S-motility, Che6 is required for type IV pilus assembly, and Che7 regulates fatty-acid metabolism (Zusman, et al. 2007). Multiple chemosensory systems in bacteria are thought to have evolved to allow for their temporal regulation during different stages of the cell cycle.

The soil bacterium *B. subtilis* uses three adaptation systems. It employs a selective methylation system, where methylation of certain residues on receptors activates CheA, and methylation of others deactivates CheA (Zimmer, et al. 2000). The second adaptation system is the CheC-CheD-CheYp system. In this system, attractant stimulation increases the formation of CheA-P, which in turn promotes CheYp production. Increased CheYp levels lead to more CheC-CheYp complexes, which then recruits CheD away from the receptors,

inhibiting CheA (Rao, Glekas and Ordal 2008). The CheC-CheD-CheYp system is also thought to coordinate selective methylation (Rao, Kirby and Arkin 2004).

The third adaptation system in *B. subtilis* uses the CheV protein, which has an N-terminal CheW-like domain and a C-terminal REC domain. Attractant binding activates the CheA kinase, which phosphorylates the D235 on the REC domain of CheV. CheV-P than disrupts the coupling between the receptors and CheA, allowing adaptation to that concentration of attractant (Alexander, et al. 2010). The multiple adaptation systems used by *B. subtilis* is thought to provide robustness in chemotaxis, and the different adaptation systems might be used for different levels of chemoeffector signals (Rao, Glekas and Ordal 2008). The chemotaxis system of *R. sphaeroides*, the organism used in this study, is described in Section 1.3.2.

1.3.2 *Rhodobacter sphaeroides*

1.3.2.1 Physiology

Rhodobacter sphaeroides is a photosynthetic, purple non-sulphur bacterium; belonging to the α-subgroup of proteobacteria (other species of α-proteobacteria include: *R. meliloti*, *Caulobacter crescentus*, *Magnetospirillum magneticum* and *Acetobacter aceti*).

R. sphaeroides has a highly versatile metabolism, and is able to grow aerobically, anaerobically in the dark, photoheterotrophically, or by fermentation (White 2007). Photosynthesis is carried out inside intracytoplasmic membranes (ICM), which are invaginations of the cytoplasmic membrane (Mackenzie, Eraso, et al. 2007). The organism's major attractants are: organic acids, sugars, polyols, glutamate, ammonia, K^+, and Rb^+ (Armitage 1992).

The genome of the *R. sphaeroides* strain 2.4.1 was sequenced and annotated, however the genome sequence of the more motile strain WS8 used in this study was found to be 98.5% identical with that of 2.1.4 (Mackenzie, Choudhary, et al. 2001). The *R. sphaeroides* genome consists of two circular chromosomes: CI (~3.2 Mb) and CII (~0.9 Mb) (Suwanto and Kaplan 1989).

1.3.2.2 Motility

R. sphaeroides has a single, unidirectional (CW), medially (subpolar) located flagellum (Armitage and Macnab 1987). Change in direction is achieved by transient stops in flagellar rotation (Armitage 1992).

1.3.2.3 The *R. sphaeroides* chemotaxis pathway

R. sphaeroides contains multiple homologues of the chemosensory proteins in *E. coli*: four CheAs, four CheWs, six CheYs, two CheBs, three CheRs, thirteen chemoreceptors, and one CheD (a *B. subtilis* homologue). The large (CI) chromosome of *R. sphaeroides* contains the

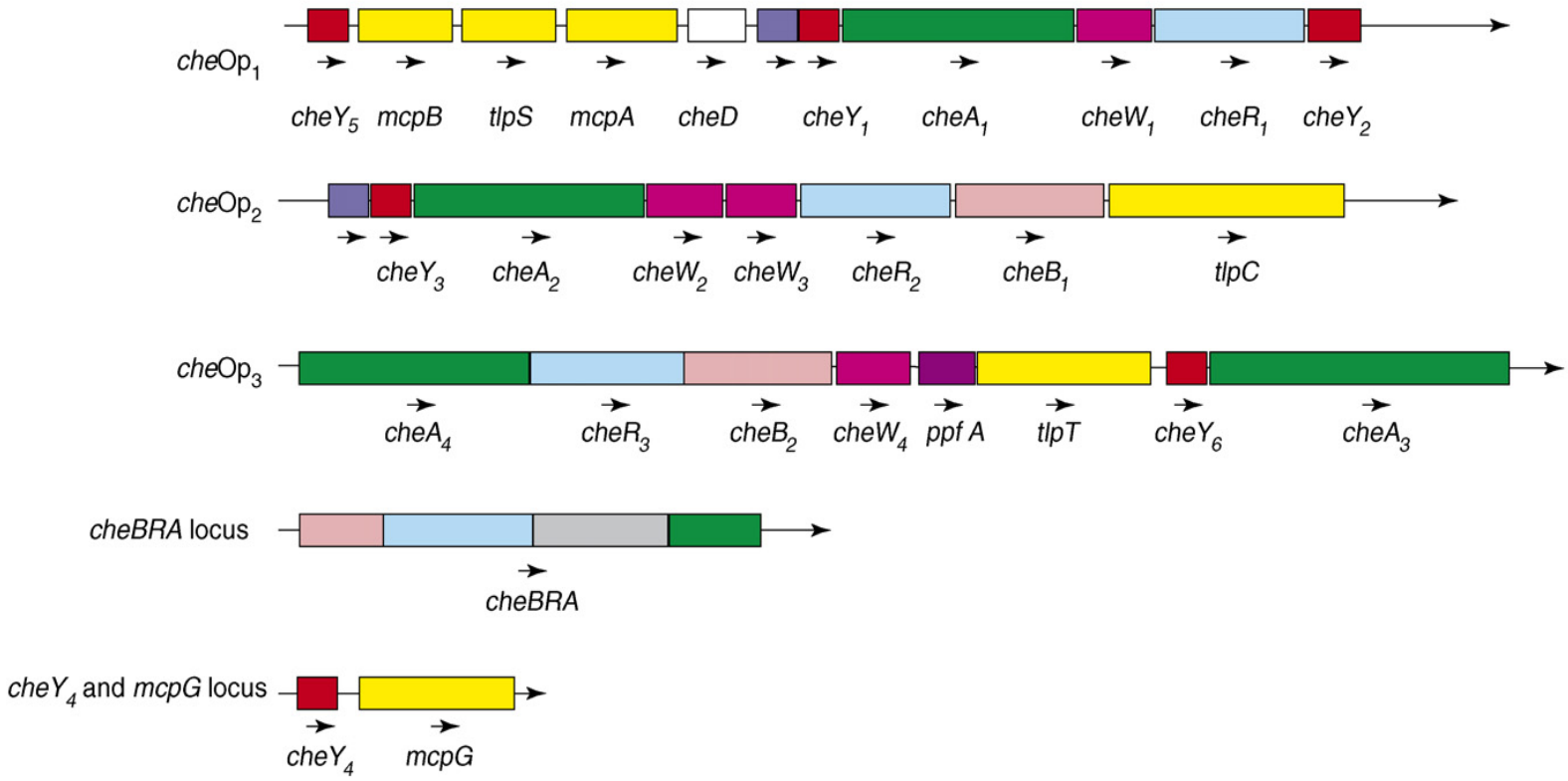


Figure 7: The chemotaxis operons of *R. sphaeroides*. The figure was taken from Porter, Wadhams and Armitage 2008.

three major chemotaxis operons, *che*Op$_1$, *che*Op$_2$, and *che*Op$_3$, as well as the *che*BRA locus (Figure 7) (Mackenzie, Choudhary, et al. 2001). Unlinked loci on CI encode for the chemoreceptors McpM and TlpL (which is clustered with genes encoding flagellar motor proteins, *motAB*) (Thompson 2005). The small (CII) chromosome contains the *cheY$_4$* and *mcpG* locus (Figure 7). There are five other unlinked loci on CII encoding for the chemoreceptors McpH, McpR, McpV, McpE, and McpJ (Thompson 2005).

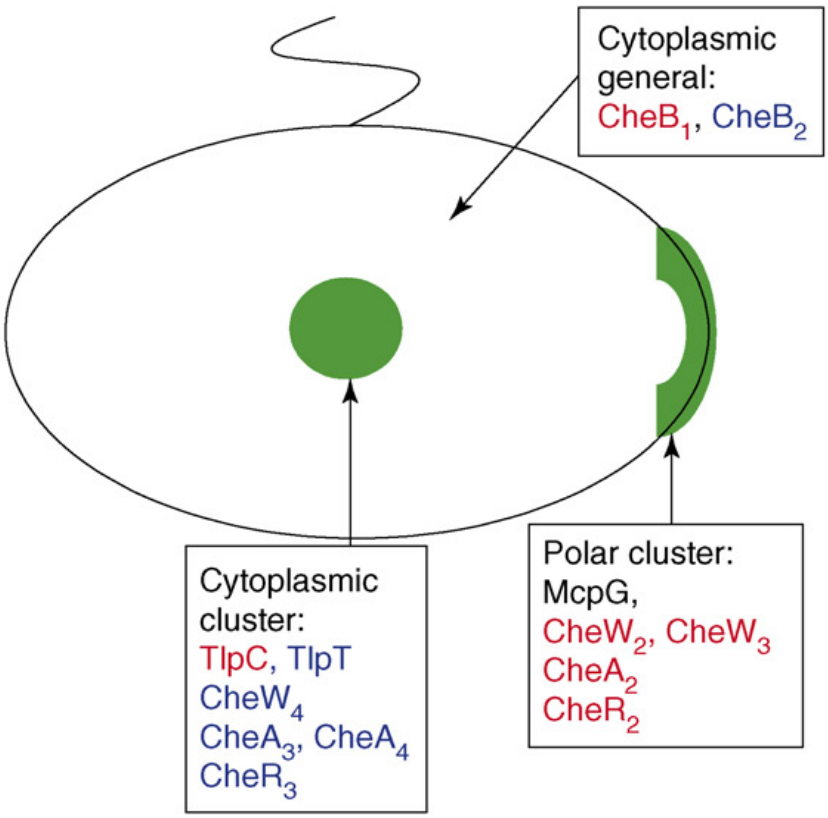


Figure 8: The known localisation of the chemotaxis protein in *R. sphaeroides*. Proteins from *che*Op$_2$ are shown in red, proteins from *che*Op$_3$ are shown in blue, and those from unlinked loci are shown in black. The figure was taken from Wadhams, Warren, et al. 2003.

All of the genes encoded by the operons *che*Op$_2$ and *che*Op$_3$ were found to be required for normal chemotaxis under laboratory conditions (Porter, Warren, et al. 2002). Most chemosensory proteins encoded by *che*Op$_2$ along with the MCPs form clusters at the cell poles, while proteins encoded by *che*Op$_3$ and the transducer-like proteins (TLPs) are found in the cytoplasm (Figure 8) (Mackenzie, Eraso, et al. 2007). The differentially localized proteins form two distinct signalling complexes, one polar and one cytoplasmic, enabling the cell to sense changes both outside and inside the cell, respectively (Porter, Wadhams and Armitage 2008).

The current working model of the *R. sphaeroides* chemotaxis pathway is shown in

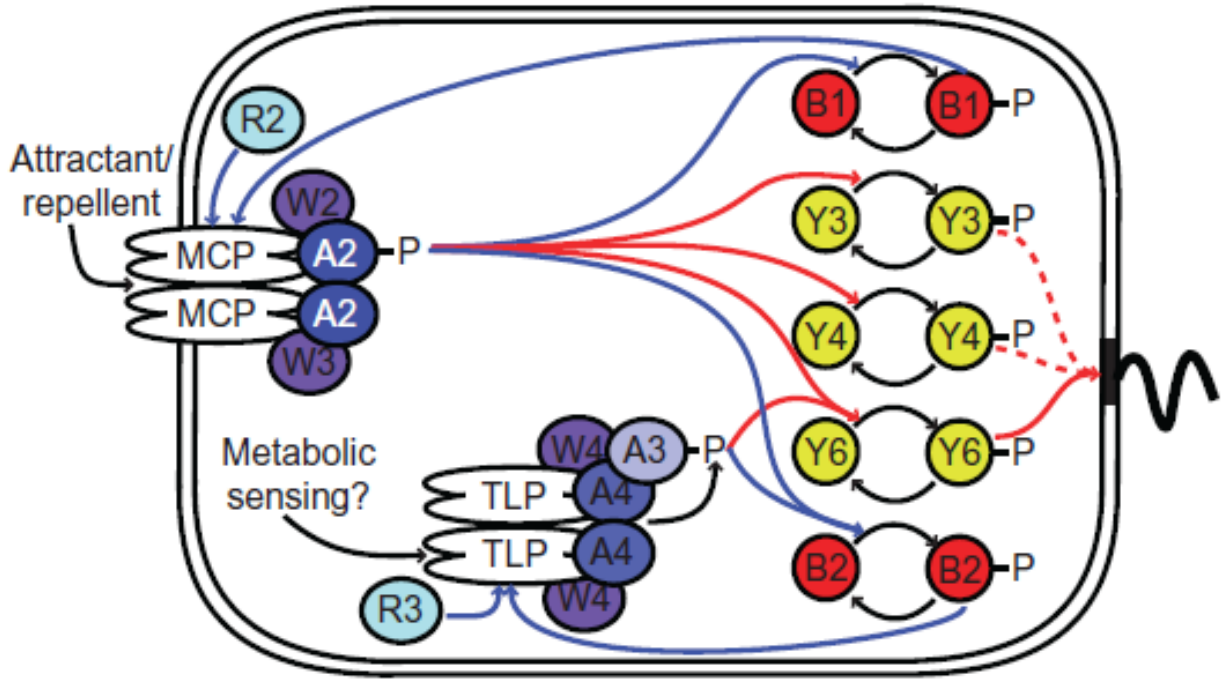


Figure 9: Diagram showing the chemosensory network of *R. sphaeroides*. Red arrows indicate control of flagellar rotation and blue arrows indicate adaptation processes. Figure taken from Scott, et al. 2010.

Figure 9. The polar cluster contains the proteins: $CheA_2$, $CheR_3$, $CheW_2$, $CheW_3$, and the MCPs. The cytoplasmic cluster contains the proteins $CheA_3$, $CheA_4$, $CheR_3$, $CheW_4$, and the TLPs. $CheB_1$ and $CheB_2$ are found dispersed in the cytoplasm (Wadhams, Warren, et al. 2003). The two pathways function together to control flagellar movement through $CheY_3$, $CheY_4$, and $CheY_6$.

1.3.2.4 MCPs in *R. sphaeroides*

R. sphaeroides has nine transmembrane MCPs: McpA, McpB, McpE, McpG, McpJ, McpH, McpM. McpR, and McpV. It also has four cytoplasmic TLPs: TlpC, TlpL, and TlpT. The deletion of either one of *mcpA*, *mcpB* (by deleting the entire *che*Op_1), or *mcpE* did not

produce chemotactic phenotypes (Ward, et al. 1995, Shah, et al. 2000, and Thompson 2005). Fluorescent tagging of McpG showed that this receptor localized to the cell poles, and deletion of *mcpG* did not result in a phenotype (Wadhams, Martin and Armitage 2000).

Deletion of *mcpH* abolishes chemotaxis, and McpH was shown to localize to the cell poles (Thompson 2005). McpJ was also found to be localized to the cell poles and *ΔmcpJ* cells exhibited a super-swarming phenotype (Mantotta 2002). Deletion of *mcpR* resulted in reduced chemotaxis, whereas the deletion of *mcpV* did not result in a chemotactic phenotype (Thompson 2005).

The deletion of *tlpC* from the *R. sphaeroides* genome abolished chemotaxis, and TlpC was found to be localized close to the centre of the cell (Wadhams, Martin and Porter, et al. 2002). Cells lacking TlpL showed reduced chemotaxis, while in *ΔtlpT* cells chemotaxis was abolished. TlpT was shown to localize in the cytoplasm (Thompson, Wadhams and Armitage 2006). Cells in which *tlpS* was deleted showed no apparent phenotype (Thompson 2005).

1.3.2.5 CheAs in *R. sphaeroides*

Deletion, localisation, and phosphorylation analyses have been used to determine the function of each CheA homologue in *R. sphaeroides*. A strain with an inactive homologue of the *cheA*$_1$ gene retained chemotaxis, and the normal behaviour of cells lacking a functional CheA$_1$ was further confirmed with *ΔcheA*$_1$ cells (Ward, et al. 1995 and Martin, Wadhams and

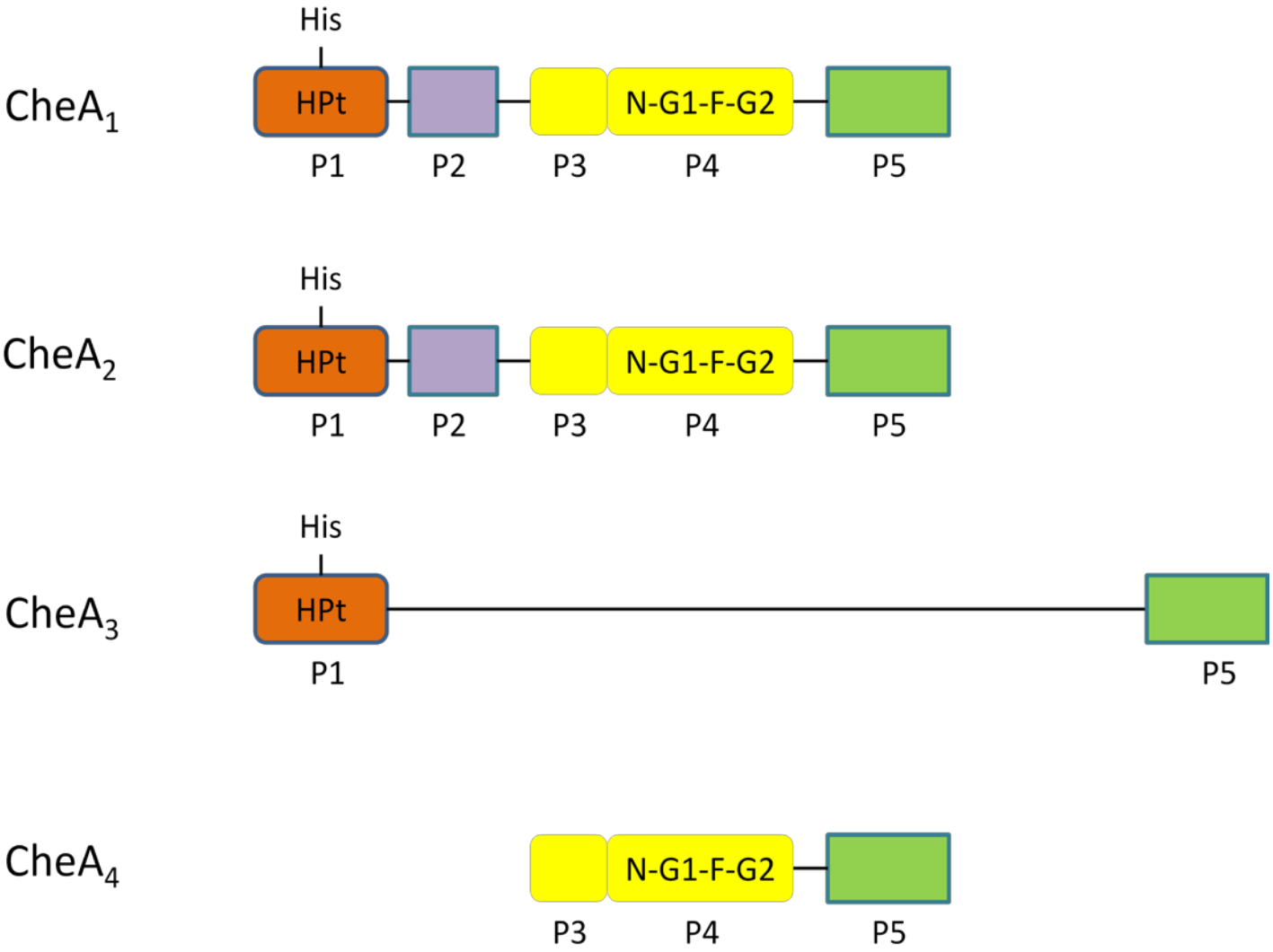


Figure 10: Domain organisation of *R. sphaeroides* CheAs. P1 is the phosphoryl-accepting domain, P2 is the RR binding domain, P3 is the dimerization domain, P4 is the CA domain, and P5 is the CheW-binding and regulatory domain. Figure adapted from Porter, Warren, et al. 2002.

Armitage 2001). $CheA_2$, $CheA_3$, and $CheA_4$ (along with the entire *che*Op_2 and *che*Op_3) were found to be essential for chemotaxis (Shah, et al. 2000, Martin, Wadhams and Armitage 2001 and Porter, Warren, et al. 2002). $CheA_2$ was found to be localized to the cell poles, while $CheA_3$ and $CheA_4$ localized in the cytoplasmic cluster (Wadhams, Warren, et al. 2003 and Martin, Usha, et al. 2003).

The domain of the four *R. sphaeroides* CheAs is shown in Figure 10. $CheA_1$ and $CheA_2$ resemble the prototypical *E. coli* CheA. $CheA_3$ lacks the domains P2-P4, while $CheA_4$ lacks domains P1-P2 (Porter, Warren, et al. 2002). *In vitro* studies have shown that $CheA_1$ could phosphorylate only the RRs that are encoded from *che*Op_1 and $CheY_3$, whereas $CheA_2$ could phosphorylate all of the eight RRs (Porter and Armitage 2002). Other *in vitro* studies demonstrated that $CheA_3$ associates with a $CheA_4$ homodimer and becomes phosphorylated by $CheA_4$ on H51. $CheA_3$-P can then subsequently phosphorylate only the RRs from *che*Op_3 and $CheY_1$ (Porter and Armitage 2004).

The middle region (residues 155-948) of $CheA_3$ was found to function as an aspartyl-phosphate phosphatase specific for $CheY_6$ (Porter, Roberts, et al. 2008). Domain swapping experiments involving $CheA_2$ and $CheA_3$ have shown that the P1 domain in these kinases determines which RRs they phosphorylate. The P5 domains of $CheA_2$, $CheA_3$, and $CheA_4$ determine their localisation at either the cytoplasmic or the polar cluster (Scott, et al. 2010).

1.3.2.6 CheWs in *R. sphaeroides*

Deletion analysis was used in previous studies to determine the functions of the four different CheW homologues in *R. sphaeroides*. Deletion of *cheW*$_1$ had no significant effect on chemotaxis or transmembrane receptor localisation under laboratory conditions. $CheW_2$ was found to be required for both MCP localisation and chemotaxis, whereas $CheW_3$ was required

for these functions only under photoheterotrophic conditions (Martin, Wadhams and Armitage 2001). The presence of $CheW_4$ was required for normal chemotaxis and cytoplasmic receptor localisation (Porter, Warren, et al. 2002).

1.3.2.7 CheYs in *R. sphaeroides*

In vivo experiments showed that two CheYs: $CheY_6$ plus either $CheY_3$ or $CheY_4$ is required for chemotaxis in *R. sphaeroides* (S. L. Porter, G. W. Wadhams, et al. 2006). Chemotaxis roles for the *che*Op_1-encoded RRs were not found, even though all six CheYs were able to bind to FliM *in vitro* (Ferre, et al. 2004). Some of the CheY homologues may not be able to stop flagellar rotation, and their binding to FliM could be to create competition against the homologues which can stop rotation (S. L. Porter, G. W. Wadhams, et al. 2006). The CheY homologues were mainly found to be dispersed throughout the cytoplasm, with some localisation of $CheY_3$ and $CheY_6$ in the cytoplasmic cluster and discrete localisation of $CheY_4$ in both the polar and cytoplasmic clusters.

1.3.2.8 Signal termination in *R. sphaeroides* chemotaxis

Because *R. sphaeroides* lacks a CheZ homologue, an alternative signal termination method has to be used. The rapid auto-dephosphorylation rate of $CheY_6$ could allow it to be used as a phosphatase, with $CheA_3$ accelerating its rate of dephosphorylation. Also, the remaining homologues of CheYs could be used as phosphate sinks (Porter, Wadhams and Armitage 2008).

1.4 Aims of the study

The aim of this study was to identify putative methylation sites on the *R. sphaeroides* chemoreceptors, and to observe the *in vivo* effects of mutating these sites on chemotaxis. The specific aims could be listed as:

- Identify putative methylation sites on all thirteen *R. sphaeroides* chemoreceptors
- Observe the effect of mutating these putative sites (both individually and in combinations) on the cytoplasmic TlpT receptor via chemotaxis assays.
- Perform a similar analysis on the transmembrane McpH receptor

2 Materials and Methods

2.1 Plasmids

Name	Description	Source
pUC19*che*Op$_3$	Plasmid containing part of *R. sphaeroides che*Op$_3$.	Steven L Porter*
pUC19	High copy number cloning vector. Ap^R	(Yanisch-Perron, Vieira and Messing 1985)
pUC19*tlpT*	The 2.4 kb region containing *tlpT* and upstream and downstream 500 bp (made by *Eco*RI/*Pst*I digestion of [pUC19*che*Op$_3$]) in pUC19.	This study
pUC19*tlpT*M$_0$	pUC19 containing *tlpT*(E96A)	This study
pUC19*tlpT*M$_2$	pUC19 containing *tlpT*(E296A)	This study
pUC19*tlpT*M$_3$	pUC19 containing *tlpT*(Q451A)	This study

pUC19*tlpT*M$_4$	pUC19 containing *tlpT*(Q475A)	This study
pUC19*tlpT*M$_5$	pUC19 containing *tlpT*(Q528A)	This study
pUC19*tlpT*M$_{12}$	pUC19 containing *tlpT*(Q261A, E296A)	This study
pUC19*tlpT*M$_{13}$	pUC19 containing *tlpT*(Q261A, Q451A)	This study
pUC19*tlpT*M$_{14}$	pUC19 containing *tlpT*(Q261A, Q475A)	This study
pUC19*tlpT*M$_{15}$	pUC19 containing *tlpT*(Q261A, Q528A)	This study
pUC19*tlpT*M$_{23}$	pUC19 containing *tlpT*(E296A, Q451A)	This study
pUC19*tlpT*M$_{24}$	pUC19 containing *tlpT*(E296A, Q475A)	This study
pUC19*tlpT*M$_{25}$	pUC19 containing *tlpT*(E296A, Q528A)	This study
pUC19*tlpT*M$_{34}$	pUC19 containing *tlpT*(Q451A, Q475A)	This study
pUC19*tlpT*M$_{35}$	pUC19 containing *tlpT*(Q451A, Q528A)	This study
pUC19*tlpT*M$_{45}$	pUC19 containing *tlpT*(Q475A, Q528A)	This study
pUC19*tlpT*M$_{123}$	pUC19 containing *tlpT*(Q261A, E296A, Q451A)	This study
pUC19*tlpT*M$_{124}$	pUC19 containing *tlpT*(Q261A, E296A, Q475A)	This study
pUC19*tlpT*M$_{125}$	pUC19 containing *tlpT*(Q261A, E296A, Q528A)	This study
pUC19*tlpT*M$_{134}$	pUC19 containing *tlpT*(Q261A, Q451A, Q475A)	This study
pUC19*tlpT*M$_{135}$	pUC19 containing *tlpT*(Q261A, Q451A, Q528A)	This study
pUC19*tlpT*M$_{145}$	pUC19 containing *tlpT*(Q261A, Q475A, Q528A)	This study
pUC19*tlpT*M$_{235}$	pUC19 containing *tlpT*(E296A, Q451A, Q528A)	This study
pUC19*tlpT*M$_{245}$	pUC19 containing *tlpT*(E296A, Q475A, Q528A)	This study
pUC19*mcpH*	The 2.7 kb region containing *mcpH* and upstream and downstream 500 bp (made by *Eco*RI/*Hind*III digestion of region PCR amplified from WS8N genome) in pUC19.	This study

pUC19*mcpH*M$_1$	pUC19 containing *mcpH*(Q295A)	This study
pUC19*mcpH*M$_3$	pUC19 containing *mcpH*(E308A)	This study
pUC19*mcpH*M$_4$	pUC19 containing *mcpH*(Q455A)	This study
pUC19*mcpH*M$_{44}$	pUC19 containing *mcpH*(Q455A, Q456A)	This study
pUC19*mcpH*M$_5$	pUC19 containing *mcpH*(Q462A)	This study
pUC19*mcpH*M$_{55}$	pUC19 containing *mcpH*(Q461A,Q462A)	This study
pUC19*mcpH*M$_6$	pUC19 containing *mcpH*(Q469A)	This study
pK18*mobsacB*	Allelic exchange suicide vector mobilized by *E. coli* S17-1*λpir*. Km^R Suc^S	(Schäfer, et al. 1994)
pK18*tlpT*M$_0$	Construct for replacing *tlpT* with *tlpT*(E96A) in *R. sphaeroides* genome. pK18*mobsacB* derivative	This study
pK18*tlpT*M$_2$	Construct for replacing *tlpT* with *tlpT*(E296A) in *R. sphaeroides* genome. pK18*mobsacB* derivative	This study
pK18*tlpT*M$_3$	Construct for replacing *tlpT* with *tlpT*(Q451A) in *R. sphaeroides* genome. pK18*mobsacB* derivative	This study
pK18*tlpT*M$_4$	Construct for replacing *tlpT* with *tlpT*(Q475A) in *R. sphaeroides* genome. pK18*mobsacB* derivative	This study
pK18*tlpT*M$_5$	Construct for replacing *tlpT* with *tlpT*(Q528A) in *R. sphaeroides* genome. pK18*mobsacB* derivative	This study

Table 2: Plasmids used in the study are listed above. For the *2*- and *3*-combinations of the *tlpT* mutants *University of Exeter

2.2 Strains

2.2.1 *E. coli*

The *E. coli* strains used in the study are listed in Table 3.

Name	Description	Source
XL-1 Blue	General cloning strain and expression host, Tet^R	Stratagene
DH5α	General cloning strain and expression host, Nal^R	(Woodcock, et al. 1989)
S17-1λ*pir*	Strain capable of mobilizing the suicide vector pK18*mobsacB* into *R. sphaeroides*, Sm^R	(Penfold and Pemberton 1992)

Table 3: *E. coli* strains used in the study are listed above.

2.2.2 *R. sphaeroides*

The *R. sphaeroides* strains used in this study are given in Table 4.

WS8N	Spontaneous Nal^R mutant of wild-type WS8	(Sockett, Foster and Armitage 1990)
JPA1331	*ΔtlpT* derivative of WS8N. Non-chemotactic	(Porter, Warren, et al. 2002)
JPA1213	$CheY_{6\ (D56N)}$ mutant of WS8N. Non-motile, non-chemotactic, and with increased stopping frequency	(S. L. Porter, G. W. Wadhams, et al. 2006)
JPA1036	$TlpT_{(Q96A)}$ mutant of WS8N	This study
JPA1037	$TlpT_{(Q451A)}$ mutant of WS8N	This study
JPA1038	$TlpT_{(Q475A)}$ mutant of WS8N	This study
JPA1039	$TlpT_{(Q528A)}$ mutant of WS8N	This study

Table 4: *R. sphaeroides* strains used in the study are listed above.

2.3 Growth conditions

Antibiotic concentrations used in this study are shown in Table 5.

Antibiotic	**Working concentration (µg/ml)**	
	E. coli	***R. sphaeroides***
Ampicillin	100	-
Kanamycin	25	25
Nalidixic acid	20	20
Tetracyclin	20	1
Streptomycin	25	50

Table 5: Antibiotics and their concentrations used in the study are listed. Solutions were filter sterilised and stored at -20°C.

2.3.1 Liquid cultures of *E. coli*

L-broth (A2.8) was inoculated with single colonies of *E. coli*. Liquid cultures containing the appropriate antibiotics were grown at 37°C with shaking.

2.3.2 Agar plates for *E. coli* growth

The agar plates were made from L-broth (A2.8) solidified with 2% agar. Appropriate antibiotics were added after melting the LB-Agar. Plates were incubated overnight at 37°C for *E. coli* growth.

2.3.3 Aerobically grown *R. sphaeroides*

R. sphaeroides strains were grown aerobically in succinate medium (A2.1) containing nalidixic acid with lateral shaking (2 cm distance, 210 shakes per minute) at 30°C in the dark.

2.3.4 Photoheterotrophically grown *R. sphaeroides*

Strains were grown in succinate medium (A2.1) containing nalidixic acid in full sealed bottles at 30°C in a light cabinet (Don Whitley Scientific) under bright, non-fluorescent light (35 μM m^{-2} s^{-1}).

2.3.5 Agar plates for *R. sphaeroides*

Plates were made with L-broth (A2.8) 2% agar containing nalidixic acid and other appropriate antibiotics. Sucrose selection was made with M22 (minimal medium, A2.5) containing 10% (w/v) sucrose solidified with 2% (w/v) agar. Plates were incubated at 30°C for 48 hours.

2.3.6 Storage of bacterial cells

Bacterial strains were grown to stationary phase in liquid culture with appropriate antibiotics and then mixed in a ratio of 3:2 with sterile 50% (v/v) glycerol in a cryotube (Starstedt). Tubes containing culture were flash frozen in liquid nitrogen and stored immediately at -80°C.

2.4 Genetic techniques

2.4.1 Extraction of *R. sphaeroides* genomic DNA

Chromosomal DNA was extracted from cultures grown aerobically for 48 hours or photoheterotrophically overnight, using the protocol of Giuliano, *et al.* 1988. 1.5 ml of cells was harvested by centrifugation, and the pellet was snap frozen in liquid nitrogen. The pellet was then resuspended in 0.5 ml of 65°C lysis buffer (A2.9), 1 mg of proteinase K was added,

and the mixture was incubated at 42°C for 2 hours. The DNA was twice extracted with 0.5 ml of phenol:chloroform:isoamyl alcohol (25:24:1) using grease tubes. The DNA was then precipitated with 1 ml of 100% (v/v) ethanol at -20°C for at least 30 minutes. The samples were centrifuged at 13,300 x g for 30 minutes, the supernatant was poured off, and the DNA pellet was washed with 70% (v/v) ethanol. The pellet was the dried overnight at 37°C and resuspended with 50 µl of sterile water.

2.4.2 Agarose gel electrophoresis

DNA fragments were separated by size in 0.8% (w/v) agarose (Roche) gels made with ½ x TBE solution (A2.7). 5 x DNA loading dye (A2.6) was added to each sample. Gels were run at 90-140 V, stained with ethidium bromide (EtBr) solution (1 ng/ml) for 20 minutes and viewed over a UV transilluminator.

2.4.3 Extraction of DNA from TBE agarose gels

The QIAquick Gel Extraction kit (Qiagen) was used to extract DNA from the excised gel fragments following the manufacturers' protocol. 30 µl of MilliQ water heated to 65°C was used in elution.

2.4.4 Polymerase Chain Reactions (PCRs)

PCR reactions were carried out in Techgene, TC-3000 or TC3000G thermal cyclers (Techne).

2.4.4.1 Standard PCR for cloning

Amplification of the region containing *mcpH* and the upstream and downstream 500 bp (Figure 11) was carried out using *Pfu* DNA polymerase (Promega) with the following mixture:

1 µl of template DNA
1 µl of each of the two appropriate primers at 100 µM
5 µl of 2.5 mM dNTPs
5 µl of 10 x *Pfu* polymerase buffer (Promega)
1 µl (2 U) of *Pfu* DNA polymerase (Promega)
2.5 µl of DMSO

The mixture was made up to 50 µl with MilliQ. The following PCR cycle was used:

Initial denaturation	98°C	10 min	
Denaturation	98°C	2 min	30 cycles
Annealing	68°C	1 min 30 sec	
Extension	72°C	6 min	
Final extension	72°C	12 min	

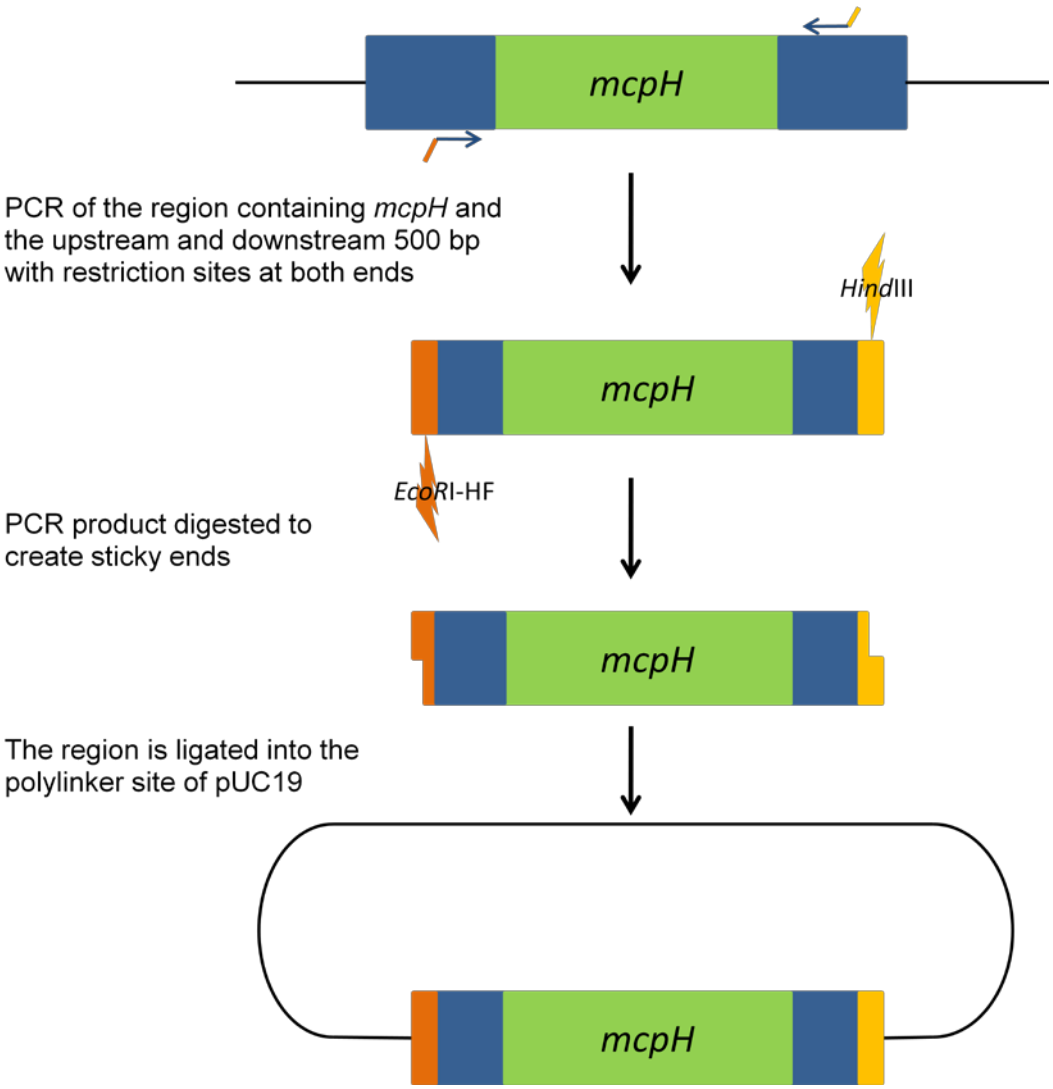


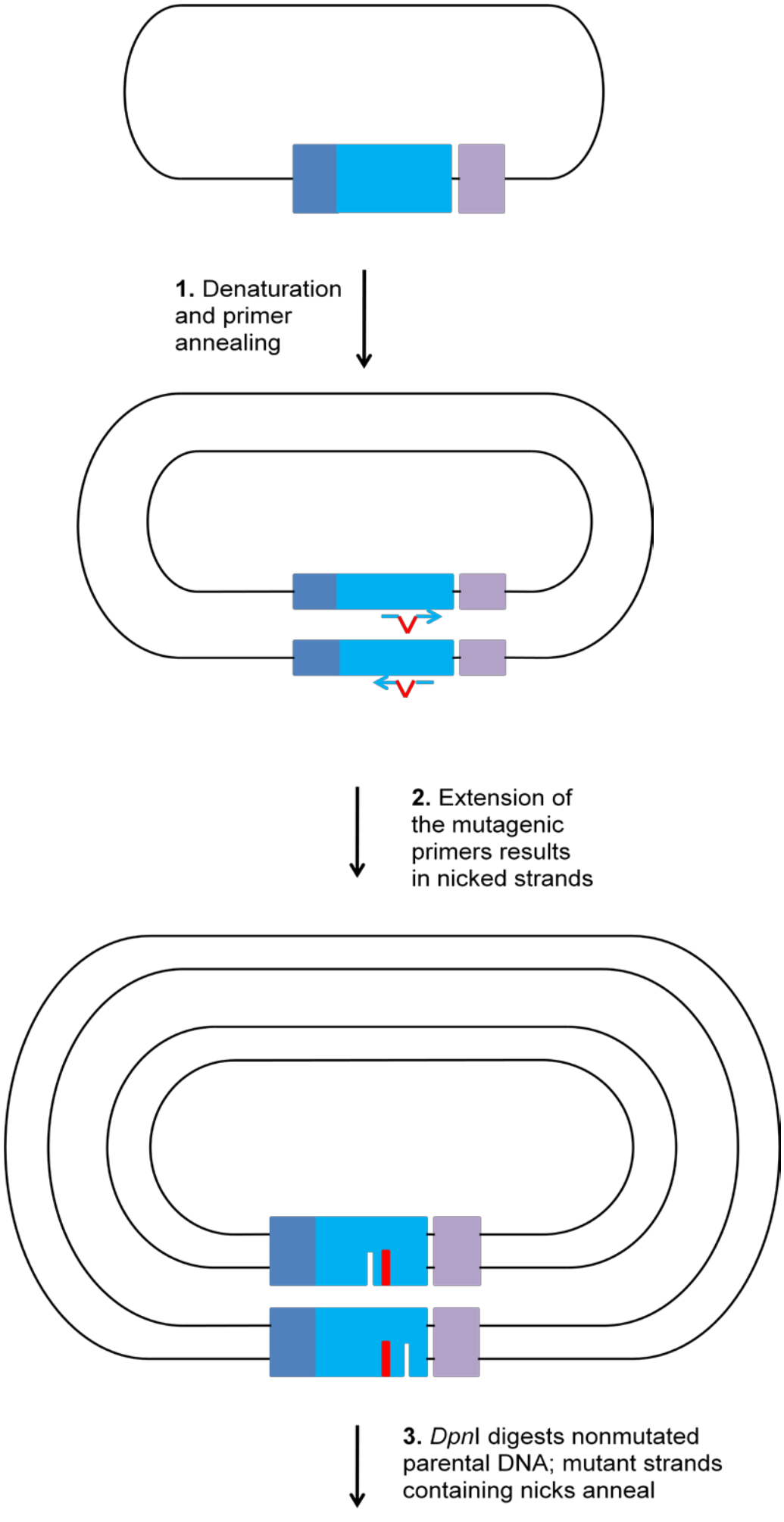
Figure 11: Construction of pUC19 based cloning construct containing the *mcpH* gene.

2.4.4.2 QuikChange mutagenesis PCR

The following conditions were used for QuikChange mutagenesis in each 50 µl reaction: 5-50 ng of template DNA, 125 ng of each primer, 0.25 mM of each dNTP, 1 x *Pfu* polymerase buffer (Promega), and 1 µl (2 U) of *Pfu* DNA polymerase (Promega). The following PCR program was used:

Initial denaturation	98°C	5 min	
Denaturation	98°C	30 sec	18 cycles
Annealing	55°C	1 min	
Extension	72°C	11 min	
Final extension	72°C	5 min	

Each reaction tube was digested with 1 µl (10 U) of *Dpn*I at 37°C for 1 hour to digest the non-mutated (parental) plasmid DNA (Figure 12). Mutant strands synthesised during the PCR cycle anneal after transformation into competent *E. coli* cells (2.4.8).


1. Denaturation and primer annealing
2. Extension of the mutagenic primers results in nicked strands
3. DpnI digests nonmutated parental DNA; mutant strands containing nicks anneal

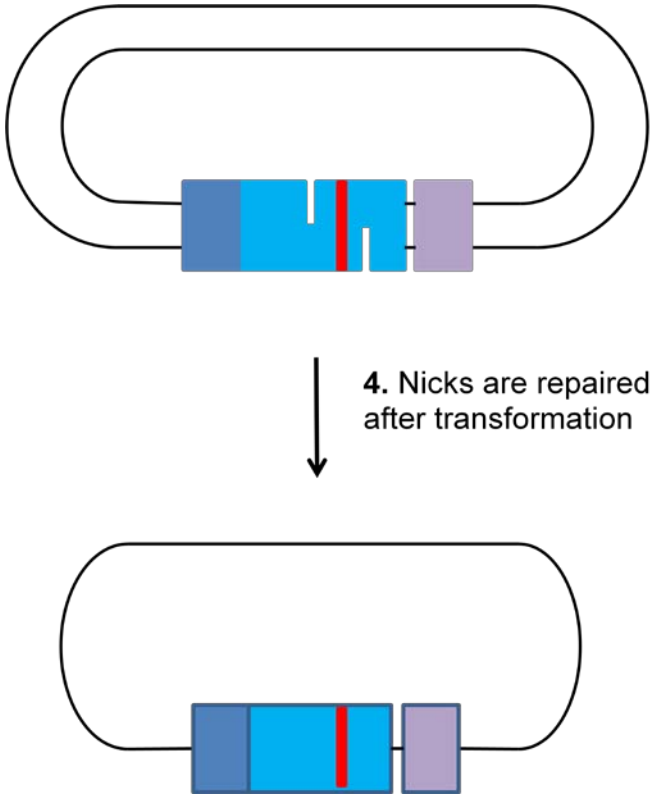


Figure 12: QuikChange mutagenesis. **(1)** Heating allows the denaturation of the plasmid and oligonucleotides containing the desired mutation anneal. **(2)** The *Pfu* DNA polymerase extends the mutagenic primers which results in the formation of nicked circular strands. **(3)** The *Dpn*I enzyme digests the methylated, nonmutated parental DNA template, and the mutant strands containing nicks anneal. **(4)** Nicks in the mutated plasmid are repaired after transformation into XL-1 cells, to give a plasmid containing mutant *tlpT* and the upstream and downstream regions.

2.4.5 Restriction enzyme digests

Restriction digests were carried out according to the manufacturers' instructions for at least two hours at 37°C in final reaction volumes of 20 µl or 50 µl; containing 1 x buffer and 2 or 10 U of BSA as required. Regions containing genes of interest amplified with the standard PCR for cloning (2.4.4.1) were restriction digested with appropriate enzymes to be inserted into pUC19 cut with the same enzymes.

2.4.6 Dephosphorylation of plasmid DNA

To prevent re-ligation of the vector with two identical ends, the 5' phosphate groups were removed by treatment with calf intestinal alkaline phosphatase (CIP, New England Biolabs). Restriction enzymes in the digest mixture were heat inactivated at 65°C (or 85°C depending on the enzyme) for 20 minutes, cooled to room temperature, and then 5-10 Units of CIP was added. The mixture was incubated for 1 hour at 37°C.

2.4.7 DNA ligations

Cohesive end ligations were performed at 16°C for at least 16 hours using T4 DNA ligase (Invitrogen) according to the manufacturer's instructions. A final reaction volume of 50 µl was used with 1 x T4 DNA ligase buffer (Invitrogen) and 1 U of T4 DNA ligase. Several insert to vector ratios were used (1:1, 2:1, 3:1, 4:1) while keeping the overall insert + vector concentration between 1-10 ng/µl. pUC19 based construct containing mutated insert was cut out with appropriate restriction enzymes (2.4.5) and ligated into pK18*mobsacB* digested with the same enzymes (Figure 13).

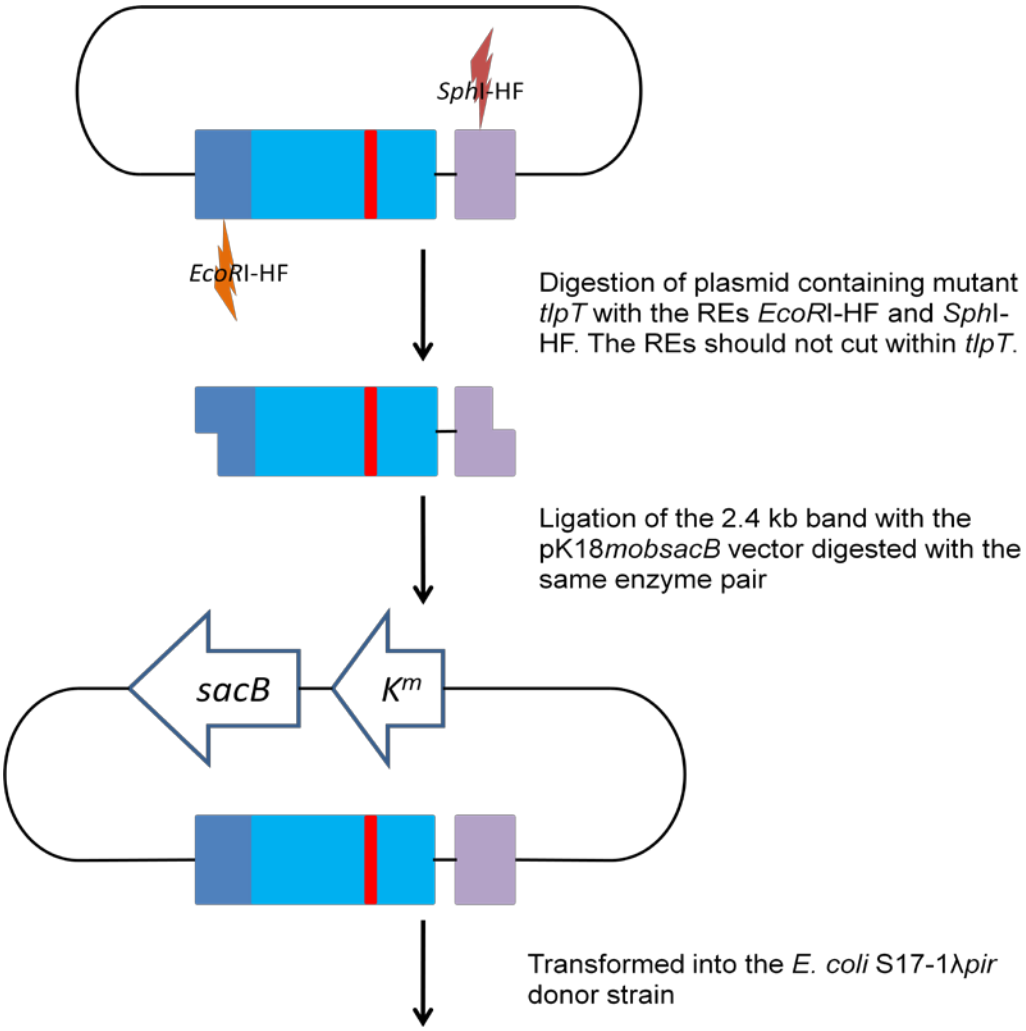


Figure 13: Construction of pK18*mobsacB* based mutant insertion construct

2.4.8 Competent cells

E. coli cells were made competent using the Hanahan Method.

2.4.9 Transformation of plasmid DNA into *E. coli*

DNA was incubated with 200 µl of competent *E. coli* cells on ice for 1 hour, and the cells were heat shocked at 42°C for 90 sec and put immediately back on ice for another 90 sec. 1 ml of L-broth was added to each tube and cells were incubated at 37°C for 1 hour to allow for the expression of antibiotic resistance genes. Cells were spread plated as per 2.3.2.

2.4.10 Plasmid preparations

Overnight liquid cultures of plasmid-containing *E. coli* were used for the preparations. Preparations were made by using either the HiSpeed Midi or Maxi Kits (Qiagen), eluting with 500 µl of MilliQ, or the QIAprep Spin Miniprep Kit (Qiagen) according to the manufacturers' instructions. The recovered DNA was stored at -20°C.

2.5 Gene insertion strategy

2.5.1 Insertion constructs

Genomic PCR was used to amplify a region containing the gene of interest and the spanning 500 bp. Primers were designed to incorporate restriction sites at both ends of the region. The region was digested with the appropriate enzymes. The pUC19 cloning vector was digested with the same enzymes and de-phosphorylated to prevent re-ligation. The region containing the gene was cloned in. pUC19 containing insert was subjected to QuikChange mutagenesis.

After the mutagenesis, pUC19 vector containing mutant insert was digested with the appropriate restriction enzymes, and the mutant insert was purified (2.4.3). the purified insert

was ligated into pK18*mobsacB*, which was digested with the same enzymes, dephosphorylated, and purified (2.4.6 and 2.4.7).

2.5.2 Conjugations

Plasmids are introduced into *R. sphaeroides* by conjugation from the donor *E. coli* strain S17-1λ*pir*. *E. coli* S17-1λ*pir* cells were made competent as per 2.4.8 and transformed with the pK18*mobsacB* based plasmid containing the mutant gene insert (2.4.9). *R. sphaeroides* cells were mixed with early log phase S17-1λ*pir* cells in a ratio of 10:1. The mixture was pipetted onto a nitrocellulose filter on an LBA plate and the plate was incubated at 30°C overnight. The cells were than washed off from the filter with L-broth and plated onto LBA plates containing nalidixic acid and kanamycin to select for transconjugants containing the pK18*mobsacB* based insertion construct (Figure 14.1).

2.5.3 Selection for 2nd round recombination

Single colonies were grown in succinate media containing Nal for 2 days at 30°C, and then plated onto M22 10% sucrose plates (2.3.5) to select for the second round recombinants that have lost the *sacB* gene. Cells which still contain *sacB* produce the SacB protein which converts sucrose into the toxic levansucrose. Sucrose resistant colonies were replica plated onto LBA/Nal/Kan and LBA/Nal plates to select for colonies that have lost Kanamycin resistance. Southern blotting with labelled fragment from *che*Op$_3$ as a probe was used to distinguish between the two possible outcomes of the second round recombination (Figure 14.2).

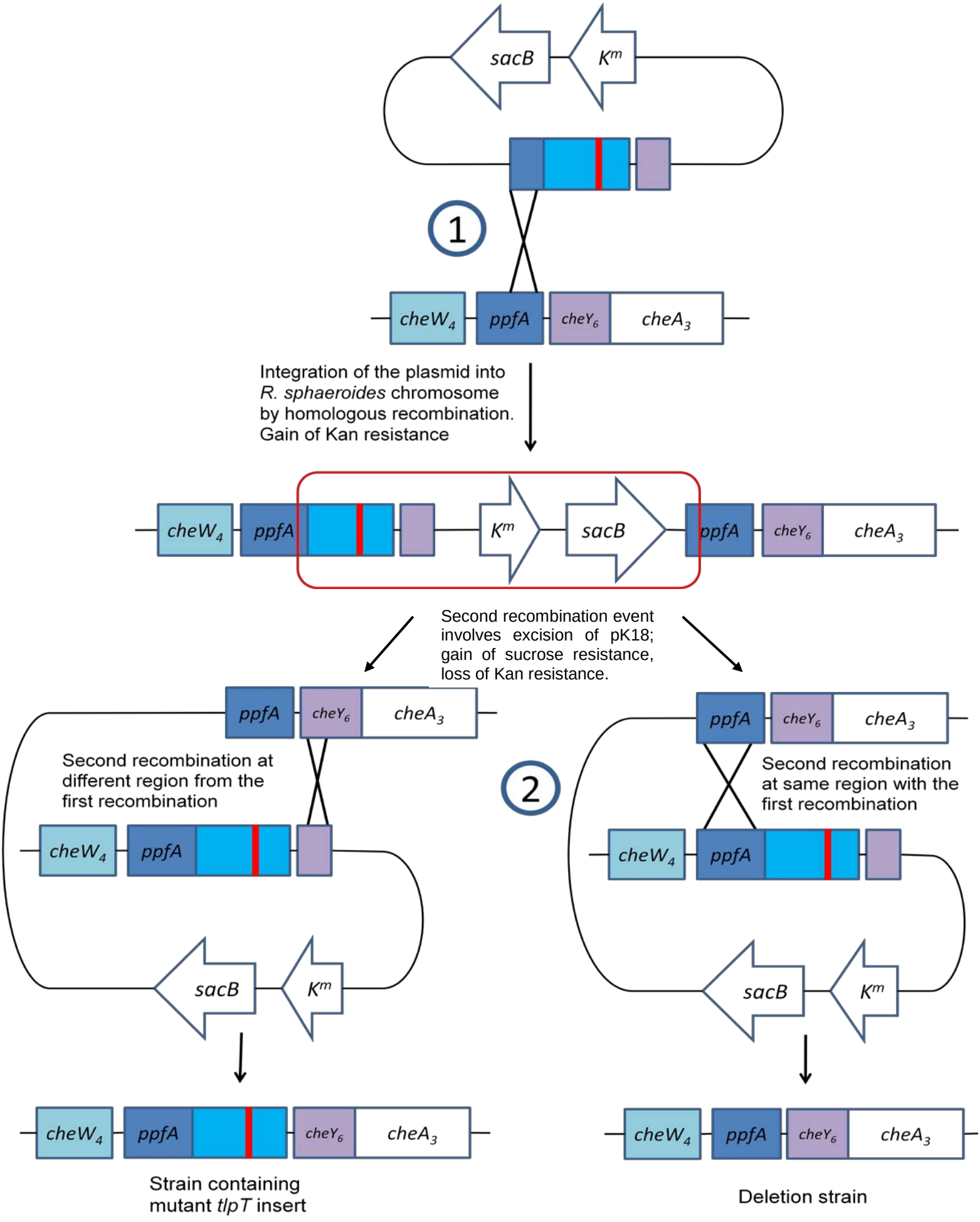


Figure 14: The double recombination method. **(1)** During the first round, the entire pK18*mobsacB* based construct is integrated into the genome of *R. sphaeroides* JPA1331 by homologous recombination. This confers kanamycin resistance. **(2)** In the second round, the vector is lost and either the original deletion strain or the strain with mutant *tlpT* insert is formed. The *sacB* gene and K^m are lost. The blue region with red line indicates *tlpT* containing the E/Q→ A mutation. Figure adapted from Porter, Wadhams and Armitage 2007.

2.5.4 DNA sequencing

Sequencing results were analyzed with the Clone Manager Software (Scientific & Educational Software version 9).

2.5.5 Preparation of labelled DNA probes

The plasmid pUC19*che*Op$_3$ was digested with the restriction enzymes *Pst*I and *Eco*RV (2.4.5) and the 1 kb band was extracted (2.4.3). The DNA was denatured at 98°C for 10 minutes and then labelled using the random hexanucleotide primers technique with the DIG DNA labelling kit (Roche), using the manufacturers' instructions.

2.5.6 Southern blots

Chromosomal DNA digested with the *Sph*I-HF enzyme overnight (2.4.5), was separated by electrophoresis on a 0.8% agarose gel at 100 Volts (2.4.2). The gel was denatured, neutralized, and capillary blotted onto Hybond-N membranes (Sambrook and Russell 2001). The membrane was dried on Whatman paper and then UV fixed. It was then pre-hybridised with hybridisation solution at 68°C, and hybridised and with DIG labelled probe (2.5.5) at 68°C overnight. The bound probe was detected using anti-digoxigenin-alkaline-phosphatase and the BCIP-NBT redox system according to the manufacturers' instructions.

2.6 Phenotypic techniques

2.6.1 Swarm plates

Swarm plates are used to measure bacterial motion. The semi-solid agar in the swarm plates was made with autoclaved M22 0.25% (w/v) agar. Chemoattractants were used at 100 µM concentration and nalidixic acid was added. The plates were left to set for at least two hours on the bench. 5 µl of photoheterotrophically grown (2.3.4) stationary phase culture was pipetted onto a single spot on the swarm plate. Motile bacteria swim outwards from the inoculation spot to generate a ring, which can then be measured. Plates were incubated 48 hours at 30°C for aerobically, or photoheterotrophically at 28°C.

2.6.2 Tethered cell analysis

Cells were tethered to a glass coverslip using anti-flagellar (α-FliC) antibody, and the coverslip was placed to a miniature flow cell (Berg and Block 1984). The stop and start behaviour of the flagellar motor can be observed by varying the chemoattractant concentration in fixed time intervals. The immobilised flagellum causes the cell to rotate, which can then be analysed under the light microscope.

Cells were grown aerobically (2.3.3), and at log phase, 1 ml of cell culture was spun down at 6,000 rpm for 3 min. Cells were washed 3 x with 1 ml of 10 mM HEPES + Chloramphenicol (30 µg/ml). In a humidity chamber, 10 µl of the gently resuspended cells were incubated with 0.5 µg of α-FliC antibody for 20-30 min on a small coverslip with edges sealed with L-grease (Apiazon). The flow cell was assembled with a large coverslip sealed on the edges with M-grease placed in the back. Buffer was syringed through the apparatus,

making sure all air bubbles were removed. The small coverslip with containing the cells was inverted onto the flow cell. The behaviour of tethered cells in response to HEPES buffer or HEPES buffer + propionate (100 µM) was video recorded under phase contrast with 40X magnification.

Camera recordings of tethered cells were analysed using the Arot7 software from Hobson tracking systems. The rotation rate for the each tracked cell was recorded every 50 ms for 15 min. The sampler program (Tom Downs, Oxford University) was used to average the data over 100 values. Average plots of the tracks of several cells were drawn using Excel.

2.7 Bioinformatics techniques

2.7.1 Multiple sequence alignments

Multiple sequence alignments were made using the online ClustalW2 tool (http://www.ebi.ac.uk/Tools/clustalw2/) using the default parameters (Larkin, et al. 2007). The Gonnet matrix with a gap opening penalty of 10.0 and a gap extension penalty of 0.2 was used.

2.7.2 InterProScan

Possible domains within receptors were identified for further analysis using the InterProScan tool, EMBL-EBI (http://www.ebi.ac.uk/Tools/InterProScan/ - Zdobnov and Apweiler 2001).

3 Results

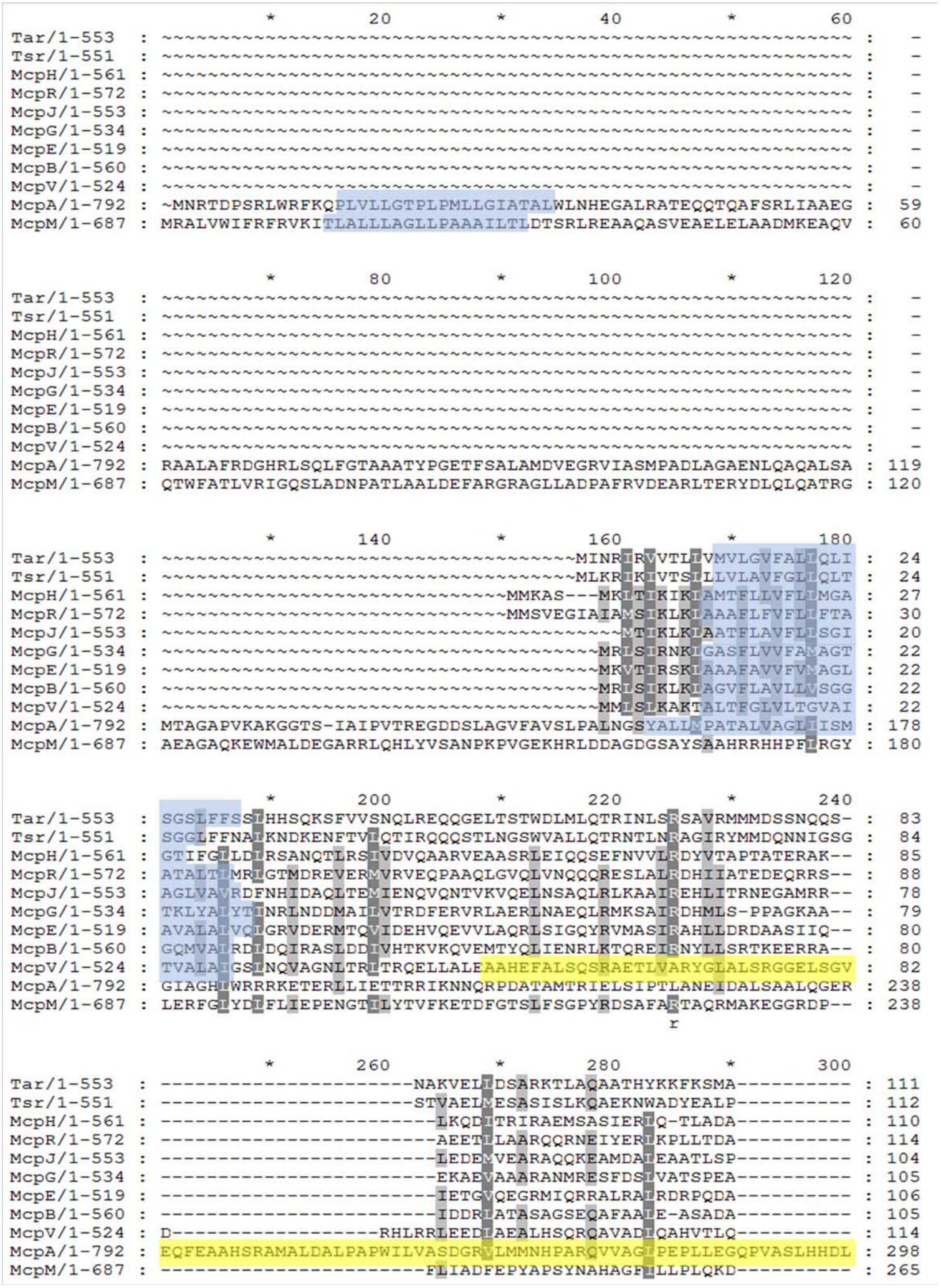
3.1 Bioinformatics results

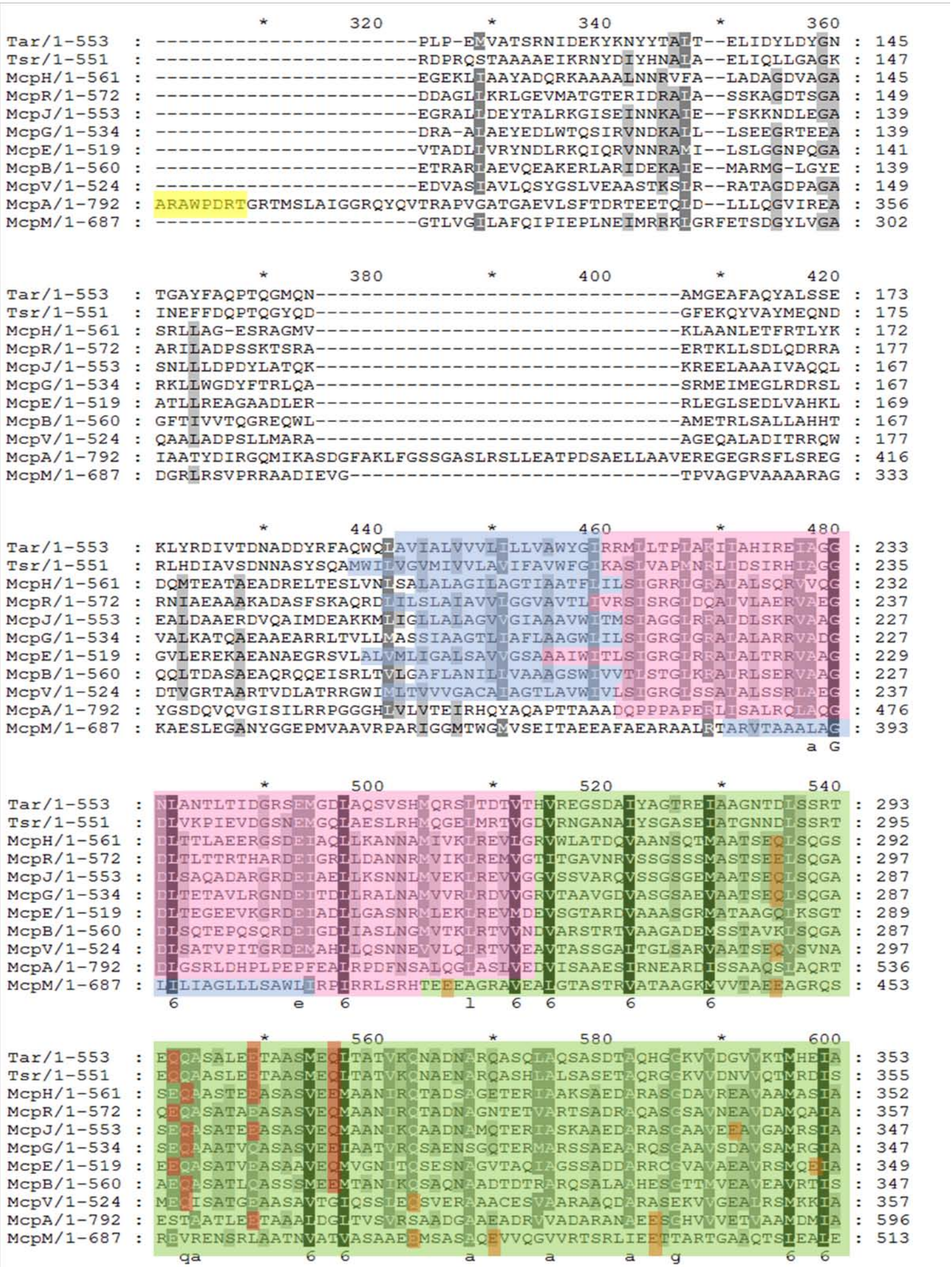
3.1.1 MCPs

The multiple sequence alignment of *Rhodobacter* MCPs with those of *E. coli* Tar and Tsr is shown in Figure 15. The functional domains in the alignment are shaded with different colours. Experimentally determined methylation sites on *E. coli* receptors and their corresponding E/Q residues on *R. sphaeroides* receptors are shown in red. Putative methylation sites have been identified in all of the thirteen chemoreceptors of *R. sphaeroides*.

In the *R. sphaeroides* receptors, all of the second of two consecutive E/Q residues within the MCP regions (light green) were designated as putative methyl-accepting sites. These remaining putative residues are shown in orange (Figure 15). Some of these orange residues are conserved across both organisms; some are conserved only within *R. sphaeroides* receptors; and some are not conserved and exist only on one *R. sphaeroides* receptor.

Eight E/Q-E/Q sites have been identified in the methylation region of McpH, three of which are homologous with the known methylation sites in *E. coli*. The homologous residues (Q295, E301, and E308) are located to the left of the HCD region. The other putative sites on McpH are: Q287, E360, Q455, Q462, and Q469.




Tar/1-553
Tsr/1-551
McpH/1-561
McpR/1-572
McpJ/1-553
McpG/1-534
McpE/1-519
McpB/1-560
McpV/1-524
McpA/1-792
McpM/1-687

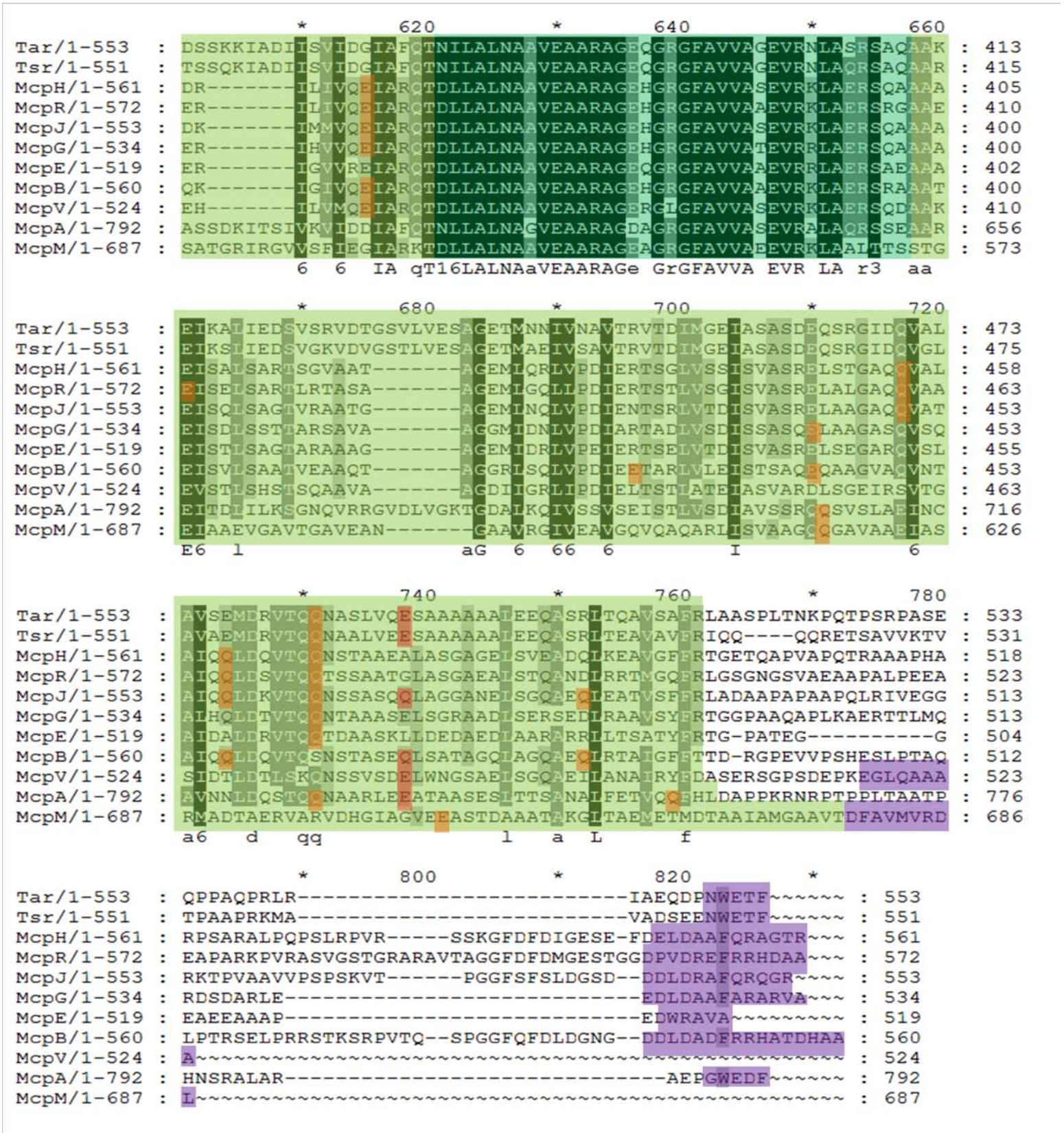
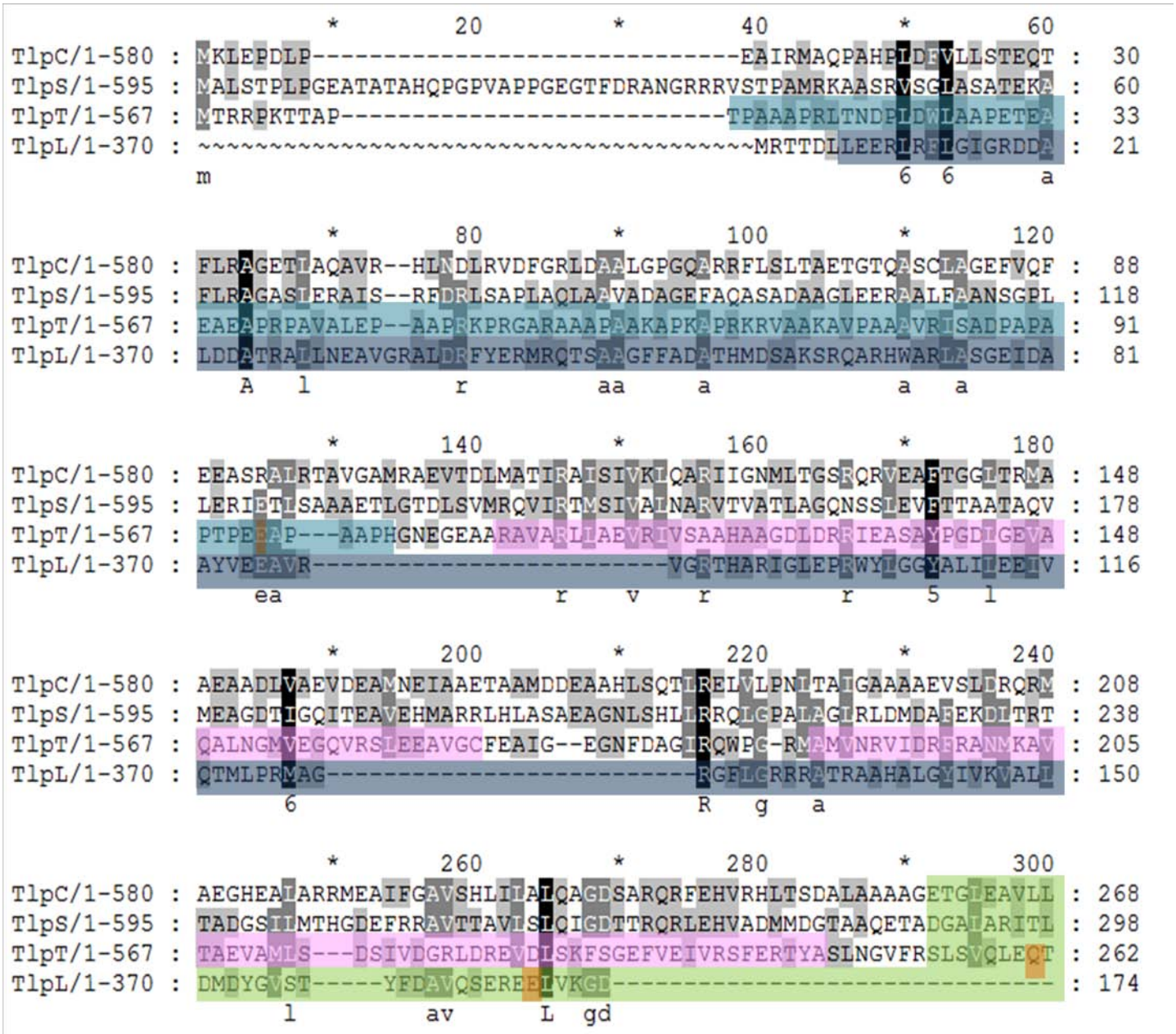


Figure 15: Alignment of the nine *R. sphaeroides* MCPs with the *E. coli* MCPs Tar and Tsr. Residues that have been experimentally determined to be methylation sites on *E. coli* receptors and the corresponding putative methylation residues on *R. sphaeroides* MCPs are shaded red. *R. sphaeroides* receptors contain additional E/Q-E/Q sites in their methylation regions, in which the second E/Q could be a methylation site. These putative sites are shaded orange. Transmembrane regions are shaded blue, HAMP domains are shaded pink, methylation regions are shaded light green, the HCD is shaded green, and the conserved C-terminal region is shaded purple. Yellow shading indicates the PAS domain in McpA. Sequences were aligned using the ClustalW2 program (http://www.ebi.ac.uk/Tools/msa/clustalw2/). Black shading indicates all highly conserved residues; dark grey shading indicates sequences that are conserved 80% or more, light grey shading indicates sequences that are conserved 60% or more.

3.1.2 TLPs

The multiple sequence alignment of TLPs from *R. sphaeroides* is shown in Figure 16. The functional domains in the alignment are shaded with different colours. The second of two consecutive E/Q residues within the MCP (methylation) regions (light green) were designated as putative methyl-accepting sites (pink).



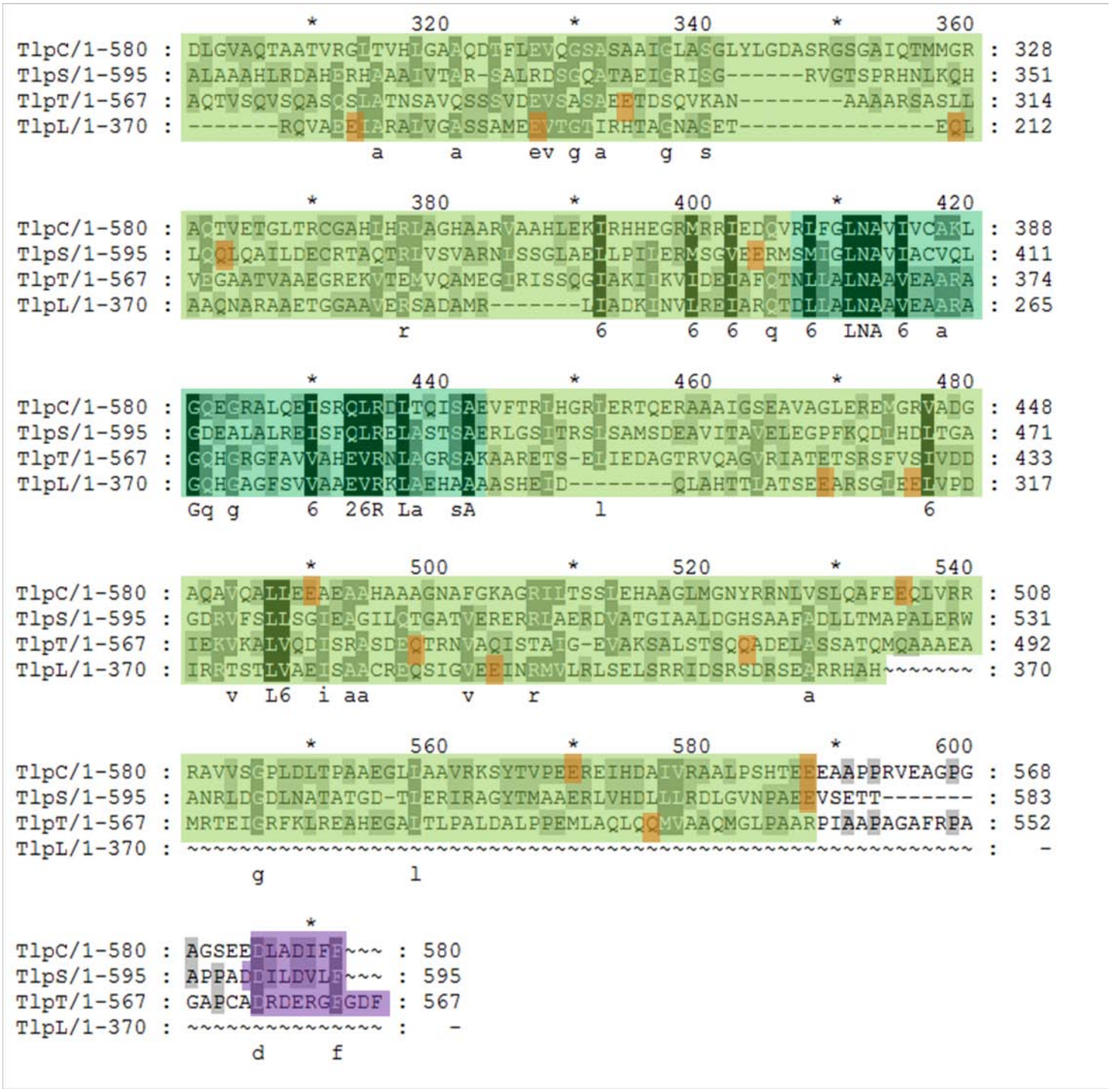


Figure 16: Alignment of the four *R. sphaeroides* TLPs. Putative methylation E/Q are shaded orange, methylation regions are shaded light green, the HCD is shaded green, and the conserved C-terminal region is shaded purple. In TlpT, HAMP domains are shaded pink and the N-terminal sensory domain is shaded aqua. The control site E96 is indicated with dark orange. The globin domain in TlpL is shaded dark blue. Sequences were aligned using the ClustalW2 program (http://www.ebi.ac.uk/Tools/msa/clustalw2/). Black shading indicates all highly conserved residues; dark grey shading indicates sequences that are conserved 80% or more, light grey shading indicates sequences that are conserved 60% or more.

Most of these putative methylation sites are not conserved among the TLPs; they are scattered throughout the methylation regions of individual receptors. Putative HAMP domains were not detected in the sequence searches for TlpC, TlpL, and TlpS; however the corresponding sequences in these proteins for the HAMP domains in TlpT are likely to have a similar function.

Five putative methylation sites have been identified on the methylation regions of TlpT, and were designated sites 1-5 from upstream to downstream. A separate site (E96) not located in the methylation region (located upstream of the HAMP domains) was designated as site 0. The effect of the mutation E96A was also tested as a control that is outside the methylation region.

3.2 QuikChange mutagenesis and the insertion of mutant chemoreceptors

Two receptors, one from each cluster, which give a non-chemotactic phenotype when deleted, were initially selected for further mutational analysis: the cytoplasmic TlpT and the polar McpH.

3.2.1 TlpT

A region of *che*Op$_3$ containing *tlpT* and the surrounding genes, previously cloned into pUC19 was supplied by Dr. S. L. Porter (Exeter). This construct (pUC19*che*Op$_3$) and the pUC19 cloning vector were digested with the enzymes *Eco*RI and *Pst*I. The host pUC19 was dephosphorylated to prevent re-ligation. The 2.4 kb band resulting from the digest of and pUC19*che*Op$_3$, which contains *tlpT* and the upstream and downstream 500 bp, was extracted

(2.4.3). The cut pUC19 vector was dephosphorylated and the *tlpT* region was cloned in (sections 2.4.6 and 2.4.7, Figure 17).

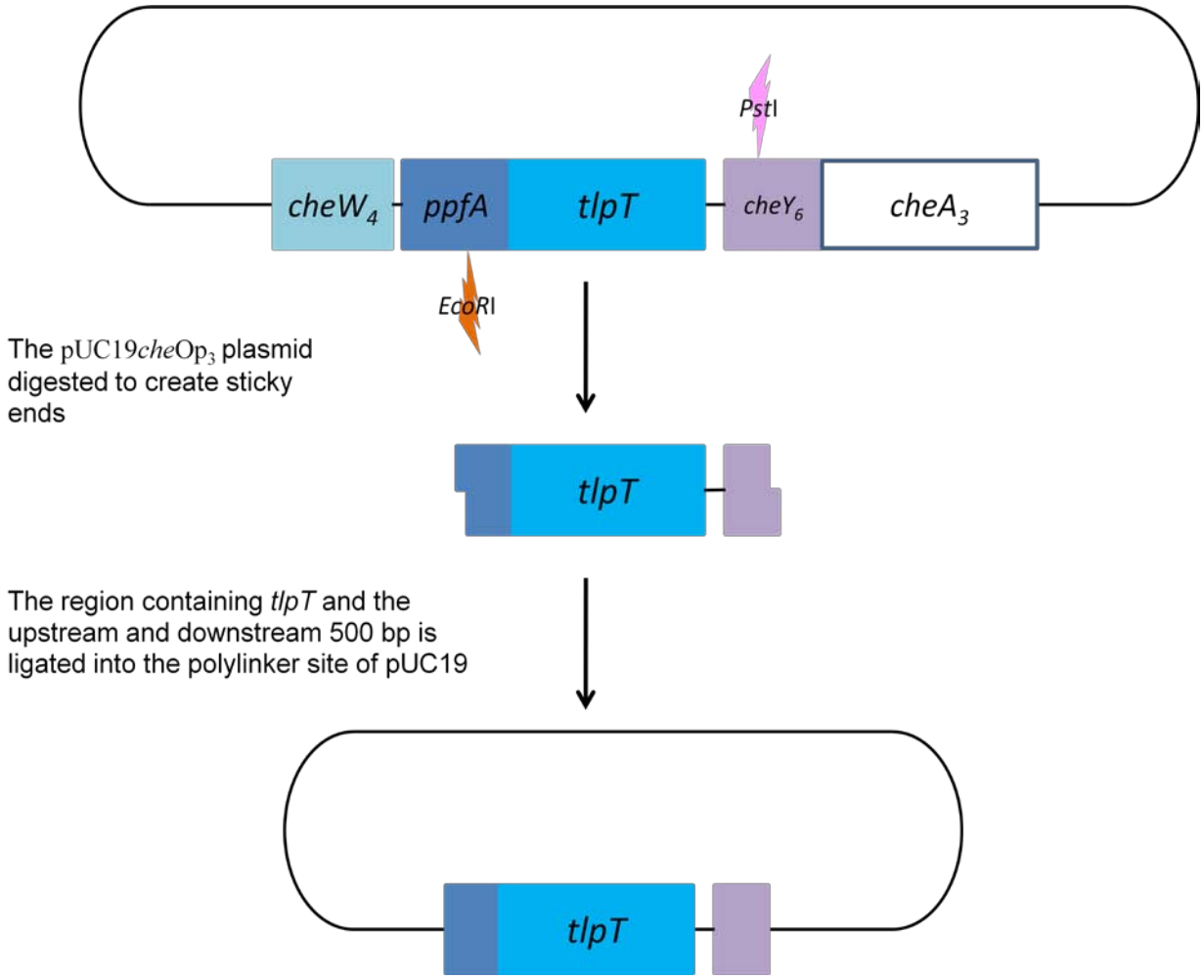


Figure 17: Construction of pUC19 based cloning construct.

The resulting plasmid, pUC19*tlpT*, was subjected to QuikChange PCR using a primer pair that converts a putative methylation site codon (Glu or Gln) to an Ala codon (2.4.4.2). Alanine was picked because of its inability to accept methyl groups and because its side chain is tiny and non-polar; which makes it unlikely to cause a disruption in the 3D structure of the receptor. Five mutant constructs, each containing a single mutant (E/Q → A) site, were made (pUC19*tlpT*M$_0$, pUC19*tlpT*M$_2$, pUC19*tlpT*M$_3$, pUC19*tlpT*M$_4$, pUC19*tlpT*M$_5$). The entire

inserted region was sequenced to confirm the presence of the desired mutation and to check for any unwanted mutations.

All of the ten *2*-combinations of the putative sites 1-5 were made with QuikChange PCR using the constructs containing one mutant site as templates (2.4.4.2). Eight out of ten of the *3*-combinations were made using the *2*-combinations as templates. For the resulting combinatorial mutants, only the regions containing the desirable mutations were sequenced for confirmation.

The mutant inserts inside pUC19 were digested with the enzymes *Eco*RI-HF and *Hind*III, or with *Eco*RI-HF and *Sph*I-HF. The pK18*mobsacB* suicide vector was digested with the same enzyme pair and dephosphorylated to prevent re-ligation, and the mutant inserts were cloned in (2.4.7). The insertion constructs pK18*tlpT*$M_{0,}$ pK18*tlpT*M_2, pK18*tlpT*M_3, pK18*tlpT*M_4, and pK18*tlpT*M_5 were generated in this manner. Cloning of the rest of the mutant *tlpT* inserts into pK18*mobsacB* was not successful.

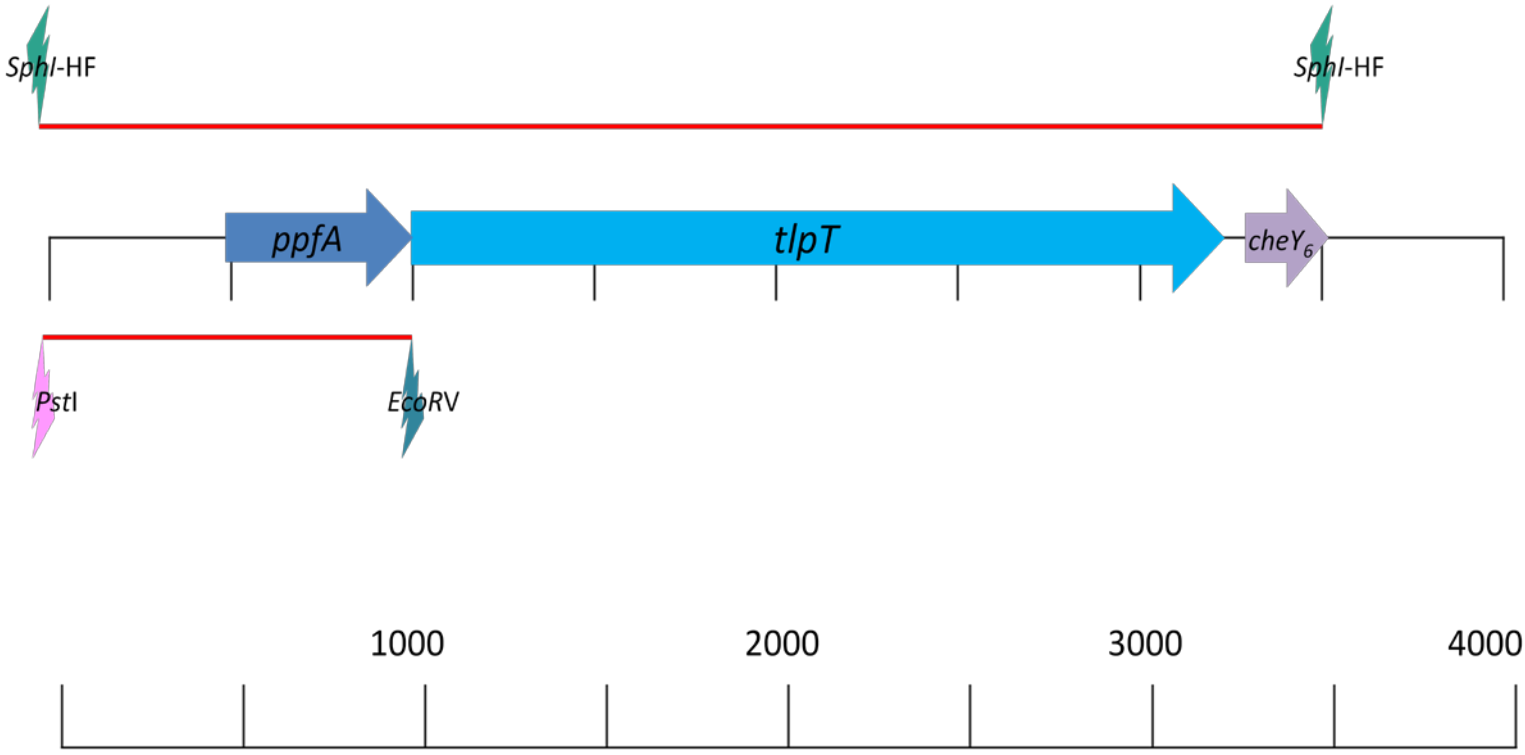


Figure 18: The region of *che*Op$_3$ containing *tlpT* and the surrounding genes. The region indicated by the red line with *Pst*I and *Eco*RV restriction sites was used to produce a DNA probe the Southern blots. The *Sph*I-HF sites used to identify mutant tlpT insertion strains are also shown on the top red line. Scale bar showing number of DNA bases, bottom.

The insertion constructs were introduced into *R. sphaeroides* JPA1331 (*ΔtlpT*) via the donor strain S17-1*λpir* for conjugal transfer. Double recombinants in which mutant *tlpT* was inserted into the genome were confirmed by Southern blot analysis using a DIG labeled DNA probe generated from the *Pst*I and *Eco*RV fragment upstream of *tlpT* in pUC19*che*Op$_3$ (Figure 18).

The *ΔtlpT* strain JPA1331 digested with *Sph*I-HF gave a band of size 1.8 kb, and strains that inserted a mutant *tlpT* molecule gave a band that corresponded to a fragment size of 3.5 kb. The strains which incorporated mutant inserts from the constructs pK18*tlpT*M$_0$, pK18*tlpT*M$_3$, pK18*tlpT*M$_4$, and pK18*tlpT*M$_5$ were designated JPA1036 (Figure 19A), JPA1037 (Figure 19B), JPA1038 (Figure 19C), and JPA1039 (Figure 19D), respectively. The mutant *tlpT* insert from pK18*tlpT*M$_2$ was not incorporated into the genome of JPA1331 in any of the colonies that were tested.

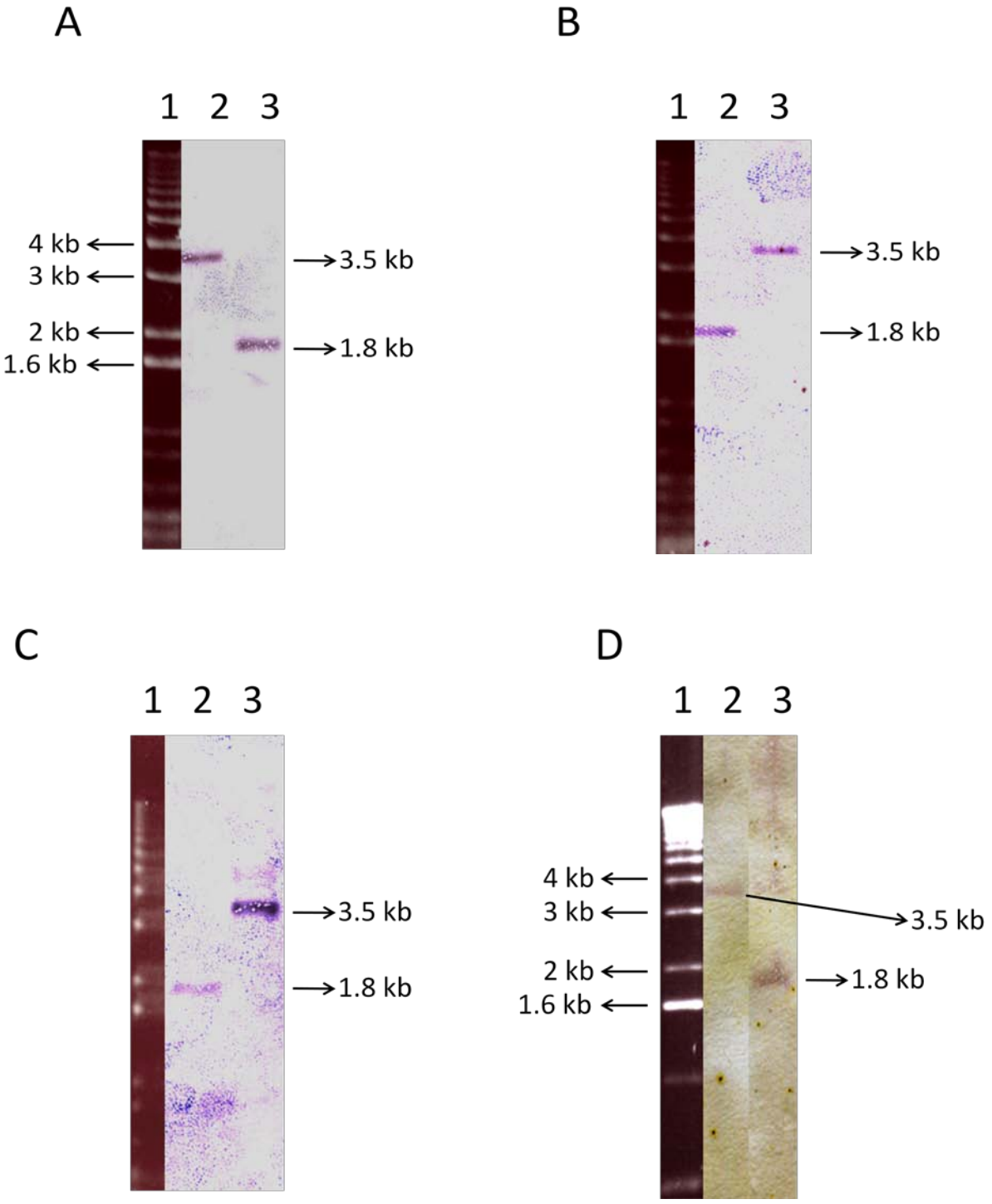


Figure 19: Southern blots confirming insertions of *tlpT* mutants into the genome of the *ΔtlpT* strain JPA1331. Chromosomal DNA was digested with *Sph*I-HF and the probe used was generated from the upstream portion of *tlpT* in *che*Op$_3$. **(A)** A 1 kb+ DNA ladder (Lane 1) and corresponding Southern blot confirming the insertion of *tlpT*M$_0$ into the chromosome of JPA1331. There is a 3.5 kb band showing a successful insertion strain (Lane 2), and a 1.8 kb band showing the original deletion strain (Lane 3). **(B)** A 1 kb+ DNA ladder (Lane 1) and corresponding Southern blot confirming the insertion of *tlpT*M$_3$ into the chromosome of JPA1331. There is a 1.8 kb band showing the deletion strain (Lane 2), and a 3.5 kb band showing the successful insertion of *tlpT*M$_3$ (Lane 3). **(C)** A 1 kb+ DNA ladder (Lane 1) and corresponding Southern blot confirming the insertion of *tlpT*M$_4$ into the chromosome of JPA1331. There is a 1.8 kb band showing the deletion strain (Lane 2), and a 3.5 kb band showing the successful insertion of *tlpT*M$_4$ (Lane 3). **(D)** A 1 kb DNA ladder (Lane 1) and corresponding Southern blot confirming the insertion of *tlpT*M$_5$ into the chromosome of JPA1331. There is a 3.5 kb bands showing the successful insertion of *tlpT*M$_5$ (Lane 2), and a 1.8 kb band showing the deletion strain (Lane 3).

3.2.2 McpH

Genomic PCR was used to amplify the region containing *mcpH* and the and the upstream and downstream 500 bp. Primers were designed to incorporate an *Eco*RI site upstream of the region and a *Hind*III site downstream of the region. The amplified region was digested with *Eco*RI and *Hind*III. The pUC19 cloning vector was digested with the same enzymes and dephosphorylated to prevent re-ligation. The region containing *mcpH* was cloned in to create the plasmid pUC19*mcpH*, and this construct was subjected to QuikChange mutagenesis.

Five constructs, each having one putative methylation site mutation (E/Q → A), were produced: pUC19*mcpH*M_1, pUC19*mcpH*M_3, pUC19*mcpH*M_4, pUC19*mcpH*M_5, and pUC19*mcpH*M_6. Two more constructs were made using primer pairs that mutated both of the consecutive Glu/Gln residues in a putative site to Ala. These constructs, pUC19*mcpH*M_{44} and pUC19*mcpH*M_{55}, were made to compare the effect of mutating a single E/Q residue to mutating both E/Q residues.

The mutant insert was digested with the enzymes *Eco*RI-HF and *Hind*III. The pK18*mobsacB* vector was digested with the same enzymes and dephosphorylated to prevent re-ligation, and the mutant insert was attempted to be cloned in. None of the ligations involving the mutant *mcpH* inserts were successful. Therefore, no mutant strains were produced.

3.3 Phenotypic results

3.3.1 Swarm plates of TlpT mutants

The chemotactic ability of the strains containing putative methylation site mutations in TlpT were compared to the wild type WS8N, *ΔtlpT* JPA1331 (non-chemotactic strain), and $CheY_{6(D56N)}$ JPA1213 (non-motile strain) in swarm plate assays (Figure 20). The $TlpT_{(E96A)}$ mutant did not result in a significant difference in phenotype under aerobic conditions, although a larger swarm size was observed in more recent plates. $TlpT_{(E96A)}$ resulted in a smaller swarm size under photoheterotrophic conditions. The $TlpT_{(Q451A)}$ mutant did not result in a significant difference in phenotype under either aerobic or photoheterotrophic growth conditions (Figure 21 andFigure 22).

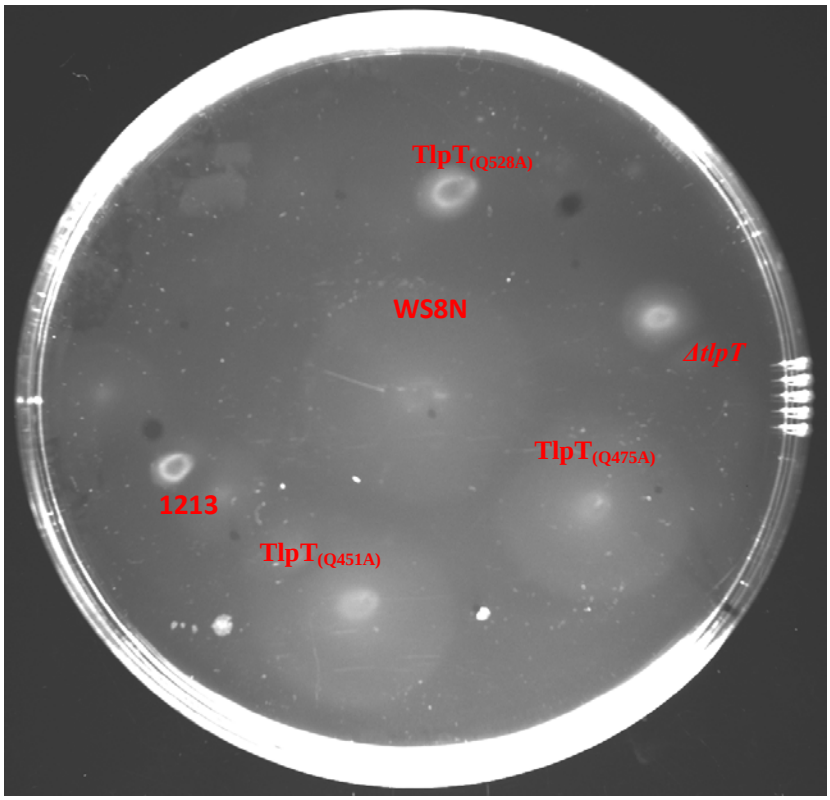


Figure 20: Photo of a propionate plate taken after 48 hours of aerobic growth.

The $TlpT_{(Q475A)}$ mutant resulted in a swarm size smaller than the wild-type under aerobic conditions in most of the tested attractants. Under anaerobic conditions, the swarm size of $TlpT_{(Q475A)}$ was still smaller than wild type (WS8N) strain, but the difference between $TlpT_{(Q475A)}$ and the *ΔtlpT* was larger.

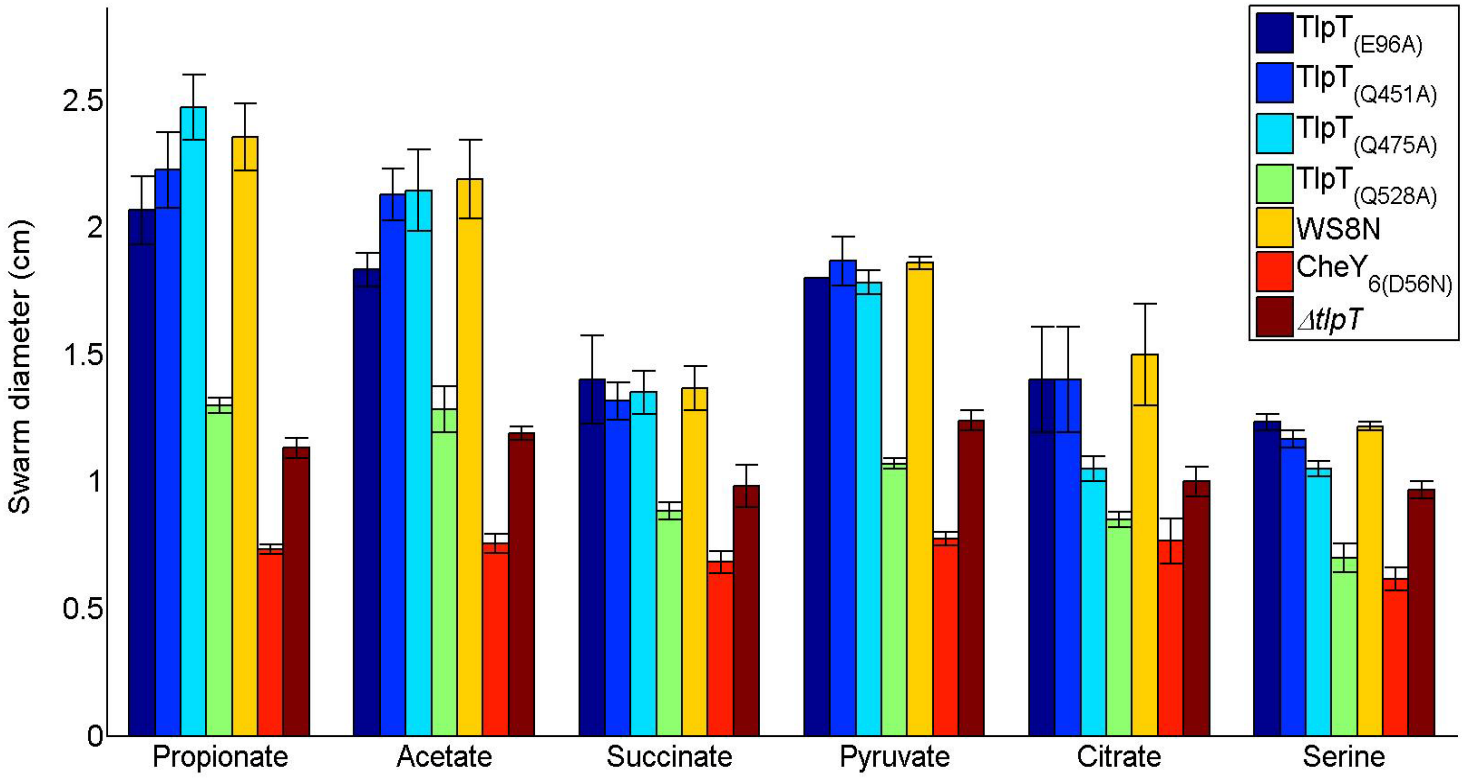


Figure 21: Swarm diameters of WS8N, *ΔtlpT* (JPA1331), $CheY_{6(D56N)}$ (JPA1213), $TlpT_{(E96A)}$, $TlpT_{(Q451A)}$, $TlpT_{(Q475A)}$, and $TlpT_{(Q528A)}$ after 48 hours under aerobic conditions. Results are the mean of at least nine data points. Error bars represent +/- one standard error of the mean.

The $TlpT_{(Q528A)}$ mutant showed a swarm size slightly larger than the *ΔtlpT* strain under aerobic growth conditions, and a slightly smaller swarm size under photoheterotrophic conditions. In both conditions, the swarm size of $TlpT_{(Q528A)}$ was larger than that of the $CheY_{6(D56N)}$ strain.

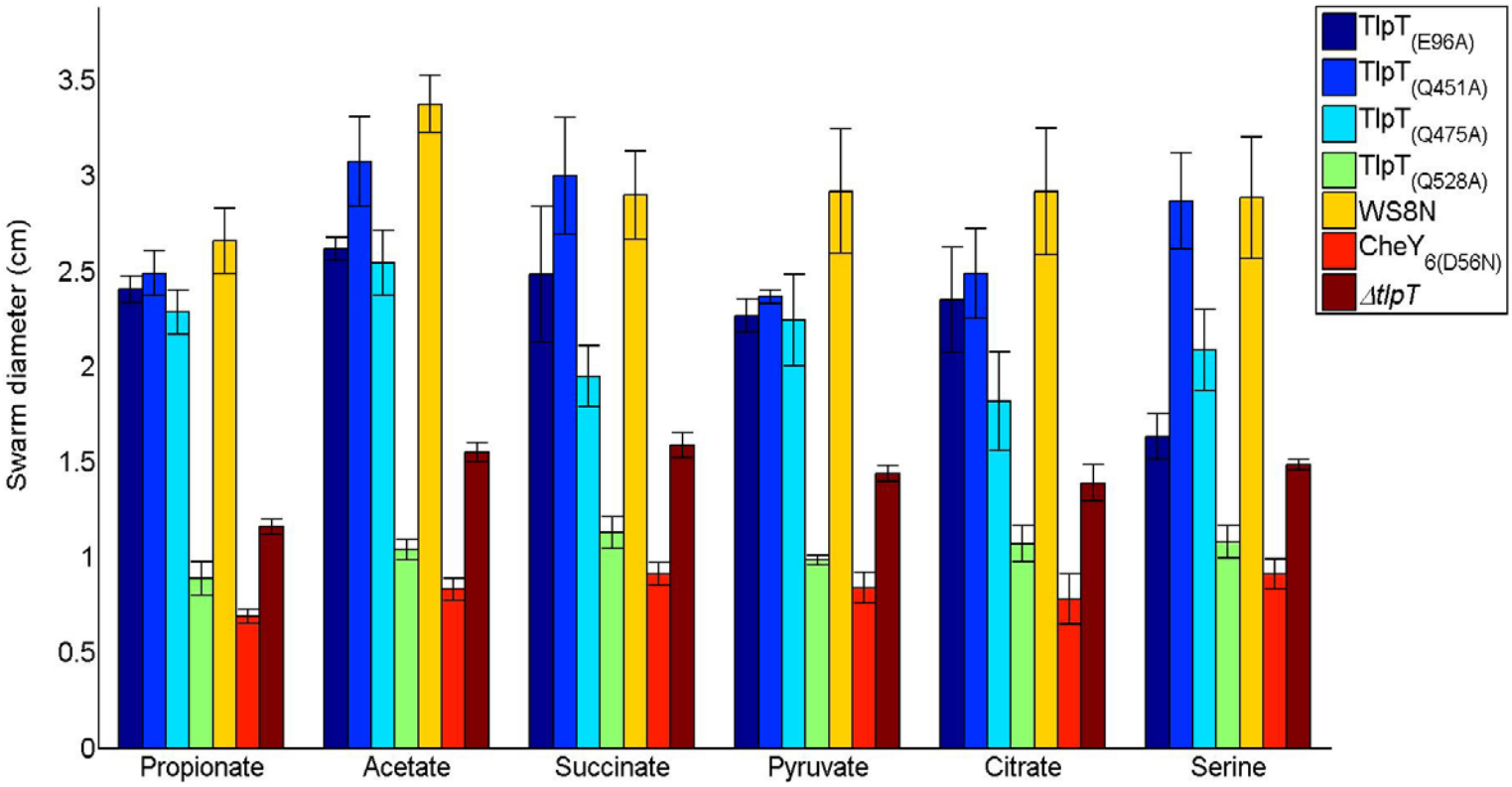
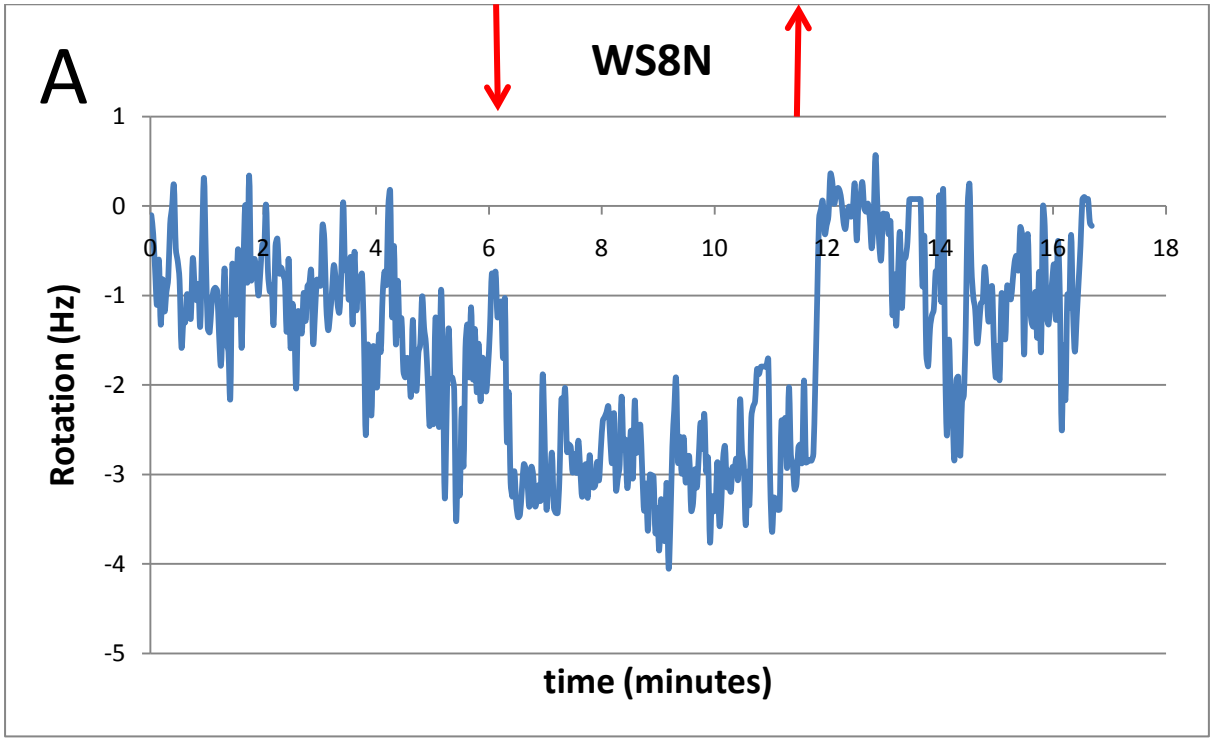


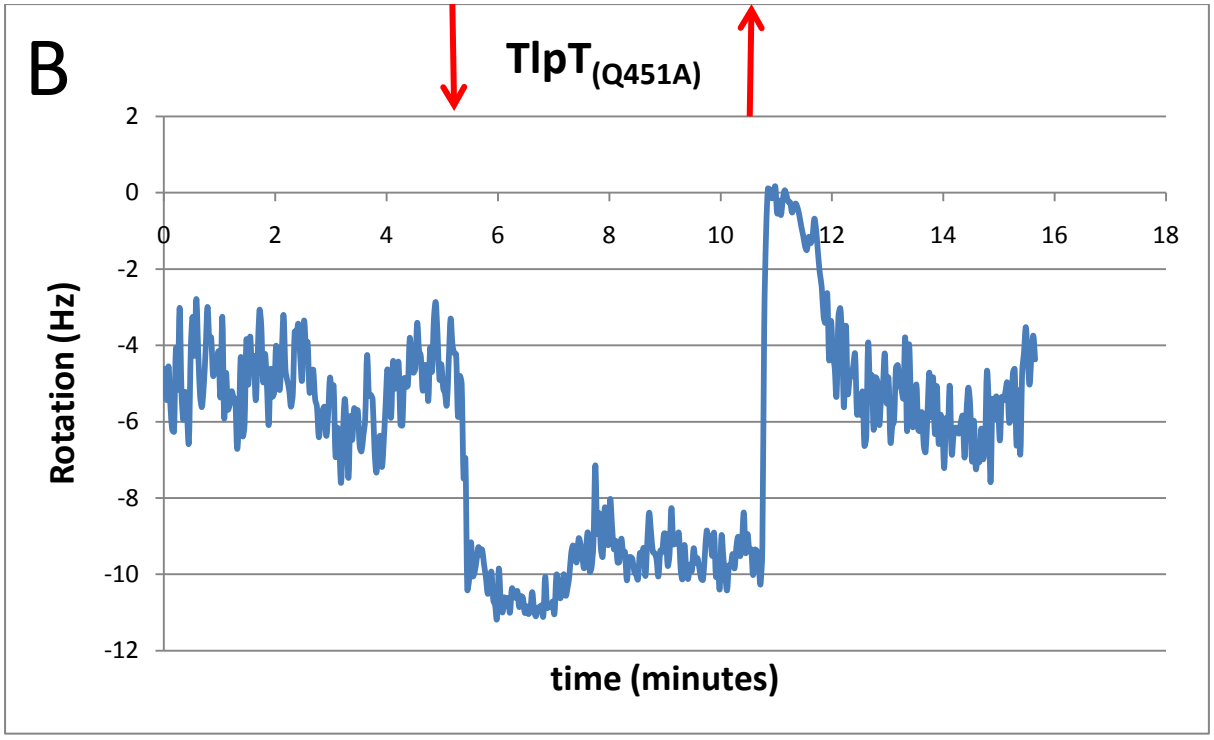
Figure 22: Swarm diameters of WS8N, *ΔtlpT* (JPA1331), $CheY_{6(D56N)}$ (JPA1213), $TlpT_{(E96A)}$, $TlpT_{(Q451A)}$, $TlpT_{(Q475A)}$, and $TlpT_{(Q528A)}$ after 48 hours under anaerobic conditions. Results are the mean of six-twelve data points. Error bars represent +/- one standard error of the mean.

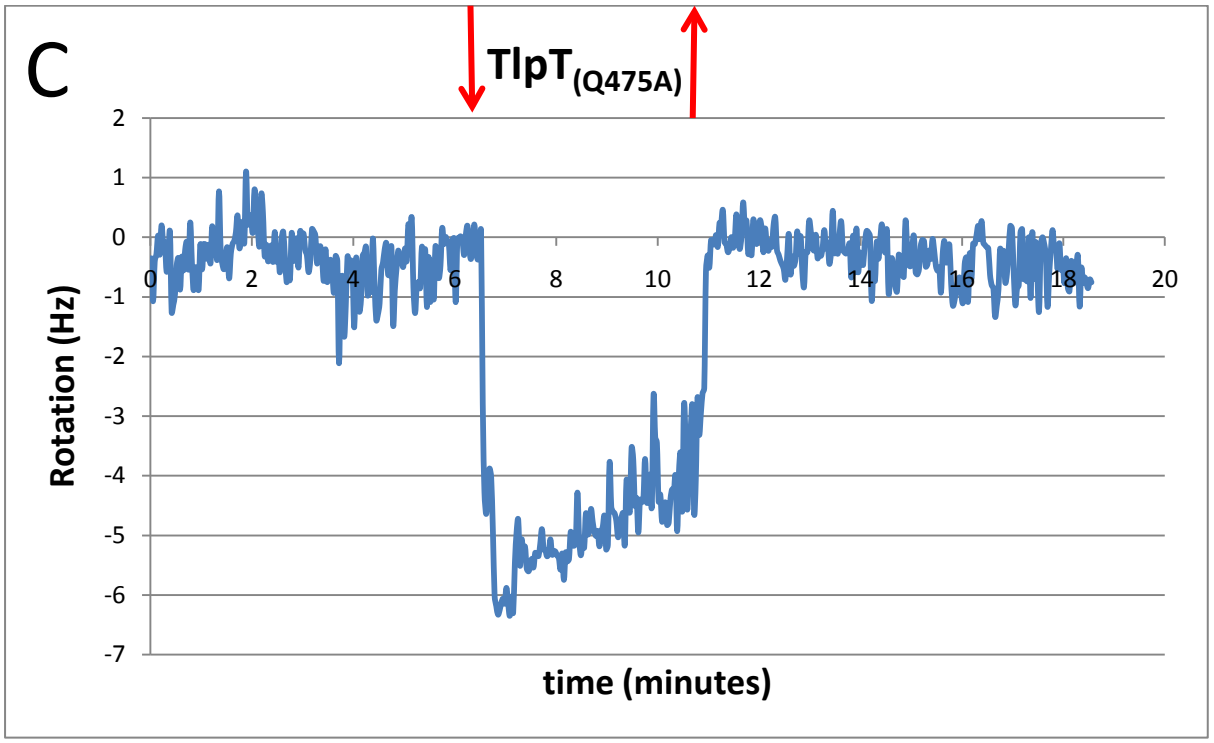
3.3.2 Tethered cell analysis of TlpT mutants

The effect of putative methylation site mutations on motor behaviour was analysed using the tethered cell assay. Wild type cells typically respond to step changes in attractant by increasing their rotation on addition of attractant followed by a sudden stop upon removal of attractant. The rotational bias then gradually returns to the pre-stimulus level after a few minutes (Figure 23A).

The results for $TlpT_{(Q451A)}$ under aerobic conditions were similar to those of wild type cells, supporting the data obtained in the swarm plate assays (Figure 23B). The behaviour of $TlpT_{(Q475A)}$ was different from that of the wild type response under aerobic conditions. These cells were non-motile before the addition of attractant and showed a larger increase in motility upon the addition of attractant. When the attractant was removed, the cells returned to their non-motile behaviour (Figure 23C). This supports the reduced motility observed on swarm plates for this strain. The *ΔtlpT* cells showed no response under aerobic conditions as expected (Figure 23D).




B
TlpT(Q451A)
2
0
-2
-4
-6
-8
-10
-12
0
2
4
6
8
10
12
14
16
18
Rotation (Hz)
time (minutes)


C
TlpT(Q475A)
2
1
0
-1
-2
-3
-4
-5
-6
-7
0
2
4
6
8
10
12
14
16
18
20
Rotation (Hz)
time (minutes)

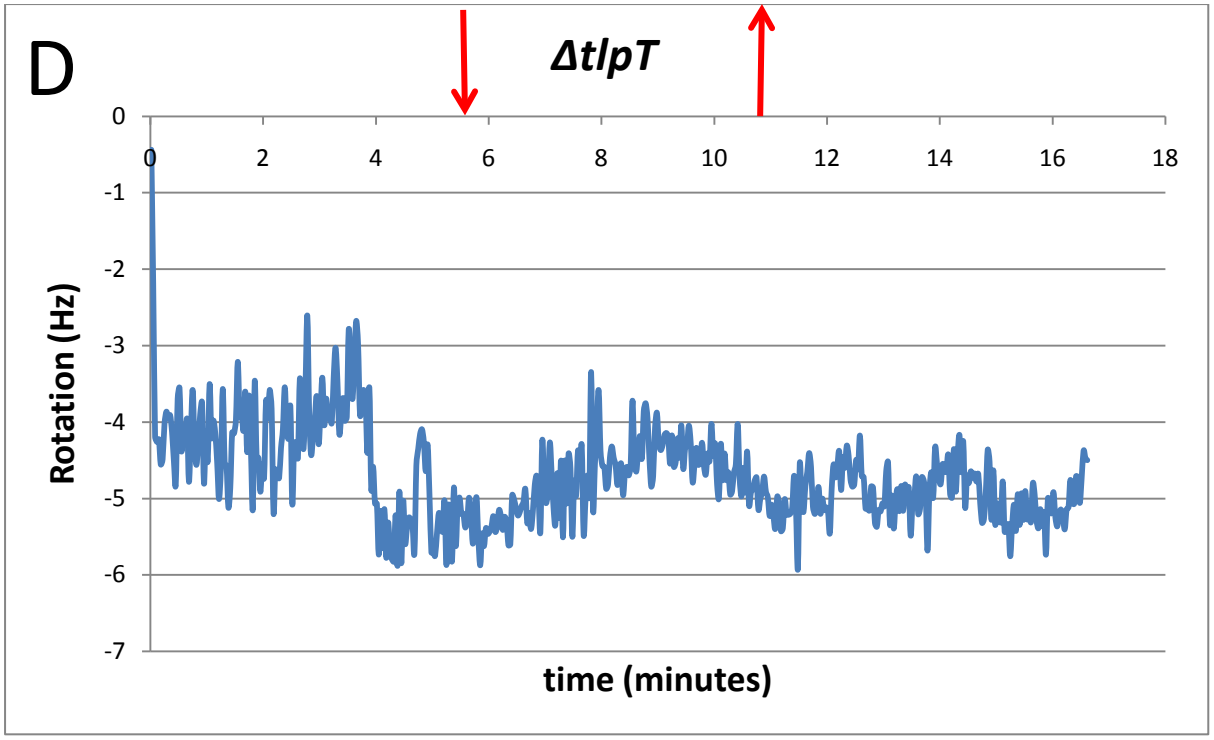


Figure 23: Behaviour of tethered cells. **(A)** A model of the wild type response averaged from four WS8N cells. **(B)** $TlpT_{(Q451A)}$ (JPA1037): a response similar to the wild type under aerobic conditions. Data averaged from seven cells. **(C)** $TlpT_{(Q475A)}$ (JPA1038): a response that differs significantly from the wild type under aerobic conditions. Data averaged from seven cells. **(D)** *ΔtlpT* (JPA1331): no response under aerobic conditions. Data averaged from eight cells.

4 Discussion

4.1 Sequence analysis of *Rhodobacter* chemoreceptors

Alignment of *R. sphaeroides* MCPs with *E. coli* MCPs revealed the sequence homology between these receptors. The residues on *R. sphaeroides* MCPs that correspond to the residues on *E. coli* chemoreceptors that have been experimentally identified as methylation sites are likely to have functions in methylation as well. These putative residues in all of the nine *R. sphaeroides* MCPs could also be tested in mutagenesis studies for their effect on motility in future studies.

TLPs in *R. sphaeroides* do not show extensive homology with the MCPs other than the HCD region. Within each other, TLPs do not show extensive sequence homology, suggesting that they might have been taken up by *Rhodobacter* through lateral gene transfer. The putative methylation sites in TlpC, TlpL, and TlpS should also be mutated and tested for their phenotype.

Except McpA and TlpT, *R. sphaeroides* chemoreceptors do not contain the conserved C-terminal pentapeptide motif (NWETF) (1.3.1.1.6). This could mean that these receptors are methylated through interdimer methylation. The MCPs except McpA do seem to have a relatively conserved C-terminal region containing several aspartates. Therefore, it is also possible that $CheR_2$ recognizes these receptors through this different C-terminal motif, or a conserved region at another location on the receptors.

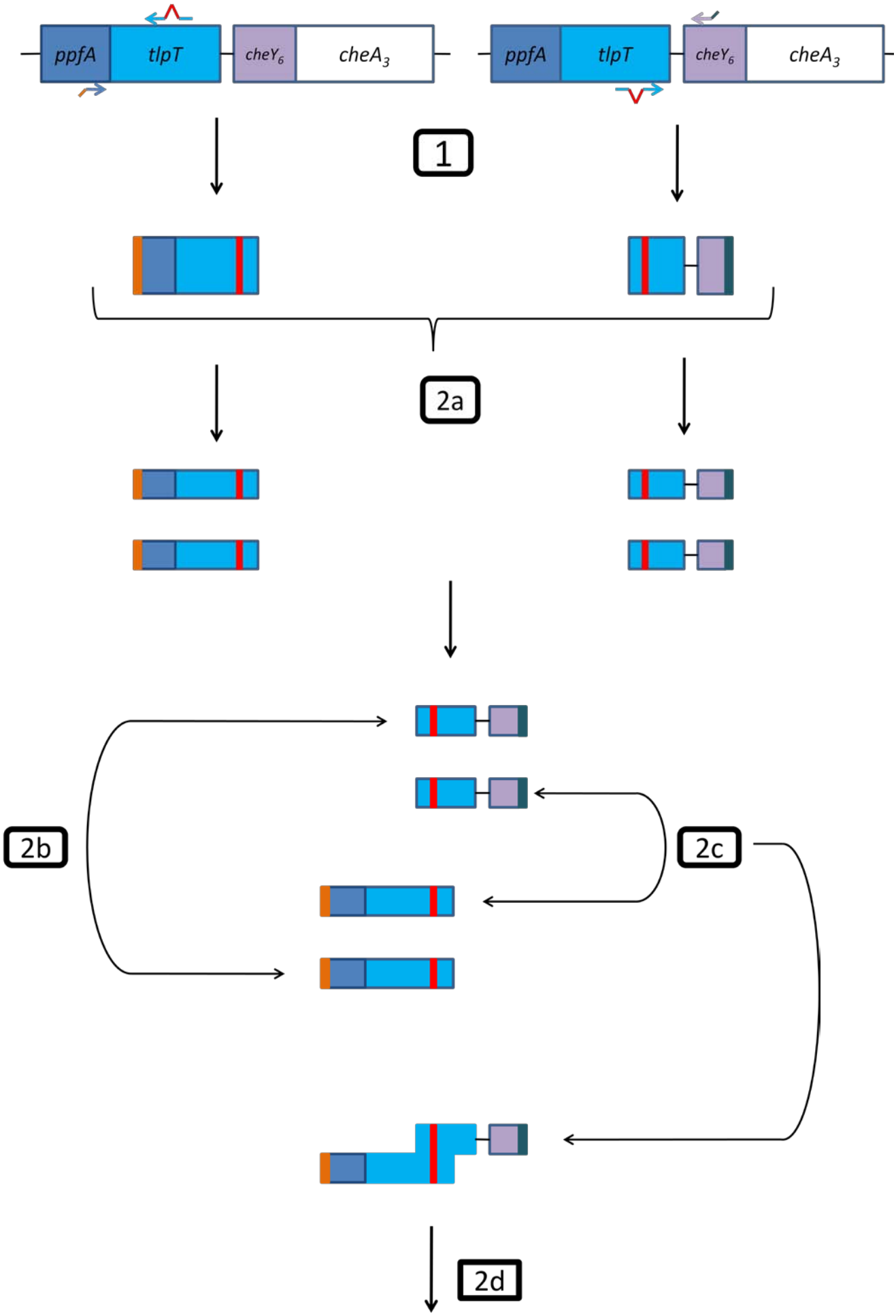
The two TLPs, TlpC and TlpS, share a conserved C-terminal motif: D-np-np-D-np-np-F (np denoting non-polar). It is therefore possible that $CheR_3$ recognizes these two TLPs through this different conserved motif. TlpL was not found to contain a conserved C-terminal motif. The *E. coli* Trg receptor, which lacks the NWETF motif, was still methylated *in vivo* (although at a slower rate); suggesting that the NWETF motif only increases the rate of methylation by the methyltransferase (Wu, et al. 1996). Therefore it is possible that TlpL is still recognized by its cognate methylesterase through a different region on its structure.

4.2 Comparison of site-directed mutagenesis techniques

The QuikChange mutagenesis method was used in creating the mutant *tlpT* and *mcpH* genes. A different method called overlap extension PCR (Figure 24) could also have been used to create these mutants. This method differs from the QuikChange method in that it uses two PCR cycles instead of one.

During the first cycle, the upstream and downstream regions including the mutation are synthesised separately (Figure 24.1). In the second cycle, these partial fragments are combined, and are extended through their overlapping mutant regions (Figure 24.2).

The QuikChange mutagenesis method was found to be the more effective method for creating constructs with mutant gene inserts. Even though upstream and downstream fragments with the correct sizes were synthesised in the first round of the oePCR, the fragments were probably unable to anneal in the second round, preventing their extension and the synthesis of the full-length mutant fragment. The QuikChange method was proved to be more practical, being able to produce the desired mutation in a single round of PCR.


ppfA
tlpT
cheY6
cheA3
ppfA
tlpT
cheY6
cheA3
1
2a
2b
2c
2d

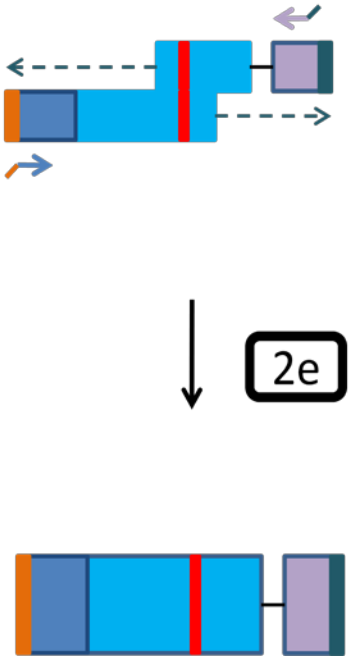


Figure 24: The oePCR method. **(1)** In the first round PCR, the upstream forward and the upstream reverse primers synthesize the upstream fragment containing a *Hind*III site **(orange)** from the template plasmid pUC19*che*Op$_3$ in one tube **(left)**. The downstream reverse and the downstream forward primers synthesize the downstream fragment containing an *Eco*RI site **(dark aqua)** from the template DNA in the other tube **(right)**. Partial fragments containing the mutation and the upstream or downstream regions were run on an agarose gel and gel extracted. **(2a)** During the second round PCR, the combined partial fragments denature. **(2b)** The upper strand of the upstream fragment and the lower strand of the downstream fragment anneal at their overlapping mutant regions. **(2c)** The lower strand of the upstream fragment and the upper strand of the downstream fragment anneal at the overlapping mutant regions. **(2d)** The molecule formed in **2c** is extended in the upstream and downstream directions with the outer primers annealing at both ends on opposite strands to yield the full length molecule **(2e)**, containing mutant *tlpT* and the upstream and downstream regions. The mutagenic base pair is shown in **red**.

4.3 Phenotypes of the *tlpT* mutants

The TlpT$_{(E96A)}$ mutant did not exhibit a chemotactic phenotype that was different from the wild type strain on both swarm plates and the tethered cell assay (data not shown). This result was expected, since E96 is not in the methylation region but is located upstream in the sensing domain. The fact that the TlpT$_{(Q451A)}$ mutant did not differ in behaviour from the wild type in both assays could mean this site is not a methylation site, or it is an alternative methylation site when the other methylation sites are unavailable.

The $TlpT_{(Q475A)}$ cells showed a smaller swarm size than the wild type strain under aerobic and anaerobic conditions. The behaviour of the $TlpT_{(Q475A)}$ strain showed a significant divergence from the wild type behaviour with the tethered cell assay, under the tested conditions. The initially nearly non-motile cells responded to attractant with a larger increase in motility than the wild type's; however they went back to their stoppy behaviour when the attractant was removed. This means that mutating residue Q475 had a significant effect on motility, and this residue could be a methylation site.

Mutating Q528 significantly impaired chemotaxis on swarm plates under the conditions tested. The $TlpT_{(Q528A)}$ mutant showed a similar phenotype to *ΔtlpT* cells, which are non-chemotactic, and its swarm size was only slightly larger than the non-motile $CheY_{6(D56N)}$ strain's swarm size. Therefore, it is highly likely that Q528 has an important function in methylation. Another possibility rises from the fact that some essential CheY homologues were found to localise in the cytoplasmic cluster, and TlpT was found to be essential for chemotaxis. This means that TlpT could be interacting with the essential CheYs, and the mutation $TlpT_{(Q528A)}$ could be interfering with this interaction. This could be preventing the CheYs from becoming phosphorylated by $CheA_3$, thereby reducing rotational switching (S. L. Porter, G. W. Wadhams, et al. 2006).

4.4 Conclusion and future work

The steady state methylation level of a receptor correlates with the intensity of the signal that it receives, and is important for adaptation to constant levels of attractant. So the more methylation sites are available on a receptor, the better it should be able to respond and adapt to an attractant. Therefore, the chemotaxis ability of a bacterium should decrease with increasing number of mutated putative methylation sites. The relative positions of the putative methylation sites on the *R. sphaeroides* TlpT are shown in Figure 25.



Figure 25: The domain structure of TlpT. Relative positions of the putative methylation sites are shown with red dots.

It has been shown in this study that mutating Q528 (site #5) on TlpT affected chemotaxis more severely than mutating Q475 (site #4). This could mean that Q528 is more rapidly methylated than Q475. A similar case was observed with the *E. coli* Tar receptor, where the mutation E309D had a more severe effect on chemotaxis that mutating the other four sites individually. E309D was determined to be the fastest methylated site (Shapiro, Chakrabarti and Koshland Jr 1995).

It is unlikely that the methylation system in *R. sphaeroides* works in a similar way to the selective methylation system found in *B. subtilis*, because the two organisms are distantly related (Figure 26). In the selective system, each methylation site has a different function, with some sites activating the HK and some sites inhibiting it. The methylation system in *R. sphaeroides* is likely to resemble that of *E. coli*'s, since the two organisms are more closely related. Therefore, the individual methylation sites should have the same function; but one

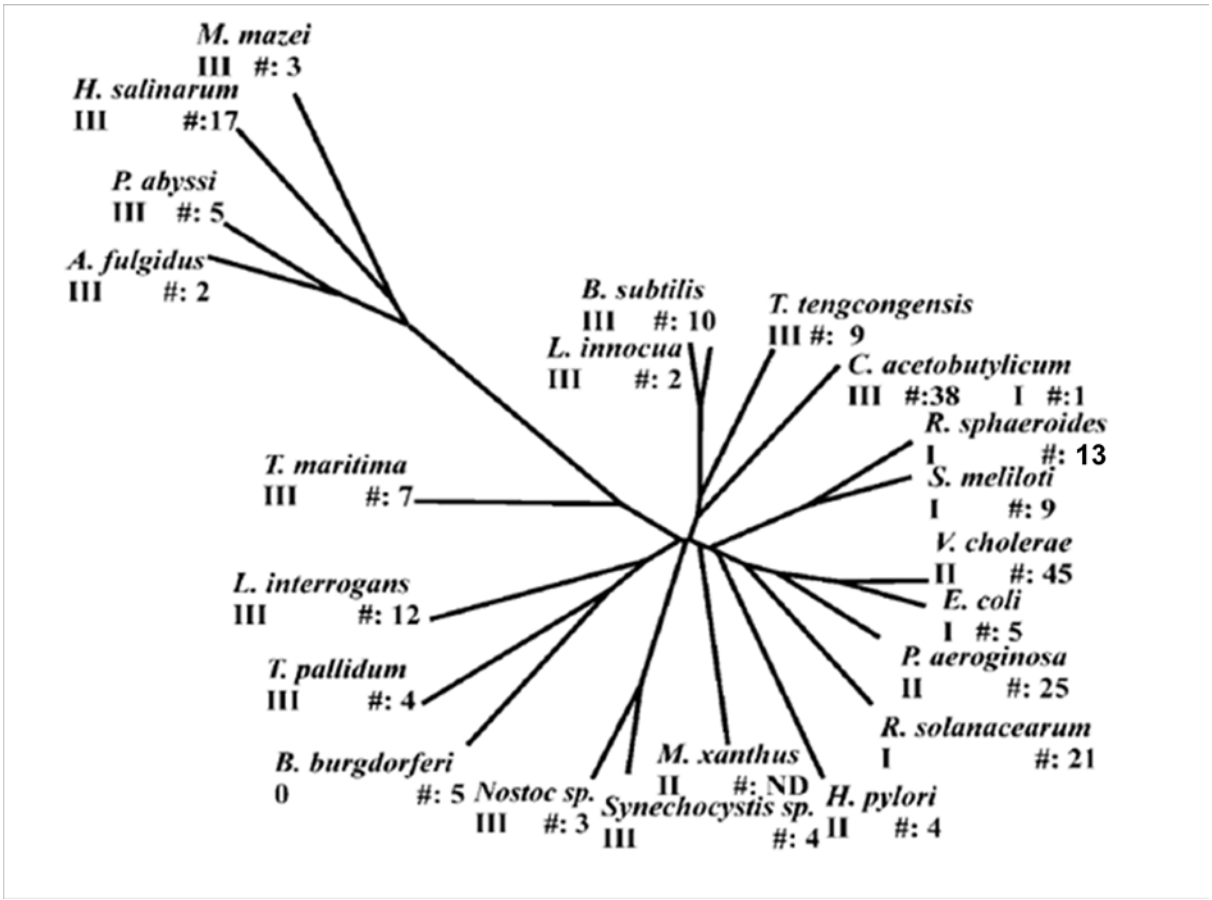


Figure 26: Phylogenetic tree showing evolutionary relationships of chemotactic bacteria and archaea species. The number of chemoreceptors of each organism and the receptor class they belong to are indicated below the organism names. *R. sphaeroides*, which belongs to the α-subgroup of proteobacteria along with *Sinorhizobium meliloti*, has thirteen class I MCPs. Tree adapted from Szurmant and Ordal 2004.

site could be more important than the other.

The function of each individual putative methylation site on TlpT could be determined by analysing the combinatorial mutants both phenotypically and biochemically.

Biochemical analysis of methylation is achieved by methylation assays. In these experiments, the methyltransferase and the receptor are mixed in the presence of radioactive SAM. The radioactivity of aliquots taken at fixed time intervals from the reaction is measured (Shapiro and Koshland Jr 1994). The extent of methylation of each putative residue can thereby be determined by amount of radioactivity produced from its reaction when all the alternative methylation sites are non-functional.

Finally, the remaining chemoreceptors in *R. sphaeroides* could be used in similar behavioural and *in vitro* assays to understand their methylation mechanism. The receptors which give chemotactic phenotypes when deleted should be given priority in analysis. The functions of other domains than the methylation domains in these receptors could also be investigated. Different domains of the receptors could be deleted, e. g. the periplasmic, HAMP, or C-terminal domains, and the effects of these deletions could be analysed.

5 References

Airola, Michael V, Kylie J Watts, Alexandrine M Bilwes, and Brian R Crane. “Structure of concatanated HAMP domains provides a mechanism for signal transduction.” *Cell* 18 (2010): 436-448.

Alexander, Roger P, Andrew C Lowenthal, Rasika M Harshey, and Karen M Otteman. “CheV: CheW-like coupling proteins at the core of the chemotaxis signaling network.” *Trends Microbiol* 18, no. 11 (2010): 494-503.

Ames, Peter, Yong A Yu, and John S Parkinson. “Methylation segments are not required for chemotactic signalling by cytoplasmic fragments of Tsr, the methyl-accepting serine chemoreceptor of Escherichia coli.” *Mol Microbiol* 19, no. 4 (1996): 737-746.

Appleby, Jeryl L, John S Parkinson, and Robert B Bourret. “Signal transduction via the multi-step phosphorelay: not necessarily a road less traveled.” *Cell* 86 (1996): 845-848.

Aravind, L, and Chris P Ponting. “The cytoplasmic helical linker domain of receptor histidine kinase and methyl-accepting proteins is common to many prokaryotic signalling proteins.” *FEMS Microbiol Lett* 176 (1999): 111-116.

Armitage, Judith P. “Behavioral responses in bacteria.” *Annu Rev Physiol* 54 (1992): 683-714.

Armitage, Judith P, and Robert M Macnab. “Unidirectional, intermittent rotation of the flagellum of Rhodobacter sphaeroides.” *J Bacteriol* 169, no. 2 (1987): 514-518.

Berg, Howard C, and Steven M Block. “A miniature flow cell designed for rapid exchange of media underhigh-power microscope objectives.” *J Gen Microbiol* 130 (1984): 2915-2920.

Bilwes, Alexandrine M, Lisa A Alex, Brian R Crane, and Melvin I Simon. “Structure of CheA, signal-transducing histidine kinase.” *Cell* 96 (1999): 131-141.

Blair, David F. “How bacteria sense and swim.” *Annu Rev Microbiol* 49 (1995): 489-522.

Boesch, Kristin C, Ruth E Silversmith, and Robert B Bourret. “Isolation and characterization of nonchemotactic CheZ mutants of Escherichia coli.” *J Bacteriol* 182, no. 12 (2000): 3544-3552.

Boyd, A, K Kendall, and Melvin I Simon. “Structure of the serine chemoreceptor in Escherichia coli.” *Nature* 301 (1983): 623-626.

Chervitz, Stephen A, and Joseph J Falke. “Lock on/off disulfides identify the transmembrane signaling helix of the aspartate receptor.” *J Biol Chem* 270 (1995): 24043-24053.

Chervitz, Stephen A, and Joseph J Falke. “Molecular mechanism of transmembrane signaling by the aspartate receptor.” *Proc Natl Acad Sci* 93 (1996): 2545-2550.

Djordjevic, Snezana, and Ann M Stock. “Chemotaxis receptor recognition by protein methyltransferase CheR.” *Nat Struct Biol* 5, no. 6 (1998): 446-450.

Djordjevic, Snezana, Paul N Goudreau, Qingping Xu, Ann M Stock, and Ann H West. “Structural basis for methylesterase CheB regulation by a phosphorylation-activated domain.” *Proc Natl Acad Sci USA* 95, no. 4 (1998): 1381-1386.

Falke, Joseph J, and Gerald L Hazelbauer. “Transmembrane signaling in bacterial chemoreceptors.” *Trends Biochem Sci* 26 (2001): 257-265.

Falke, Joseph J, Randal B Bass, Scott L Butler, Stephen A Chervitz, and Mark A Danielson. “The two-component signaling pathway of bacterial chemotaxis: a molecular view of signal transduction by receptors, kinases, adaptation enzymes.” *Annu Rev Cell Dev Biol* 13 (1997): 457-512.

Falke, Joseph, J, and Annette H Erbse. “The piston rises again.” *Structure* 17 (2009): 1149-1151.

Ferre, Axelle, Javier de la Mora, Teresa Ballado, Laura Camarena, and Georges Dreyfus. “Biochemical study of multiple CheY response regulators of the chemotactic pathway of Rhodobacter sphaeroides.” *J Bacteriol* 186, no. 15 (2004): 5172-5177.

Gao, Rong, and Ann M Stock. “Biological insights from structures of two-component proteins.” *Annu Rev Microbiol* 63 (2009): 133-154.

Gegner, Julie A, Daniel R Graham, Amy F Roth, and Frederick W Dahlquist. “Assembly of an MCP receptor, CheW and kinase CheA complex in the bacteria chemotaxis signal transduction pathway.” *Cell* 70, no. 6 (1992): 975-982.

Giuliano, G, D Pollock, H Stapp, and P A Scolnik. “A genetic-physical map of the Rhodobacter capsulatus carotenoid biosynthesis gene-cluster.” *Mol Gen Genet* 231 (1988): 78-83.

Griswold, Ian J, et al. “The solution structure and interactions of CheW from Thermotoga maritima.” *Nat. Struct. Biol.* 9, no. 2 (2002): 121-125.

Hazelbauer, Gerald L, Joseph J Falke, and John S Parkinson. “Bacterial chemoreceptors: high-performance signaling in networked arrays.” *Trends Biochem Sci* 33 (2007): 9-19.

Hulko, Michael, et al. “The HAMP domain structure implies helix rotation in transmembrane signaling.” *Cell* 126 (2006): 929-940.

Hwang, Ildoo, Huei-Chi Chen, and Jen Sheen. “Two-component signal transduction pathways in Arabidopsis.” *Plant Physiol* 129 (2002): 500-515.

Kehry, Marilyn R, Martha W Bond, Michael W Hunkapiller, and Frederick W Dahlquist. “Enzymatic deamidation of methyl-accepting chemotaxis proteins in Escherichia coli catalyzed by the cheB gene product.” *Proc Natl Acad Sci U S A* 80 (1983): 3599-3603.

Kirby, John R. “Chemotaxis-like regulatory systems: unique roles in diverse bacteria.” *Annu Rev Microbiol* 63 (2009): 45-59.

Krikos, Alexandra, Norihiro Mutoh, Alan Boyd, and Melvin I Simon. “Sensory transducers of E. coli are composed of discrete structural and functional domains.” *Cell* 33 (1983): 615-622.

Larkin, MA, et al. “Clustal W and Clustal X version 2.0.” *Bioinformatics* 23 (2007): 2947-2948.

Le Moual, Herve, and Daniel E Jr. Koshland. “Molecular evolution of the C-terminal cytoplasmic domain of a superfamily of bacterial receptors involved in taxis.” *J Mol Biol* 261 (1996): 568–585.

Lukat, Gudrun s, Benjamin H Lee, James M Mottonen, Ann M Stock, and Jeffry B Stock. “Roles of the highly conserved aspartate and lysine residues in the response regulator of bacterial chemotaxis.” *J Biol Chem* 266, no. 13 (1991): 8348-8354.

Lupas, Andrei, and Jeffry Stock. “Phosphorylation of an N-terminal regulatory domain activates the CheB methylesterase in bacterial chemotaxis.” *J Biol Chem* 264, no. 29 (1989): 17337-17342.

Mackenzie, Chris, et al. “Postgenomic adventures with Rhodobacter sphaeroides.” *Annu Rev Microbiol* 61 (2007): 283–307.

Mackenzie, Chris, et al. “The home stretch, a first analysis of the nearly completed genome of Rhodobacter sphaeroides 2.4.1.” *Photosynth Res* 70, no. 1 (2001): 19-41.

Madigan, Michael T, and John M Martinko. *Brock biology of microorganisms.* Upper Saddle River: Pearson Education, Inc., 2006.

Mantotta, Jeevani C. *Analysis of chemosensory proteins in Rhodobacter sphaeroides.* D Phil Thesis University of Oxford, 2002.

Martin, Angela C, et al. “CheR- and CheB-dependent chemosensory adaptation system of Rhodobacter sphaeroides.” *J Bacteriol* 183 (2001): 7135-7144.

Martin, Angela C, George H Wadhams, and Judith P Armitage. “The roles of the multiple CheW and CheA homologues in chemotaxis and in chemoreceptor localization in Rhodobacter sphaeroides.” *Mol Microbiol* 40, no. 6 (2001): 1261-1272.

Martin, Angela C, Nair Usha, Judith P Armitage, and Janine R Maddock. “Polar localization of CheA2 in Rhodobacter sphaeroides requires specific Che homologs.” *J Bacteriol* 185, no. 16 (2003): 4667-4671.

McEvoy, Megan M, Andrew C Hausrath, Gannon B Randolph, S James Remington, and Frederick W Dahlquist. “Two binding modes reveal flexibility in kinaseyresponse regulator interactions in the bacterial chemotaxis pathway.” *Proc. Natl. Acad. Sci. USA* 95, no. 13 (1998): 7333–7338.

McEvoy, Megan M, D Ranjith Muhandiram, Lewis E Kay, and Frederick W Dahlquist. “Structure and dynamics of a CheY-binding domain of the chemotaxis kinase CheA determined by nuclear magnetic resonance spectroscopy.” *Biochemistry* 35, no. 18 (1996): 5633-5640.

Meir, Yigal, Vladimir Jakovljevic, Olga Oleksiuk, Victor Sourjik, and Ned S Wingreen. “Precision and kinetics of adaptation in bacterial chemotaxis.” *Biophysics* 99, no. 9 (2010): 2766–2774.

Mourey, Lionel, et al. “Crystal structure of the CheA histidine phosphotransfer domain that mediates response regulator phosphorylation in bacterial chemotaxis.” *J Biol Chem* 276, no. 33 (2001): 31074-31082.

Mowbray, Sherry L, and Mats O J Sandgren. “Chemotaxis receptors: a progress report on structure and function.” *J Struct Biol* 124 (1998): 257-275.

Nowlin, Dawn M, John Bollinger, and Gerald L Hazelbauer. “Sites of covalent modification in Trg, a sensory transducer of Escherichia coli.” *J Biol Chem* 262 (1987): 6039-6045.

Nowlin, Dawn, M, John Bollinger, and Gerald L Hazelbauer. “Site-directed mutations altering methyl-accepting residues of a sensory transducer protein.” *Proteins* 3 (1988): 102-112.

Pallen, Mark J, and Nicholas J Matzke. “From The Origin of Species to the origin of bacterial flagella.” *Nat Rev Microbiol* 4: 784-790.

Pallen, Mark J, and Nicholas J Matzke. “From The Origin of Species to the origin of bacterial flagella.” *Nat Rev Microbiol* 4, no. 10 (2006): 784-790.

Parkinson, John S, and Eric C Kofoid. “Communication modules in bacterial signaling proteins.” *Annu Rev Genet* 26 (1992): 71-112.

Penfold, Robert J, and John M Pemberton. “An improved suicide vector for construction of chromosomal insertion mutations in bacteria.” *Gene* 118 (1992): 145-146.

Perez, Eduardo, Ann H West, Ann M Stock, and Snezana Djordjevic. “Discrimination between different methylation states of chemotaxis receptor Tar by receptor methyltransferase CheR.” *Biochemistry* 43 (2004): 953-961.

Perez, Eduardo, Haiyan Zheng, and Ann M Stock. “Identification of methylation sites in Thermotoga maritima chemotaxis receptors.” *J Bacteriol* 188 (2006): 4093-4100.

Porter, Steven L. *The chemotaxis proteins of Rhodobacter sphaeroides.* University of Oxford, 2002.

Porter, Steven L, and Judith P Armitage. “Chemotaxis in Rhodobacter sphaeroides requires an atypical histidine protein kinase.” *J Biol Chem* 279, no. 52 (2004): 54573-54580.

Porter, Steven L, and Judith P Armitage. “Phosphotransfer in Rhodobacter sphaeroides chemotaxis.” *J Mol Biol* 324, no. 1 (2002): 35-45.

Porter, Steven L, Anna V Warren, Angela C Martin, and Judith P Armitage. “The third chemotaxis locus of Rhodobacter sphaeroides is essential for chemotaxis.” *Mol Microbiol* 46, no. 4 (2002): 1081-1094.

Porter, Steven L, George H Wadhams, and Judith P Armitage. “In vivo and in vitro analysis of the Rhodobacter sphaeroides chemotaxis signaling complexes.” *Methods Enzymol* 423 (2007): 392-413.

Porter, Steven L, George H Wadhams, and Judith P Armitage. “Rhodobacter sphaeroides: complexity in chemotactic signalling.” *Trends in Microbiology* 16 (2008): 251-260.

Porter, Steven L, George H Wadhams, Angela C Martin, Elaine D Byles, David E Lancaster, and Judith P Armitage. “The CheYs of Rhodobacter sphaeroides.” *J Biol Chem* 281, no. 43 (2006): 32694-32704.

Porter, Steven L, Mark A J Roberts, Cerys S Manning, and Judith P Armitage. “A bifunctional kinase-phosphatase in bacterial chemotaxis.” *Proc Natl Acad Sci U S A* 105, no. 47 (2008): 18531-18536.

Posas, Francesc, Susannah M Wurgler-Murphy, Tatsuya Maeda, Elizabeth A Witten, Tran Cam Thai, and Haruo Saito. “Yeast HOG1 MAP kinase cascade is regulated by a multistep phosphorelay mechanism in the SLN1-YPD1-SSK1 "two-component" osmosensor.” *Cell* 86 (1996): 865-875.

Rao, Christopher V, George D Glekas, and George W Ordal. “The three adaptation systems of Bacillus subtilis chemotaxis.” *Trends Microbiol* 16, no. 10 (2008).

Rao, Christopher V, John R Kirby, and Adam P Arkin. “Design and Diversity in Bacterial Chemotaxis: A Comparative Study in Escherichia coli and Bacillus subtilis.” *PLoS Biol* 2, no. 2 (2004).

Roberts, Mark A J. *The cytoplasmic chemotaxis protein cluster of Rhodobacter sphaeroides.* University of Oxford, 2007.

Sambrook, Joseph, and David W Russell. *Molecular cloning: a laboratory manual.* New York: Cold Spring Harbor Laboratory Press, 2001.

Sanders, David Avram, Beth L Gillece-Castro, Ann M Stock, A L Burlingame, and Daniel E Koshland Jr. “Identification of the site of phosphorylation of the chemotaxis response regulator protein, CheY.” *J Biol Chem* 264, no. 36 (1989): 21779-21778.

Schäfer, A, A Tauch, A Jäger, J Kalinowski, G Thierbach, and A Pühler. “Small mobilizable multi-purpose cloning vectors derived from the Escherichia coli plasmids pK18 and pK19: selection of defined deletions in the chromosome of Corynebacterium glutamicum.” *Gene* 145 (1994): 69-73.

Scharf, Birgit, and Rüdiger Schmitt. “Sensory transduction to the flagellar motor of Sinorhizobium meliloti.” *J Mol Microbiol Biotechnol* 4, no. 3 (2002): 183-186.

Scott, Kathryn A, et al. “Specificity of localization and phosphotransfer in the CheA proteins of Rhodobacter sphaeroides.” *Mol Microbiol* 76, no. 2 (2010): 318-330.

Shah, Deepan S H, Steven L Porter, Angela C Martin, Paul A Hamblin, and Judith P Armitage. “Fine tuning bacterial chemotaxis: analysis of Rhodobacter sphaeroides behaviour under aerobic and anaerobic conditions by mutation of the major chemotaxis operons and cheY genes.” *EMBO J* 19, no. 17 (2000): 4601-4613.

Shapiro, Michael J, and Daniel E Koshland Jr. “Mutagenic studies of the interaction between the aspartate receptor and methyltransferase from Escherichia coli.” *J Biol Chem* 269, no. 15 (1994): 11054-11059.

Shapiro, Michael J, Indro Chakrabarti, and Daniel E Koshland Jr. “Contributions made by individual methylation sites of the Escherichia coli aspartate receptor to chemotactic behavior.” *Proc Natl Acad Sci U S A* 92, no. 4 (1995): 1053-1056.

Sockett, R Elizabeth, J C A Foster, and Judith P Armitage. “Molecular biology of the Rhodobacter sphaeroides flagellum.” *FEMS Symp* 53 (1990): 473-479.

Sourjik, Victor. “Receptor clustering and signal processing in E. coli chemotaxis.” *Trends Microbiol* 12 (2004): 569-576.

Stewart, Richard C. “Activating and inhibitory mutations in the regulatory domains of CheB, the methylesterase in bacterial chemotaxis.” *J Biol Chem* 268, no. 3 (1993): 1921-1930.

Stewart, Richard C, Amy F Roth, and Frederick W Dahlquist. “Mutations that affect control of the methylesterase activity of CheB, a component of the chemotaxis adaptation system in Escherichia coli.” *J Bacteriol* 172, no. 6 (1990): 3388-3399.

Stock, Ann M, and Sherry L Mowbray. “Bacterial chemotaxis: a field in motion.” *Curr Opin Struct Biol* 5 (1995): 744-751.

Stock, Ann M, James M Mottonen, Jeffry B Stock, and Clarence E Schutt. “Three-dimensional structure of CheY, the response regulator of bacterial chemotaxis.” *Nature* 337, no. 6209 (1989): 745-749.

Stock, Ann M, Victoria L Robinson, and Paul N Goudreau. “Two-component signal transduction.” *Annu Rev Biochem* 69 (2000): 183-215.

Stock, Jeffrey B, Alexander J Ninfa, and Ann M Stock. “Protein phosphorylation and regulation of adaptive responses in bacteria.” *Microbiol Rev* 53 (1989): 450-490.

Suwanto, Antonius, and Samuel Kaplan. “Physical and genetic mapping of the Rhodobacter sphaeroides 2.4.1 genome: presence of two unique circular chromosomes.” *J Bacteriol* 171, no. 11 (1989): 5850-5859.

Swanson, Ronald V, and Melvin I Simon. “Bringing the eukaryotes up to speed.” *Curr Biol*, 1994: 234-237.

Szurmant, Hendrik, and George W Ordal. “Diversity in chemotaxis mechanisms among Bacteria and Archaea.” *Microbiol Mol Biol Rev* 68 (2004): 301-319.

Terwilliger, Thomas C, and Daniel E Jr. Koshland. “Sites of methyl esterification and deamination on the aspartate receptor involved in chemotaxis.” *J Biol Chem* 259 (1984): 7719-7725.

Terwilliger, Thomas C, Justin Y Wang, and Daniel E Jr. Koshland. “Surface structure recognized for covalent modification of the aspartate receptor in chemotaxis.” *Proc Natl Acad Sci U S A* 83 (1986): 6707-6710.

Thompson, Stephen R. *A study of multiple chemosensory gene homologues in Rhodobacter sphaeroides.* DPhil Thesis University of Oxford, 2005.

Thompson, Stephen R, George H Wadhams, and Judith P Armitage. “The positioning of cytoplasmic protein clusters in bacteria.” *Proc Natl Acad Sci U S A* 103 (2006): 8029-8214.

Wadhams, George H, Angela C Martin, and Judith P Armitage. “Identification and localization of a methyl-accepting chemotaxis protein in Rhodobacter sphaeroides.” *Mol Microbiol* 36, no. 6 (2000): 1222-1233.

Wadhams, George H, Anna V Warren, Angela C Martin, and Judith P Armitage. “Targeting of two signal transduction pathways to different regions of the bacterial cell.” *Mol Microbiol* 50, no. 3 (2003): 763-70.

Wadhams, George H, et al. “TlpC, a novel chemotaxis protein in Rhodobacter sphaeroides, localizes to a discrete region in the cytoplasm.” *Mol Microbiol* 46, no. 5 (2002): 1211-1221.

Wadhams, George W, and Judith P Armitage. “Making sense of it all: bacterial chemotaxis.” *Nat Rev Mol Cell Biol* 5 (2004): 1024-1037.

Ward, Mandy J, David M Harrison, Martin J Ebner, and Judith P Armitage. “Identification of a methyl-accepting chemotaxis protein in Rhodobacter sphaeroides.” *Mol Microbiol* 18, no. 1 (1995): 115-121.

Welch, Martin, Kenji Oosawa, Shin-Ichi Aizawa, and Michael Eisenbach. “Phosphorylation-dependent binding of a signal molecule to the flagellar switch of bacteria.” *Prot Natl Acad Sci USA* 90, no. 19 (1993): 8787-8791.

West, Ann H, Erik Martinez-Hackert, and Ann M Stock. “Crystal structure of the catalytic domain of the chemotaxis receptor methylesterase, CheB.” *J Mol Biol* 250, no. 2 (1995): 276-290.

White, David. *The physiology and biochemistry of prokaryotes.* New York: Oxford University Press, Inc., 2007.

Woodcock, D M, P J Crowther, J Doherty, S Jefferson, and DeCruz. “Quantitative evaluation of Escherichia coli host strains for tolerance to cytosine methylation in plasmid and phage recombinants.” *Nucleic Acids Res* 17 (1989): 3469-3478.

Wu, Jiongru, Jiayin Li, David G Long, and Robert M Weis. “The receptor binding site for the methyltransferase of bacterial chemotaxis is distinct from the sites of methylation.” *Biochemistry* 35, no. 15 (1996): 4984-4993.

Yanisch-Perron, C, J A Vieira, and J Messing. “Improved M13 phage cloning vectors and host strains: nucleotide sequences of the M13mp18 and pUC19 vectors.” *Gene* 33 (1985): 103-119.

Yeh, Joanne I, Hans-Peter Biemann, Gil G Privé, Jay Pandit, Daniel E Koshland Jr, and Sung-Hou Kim. “High-resolution structures of the ligand binding domain of the wild-type bacterial aspartate receptor.” *J Mol Biol* 262 (1996): 186-201.

Zdobnov, EM, and R Apweiler. “InterProScan - an integration platform for the signature-recognition methods in InterPro.” *Bioinformatics* 17, no. 9 (2001): 847-848.

Zhao, Rui, Edward J Collins, Robert B Bourret, and Ruth E Silversmith. “Structure and catalytic mechanism of the E. coli chemotaxis phosphatase CheZ.” *Nat Struct Biol* 9, no. 8 (2002): 570-575.

Zimmer, Michael A, Joseph Tiu, Marissa A Collins, and George W Ordal. “Selective methylation changes on the Bacillus subtilis chemotaxis receptor McpB promote adaptation.” *J Biol Chem* 275, no. 32 (2000): 24264-24272.

Zusman, David R, Ansley, E Scott, Zhaomin Yang, and John R Kirby. “Chemosensory pathways, motility and development in Myxococcus xanthus.” *Nat Rev Microbiol* 5, no. 11 (2007): 862-872.

A1 Appendix 1 – Primers

A1.1 TlpT primers

Primer	Sequence	Description
*tlpT*M2DF	GTCTCGGCCTCGGCCGAAGCGACCGACAGCCAGGTGAAG	Downstream forward of a pair of primers used to create the mutation E296A in *tlpT*.
*tlpT*M2UR	CTTCACCTGGCTGTCGGTCGCTTCGGCCGAGGCCGAGAC	Upstream reverse of a pair of primers used to create the mutation E296A in *tlpT*.
*tlpT*M3DF	GCGCCTCGGACGAGGCGACGCGCAACGTGGCC	Downstream forward of a pair of primers used to create the mutation Q451A in *tlpT*.
*tlpT*M3UR	GGCCACGTTGCGCGTCGCCTCGTCCGAGGCGC	Upstream reverse of a pair of primers used to create the mutation Q451A in *tlpT*.
*tlpT*M4DF	GCTTTCGACCAGCCAGGCGGCGGATGAGCTGGC	Downstream forward of a pair of primers used to create the mutation Q475A in *tlpT*.
*tlpT*M4UR	GCCAGCTCATCCGCCGCCTGGCTGGTCGAAAGC	Upstream reverse of a pair of primers used to create the mutation Q475A in *tlpT*.
*tlpT*M5DF	GATGCTGGCCCAGCTTCAGGCGATGGTGGCGGCCCAGATG	Downstream forward of a pair of primers used to create the

		mutation Q528A in *tlpT*.
*tlpT*M5UR	CATCTGGGCCGCCACCATCGCCTGAAGCTGGGCCAGCATC	Upstream reverse of a pair of primers used to create the mutation Q528A in *tlpT*.

Table 6: The above table shows the mutagenic primers used to mutate putatively methylated E/Q to A in *tlpT*. Mismatch bases are shown in red.

A1.2 McpH primers

A1.2.1 Outer primers

Primer	Restriction site	Sequence	Description
*mcpH*UF	*Eco*RI	GCCGAATTCGGGCATGCGCCGTCGTCC	Upstream forward outer primer that binds to ~500 bp upstream of *mcpH*.
*mcpH*DR	*Hin*dIII	GGCAAGCTTAGCCAGCCCCGAGGCAGG	Downstream forward outer primer that binds to ~500 bp downstream of *mcpH*.

Table 7: The above primers were used to amplify the region containing *mcpH* and the upstream and downstream 500 bp of it from WS8N genomic DNA template. Restriction sites are shown in red.

A1.2.2 QuikChange primers

Primer	Sequence	Description
*mcpH*1UR	CTCTTCGGTGGAGGCCGCCGCCTCGCTGCTGCCCTGCGACAG	Upstream reverse of a pair of primers used to create the mutation Q295A in *mcpH*.
*mcpH*1DF	CTGTCGCAGGGCAGCAGCGAGGCGGCGGCCTCCACCGAAGAG	Downstream forward of a pair of

		primers used to create the mutation Q295A in *mcpH*.
*mcpH*2UR	CTCGACCGAGGCCGAGGCCGCTTCGGTGGAGGCCGCCTGCTC	Upstream reverse of a pair of primers used to create the mutation E301A in *mcpH*.
*mcpH*2DF	GAGCAGGCGGCCTCCACCGAAGCGGCCTCGGCCTCGGTCGAG	Downstream forward of a pair of primers used to create the mutation E301A in *mcpH*.
*mcpH*3UR	GATGTTGGCGGCCATCGCCTCGACCGAGGCCGAGGC	Upstream reverse of a pair of primers used to create the mutation E308A in *mcpH*.
*mcpH*3DF	GCCTCGGCCTCGGTCGAGGCGATGGCCGCCAACATC	Downstream forward of a pair of primers used to create the mutation E308A in *mcpH*.
*mcpH*4UR	CTGGATGGCGAGCGCCACCGCCTGCGCCCCCGTCGACAGTTC	Upstream reverse of a pair of primers used to create the mutation Q455A in *mcpH*.
*mcpH*4DF	GAACTGTCGACGGGGGCGCAGGCGGTGGCGCTCGCCATCCAG	Downstream forward of a pair of primers used to create the mutation Q455A in *mcpH*.
*mcpH*5UR	CTGGGTGACCTGATCGAGCGCCTGGATGGCGAGCGCCACCTG	Upstream reverse of a pair of primers used to create the mutation Q462A in *mcpH*.
*mcpH*5DF	CAGGTGGCGCTCGCCATCCAGGCGCTCGATCAGGTCACCCAG	Downstream forward of a pair of primers used to create the mutation

		Q462A in *mcpH*.
*mcpH*6UR	CTCAGCGGCGGTGCTGTTCGCCTGGTGACCTGATCGAGCTG	Upstream reverse of a pair of primers used to create the mutation Q469A in *mcpH*.
*mcpH*6DF	CAGCTCGATCAGGTCACCAGGGCGAACAGCACCGCCGCTGAG	Downstream forward of a pair of primers used to create the mutation Q469A in *mcpH*.
*mcpH*4URb	CTGGATGGCGAGCGCCACCGCCGCCGCCCCCGTCGACAGTTC	Upstream reverse of a pair of primers used to create the mutations Q454A and Q455A in *mcpH*.
*mcpH*4DFb	GAACTGTCGACGGGGGCGGCGGCGGTGGCGCTCGCCATCCAG	Downstream forward of a pair of primers used to create the mutations Q454A and Q455A in *mcpH*.
*mcpH*5URb	CTGGGTGACCTGATCGAGCGCCGCGATGGCGAGCGCCACCTG	Upstream reverse of a pair of primers used to create the mutations Q461A and Q462A in *mcpH*.
*mcpH*5DFb	CAGGTGGCGCTCGCCATCGCGGCGCTCGATCAGGTCACCCAG	Downstream forward of a pair of primers used to create the mutations Q461A and Q462A in *mcpH*.

Table 8: The above table shows the mutagenic primers used to mutate putatively methylated E/Q to A in *mcpH*. Mismatch bases are shown in red.

A2 Appendix 2 – Reagent recipes

A2.1 Succinate medium

Ingredient	Quantity
1 M Phosphate buffer, pH 7.0	20 ml
Concentrated base (A2.2)	20 ml
Ammonium sulphate	0.5 g
Growth factors (A2.4)	2 ml
Sodium succinate	2.0 g
NaCl	0.5 g
Casamino acids	1 g

The ingredients are made up to a final volume of 1 L with MilliQ water. The mixture is then adjusted to pH 7.2 with KOH and autoclave sterilised at 116°C.

A2.2 Concentrated Base

Ingredient	Quantity
Nitriloacetic acid	5.94 g
Metals 44 solution (A2.3)	25 ml
$MgSO_4 \cdot 7H_2O$	14.5 g
$CaCl_2 \cdot 6H_2O$	2.5 g

$FeSO_4 \cdot 7H_2O$	50 mg
Ammonium molybdate($\cdot 4H_2O$)	4.6 mg

The ingredients are made up to a final volume of 1 L with distilled water. The mixture is then adjusted to pH 6.8 with KOH, autoclave sterilised at 116°C, and stored at 4°C.

A2.3 Metals 44 Solution

Ingredient	**Quantity**
EDTA	2.5 g
$ZnSO_4 \cdot 7H_2O$	11 g
$FeSO_4 \cdot 7H_2O$	5 g
$MnSO_4 \cdot 4H_2O$	2 g
$CuSO_4 \cdot 5H_2O$	0.39 g
$CoCl_2 \cdot 6H_2O$	0.2 g
H_3BO_3	0.12 g
3 M Sulphuric acid	1.5 ml

The ingredients are made up to a final volume of 1 L with distilled water, filter sterilised, and stored at 4°C.

A2.4 Growth Factors

Ingredient	**Quantity**

Biotin	2 mg
$NaHCO_3$	50 mg
Niacin	100 mg
Thiamine	50 mg

The ingredients are dissolved in MilliQ water to a final volume of 100 ml and filter sterilized.

A2.5 M22 medium

Same as the succinate medium, except that sodium succinate and casamino acids are omitted in M22.

A2.6 DNA loading dye (5x)

Ingredient	**Quantity**
Bromophenol blue	0.25% (w/v)
Xylene cyanol	0.25% (w/v)
Glycerol	70% (w/v)
RNAse	Trace

The concentration of the loading dye is reduced to 1x when added to samples.

A2.7 TBE (10x)

Ingredient	Quantity
Tris base	108 g
Boric acid	55 g
EDTA	7.4 g

The ingredients are dissolved in 1 L of distilled water. When running agarose gels, 10x TBE is diluted to ½ x with MilliQ water.

A2.8 L-broth

Ingredient	Quantity
Tryptone	10 g
Yeast extract	5 g
NaCl	5 g

The ingredients are made up to 1 L with distilled water, adjusted to pH 7.0 with NaOH, and autoclave sterilized.

A2.9 Chromosomal DNA preparation lysis buffer

Ingredient	Quantity
Tris-HCl, pH 8.0	10 mM

EDTA	1 mM
SDS	1%